Probing the Unruh and Hawking effects using Unruh-DeWitt detectors

by

Aida Ahmadzadegan

A thesis
presented to the University of Waterloo
in fulfillment of the
thesis requirement for the degree of
Doctor of Philosophy
in
Physics

Waterloo, Ontario, Canada, 2017

Examining Committee Membership

The following served on the Examining Committee for this thesis. The decision of the Examining Committee is by majority vote.

External Examiner	MILES BLENCOWE Professor
Supervisor	ROBERT MANN Professor
Co-Supervisor	DANIEL TERNO Associate Professor
Internal Member	ROGER MELKO Associate Professor
Internal-external Member	ACHIM KEMPF Professor
Other Member	EDUARDO MARTÍN-MARTÍNEZ Assistant Professor

Author's Declaration

This thesis consists of material all of which I authored or co-authored: see Statement of Contributions included in the thesis. This is a true copy of the thesis, including any required final revisions, as accepted by my examiners.

I understand that my thesis may be made electronically available to the public.

Statement of Contributions

The results that are presented in this thesis were previously published in four co-authored publications [1–4]. In the leading research to these four publications, I was responsible for all the calculations and writing the first drafts of the papers. These were then co-edited with my collaborators before the submission for publication. The core chapters 4, 5, 6, 7, and Appendix A of this thesis are adapted from aforementioned four publications.

Abstract

Quantum field theory is so far the best description of the fundamental laws of Nature, yet it does not fully incorporates gravitation. The first attempt toward unifying the quantum field theory and gravity is a semi-classical theory of gravity, that in its basic form treats the gravitational background as fixed and focuses on the dynamics of matter fields instead. Well-known phenomena such as the Unruh effect and Hawking radiation provide elegant partial unification of these theories but still present a number of unresolved issues. One can attempt to address some of these challenging issues by relying on the semi-classical theory of gravity but not all of them are resolvable in the absence of a complete theory of quantum gravity, without fully incorporating both principles of general relativity and quantum theory. In recent years, however, the core ideas of quantum field theory combined with basic concepts of quantum information theory such as quantum entanglement have provided powerful approaches to address such questions. Perhaps quantum information theoretic methods could be a step towards uncovering the fundamental principles of quantum gravity.

In this context, the new sub-discipline of relativistic quantum information underlies the present thesis. Here, the fundamental features of radiation-matter interaction are explored in various physical settings of quantum field theory in curved spacetimes using Unruh-DeWitt particle detectors. In the first part of this thesis, a new model for computing the response of a particle detector in localized regions of general curved spacetimes is introduced to circumvent the mathematical complexity of standard methods for calculating the response function. Also, signatures of transition probabilities of atoms that are relativistically moving through optical cavities are shown to be very sensitive to their spatial trajectories. This allows to use internal atomic degrees of freedom to measure small time-dependent perturbations in the proper acceleration of an atomic probe, or in the relative alignment of a beam of atoms and a cavity. Further, the extent to which the Unruh spectrum of non-uniformly accelerated trajectories can be modulated and carry information is determined. Invoking the equivalence principle, one can argue that these results indicate that Hawking radiation could also be correspondingly strongly modulated and could, therefore, be carrying away significant amounts of information. Furthermore, showing how and to what extent the Unruh effect can be amplified is of interest in developing its experimental probes.

The last topic that is considered in this work concerns foundational issues associated with relativistic quantum information. Motivated by recent suggestions that gravity might remain classical, and by claims that Gaussian quantum mechanics is effectively a classical theory, the dynamics of a hybrid classical-quantum system is investigated. While many

explicit quantum effects can be represented classically, we demonstrate that quantum aspects of the system cannot be fully masked. These results could have implications for the no-cloning theorem, quantum teleportation, and the Einstein-Podolski-Rosen (EPR) thought experiment. Also they could be of importance in the ongoing discussion as to whether or not gravity should be quantized.

Acknowledgements

It is my pleasure to acknowledge the roles of several individuals who were by my side during my doctorate.

First and foremost I would like to express my gratitude to Robert Mann, my Ph.D. supervisor, who gave me the opportunity to work in a research environment that stimulates original thinking and initiative. He has been a compassionate leader who has given me the freedom to choose my path in physics, to follow my interests, to make mistakes and to learn from them. His generosity, honesty and patience have given me numerous opportunities to freely discuss my problems and to benefit from his insightful mind. It is rare for a supervisor to go out of his way to make the seemingly impossible become possible. I will always be grateful for his complete, unconditional support during my Ph.D.

I would like to extend my deepest gratitude to Achim Kempf whom I have always admired for his intellectual brilliance and empathy. As my mentor, collaborator, and friend during the last few years, our discussions have inspired me and fueled my motivation and excitement for doing research. My trust in his outstanding mentorship and his unique way of thinking has always made my decisions easier. I have been fortunate to have his unwavering support and attention during the last years of my Ph.D. and I will always look up to him.

I would also like to thank Daniel Terno, my Ph.D. co-supervisor. During my time collaborating with him in Australia, he provided a unique perspective on approaching the many challenges I faced, and helped me to experience a different style of working and research! I greatly appreciate his most helpful commentary and advice.

I would like to extend my thanks to those friends and colleagues who made my life more joyful in Waterloo since my arrival in 2012. In a research environment where some individuals may hide their insecurities and lack of confidence under a mask of competition and intimidation, it is always heartening to find sincere, dedicated and peaceful people like Eduardo Martín-Martínez, Eric Brown, Wilson Brenna, Paul MacGrath, and Robert Jonsson. These are among the smartest, most confident and humble young researchers whose friendship I sincerely cherish. As future leaders in their fields, they will be among those who keep the culture of research in academia rich and who can keep academia a healthy, joyful and encouraging place for beautiful minds to fulfill their potentials.

My heart-felt regard goes to a very special person, my husband, Roman Shapiro who never stopped believing in me. When the challenges and inherent instability of academic life have caused me to doubt myself, his continued and unconditional love, support and understanding have been a constant source of stability.

Last but not least, I would like to thank my parents and my brother who have been my full supporters in all my ups and downs. This work could not have happened without the emotional support they gave me when I needed it most.

Dedication

For the ancestors who paved the path before me upon whose shoulders I stand.

Table of Contents

List of Figures

Chapter 1

Introduction

1.1 Motivation and Context

The main body of work presented in this thesis is investigating the fundamental features of the interaction between radiation and matter in different physical settings of quantum field theory in curved spacetimes using Unruh-DeWitt (UDW) particle detectors [5]. The motivation of this work is twofold. First, by exploring the Unruh effect and its relation to Hawking radiation using particle detectors we can obtain hints towards a new approach to the black hole information loss problem, which has defied explanation for decades [6, 7]. Second and on the more practical side, we are concerned with confronting the theoretical and experimental aspects of physics. To this end, we will compare responses of particle detectors with both uniform and nonuniform accelerations in Minkowski spacetime. One of the main topics we investigate is the possibility of amplifying the Unruh effect and therefore bringing it closer to observability with the current technology. So far, the Unruh effect and most studies of the relationship between acceleration and entanglement are for idealized cases when the detector is turned on forever while uniformly accelerating. However, to offer reasonable prospects for testing fundamental physical phenomena such as the Unruh effect in the lab, it is essential to study non-idealized cases of nonuniform acceleration. This could also be of special importance as the entanglement present in quantum states depends on the observer trajectory [8–10]. It was recently shown for the localized fermionic Gaussian states that how increasing the uniform acceleration affects the vacuum entanglement and entanglement of Bell states differently [11]. Similar studies can be done to investigate the effect of nonuniform accelerations on such states.

The primary underlying framework of this thesis is Quantum Field Theory (QFT) –

a discipline in the overlap of quantum theory, general relativity and field theory, which holds a central position in our description of Nature. Originally, QFT emerged from the inability of relativistic quantum theory to fully explain the particle interactions, including annihilation and creation processes. The problem was that the deterministic behavior of the wave function described by the Schrödinger equation in quantum theory did not have any probabilistic dynamics. By fixing the initial conditions, the wave function is just a classical field with a precise evolution through the Schrödinger equation (or Klein-Gordon and Dirac equations) without any uncertainty. But in quantum theory we expect all quantities including the wave function to be subject to uncertainty, and that historically, brought researchers to the idea of second quantization, where one applies quantum theory to the wave function itself. In modern QFT, it is not exactly wave functions but general quantum fields that are subject to quantum fluctuations, leading to loss of conservation of particle number.

QFT is resulting from the application of the principles of quantum theory to the classical systems of fields. It has provided a very successful theoretical framework for studying elementary particles and their interactions for the last 70 years. QFT has succeed in predicting the outcomes of high energy particle experiments such as the existence of the Higgs boson [12], asymptotic freedom [13], and the anomalous magnetic moment of the electron [14]. The methods of quantum field theory have also been used in condensed matter physics for studying complex quantum phenomena in solids, a critical requirement for understanding, for example, superconductivity and superfluidity.

The validity of both QFT and Einstein's general theory of relativity have been confirmed via highly accurate experiments, the latest being those at LHC and from LIGO, respectively. These theories seem to be the best available candidates to form the basis for the underlying unified theory of nature. However, after more than forty years of rigorous attempts to quantize the gravitational field [15, 16], a complete quantum theory of gravity is still lacking. In the absence of such a theory, we can still consider a semiclassical approximation in which the gravitational field is considered as a classical background that interacts with quantized matter fields. This approach leads to the topic of QFT in a curved spacetime, which has been studied in detail for several decades [17–19]. Treating gravitation classically, we can describe the spacetime structure with a manifold, M, and a metric $g_{\mu\nu}$ on which the propagating matter fields are treated as quantum fields. As long as we stay with energies well below the Planck scale, one can expect to at least be able to construct a satisfactory theory for linear fields in a curved background. This leads to interesting predictions such as the Unruh effect [20], particle creation in an expanding universe, and Hawking radiation, which is particle radiation from a black hole with a radius much larger than the Planck length.

Exploring quantum field theory in curved spacetimes, one finds that there is no global notion of 'particle'. This is quite unlike in a flat background where the Poincaré symmetry can be used to pick out a preferred vacuum state, yielding in turn a preferred definition of particles. However, even in this setting the notion of particle is an observer-dependent concept. It has been shown [20] that when a uniformly accelerating detector is interacting with a quantum field along its worldline, it observes particles in the vacuum state of its inertial counterpart. The accelerating observer would describe itself as being in a thermal bath with a temperature proportional to its acceleration. This phenomenon is known as the Unruh effect. The accelerating observer in this example is a particle detector, which is modeled as a two level quantum system, known as an Unruh-DeWitt detector [17, 20]. These particle detectors have been proven to be effective tools in studying new phenomena that arise when the basic concepts of quantum information get revised in relativistic settings. A number of their applications are demonstrated in [21].

These particle detectors play a crucial role in the research field of Relativistic Quantum Information (RQI) where the foundation of the work presented in this thesis lies. One can interpret RQI as a new bridge between relativistic quantum field theory and information theory where information-theoretic approaches and notions from quantum information can be applied to questions in quantum field theory in curved spacetimes. These simple models of quantum systems provide us with operational insight into various active topics of research today, such as the black hole information paradox, the entropy of black holes, the vacuum entanglement of quantum fields, and black hole thermodynamics.

In quantum-informatic studies, UDW detectors are used to find the detector-field correlation functions of interest in the fidelity of quantum teleportation between two accelerating observers [9], energy teleportation between two particle detectors which are locally interacting with the field [22, 23], and measuring the entanglement between localized systems which is shown to be an observer-dependent property. Recently it has been shown that entanglement can even be harvested from the vacuum of a quantum field. For example, two uncorrelated quantum systems (such as two Hydrogen atoms [24]) that are timelike or spacelike separated can become entangled just by interacting locally with the quantum field around them, even if the field is in the vacuum state (in other words the field is 'empty', containing no photons in the case of the electromagnetic field) [25–28]. This is due to quantum correlations in the fluctuations of fields such as the electromagnetic field. This phenomenon of entanglement harvesting illustrates once more how the laws of (quantum) physics dictate what can be done with information, even beyond the limits of what classical intuition would indicate. The extracted entanglement can also be a tool to distinguish spacetimes with different geometries [29–33].

One of the main motivations for exploring ideas such as quantum correlations and quan-

tum entanglement rests in both their theoretical and practical implications. For example, knowledge about quantum correlations and effects produced by the gravitational interactions can set a basis for experimental proposals aimed at finding signatures of quantum gravity effects that cannot be observed directly. This could be a step towards uncovering the fundamental principles of quantum gravity. On a more practical side, by gaining new insights one can propose using relativistic quantum fields as a resource for quantum technological tasks such as information processing and metrology. In general, the real-world implementation and application of the RQI tool box includes phenomena such as teleportation, superdense coding, and the study of quantum channels, to fully relativistic quantum field theory in flat and curved background spacetimes.

Unruh-DeWitt detectors are also useful in probing both the Unruh effect and Hawking radiation from black holes [6], two of the most well-known and well-studied phenomena in the field of QFT in curved spacetimes. The Unruh effect is one of the more conceptually striking phenomena in QFT since it provides evidence that the notion of particle is observer dependent. The discovery of this effect, which was initiated by discoveries of Fulling and Davies [34, 35], was first derived using time-dependent perturbation theory [20]. The generalized version of this phenomenon in the presence of curved backgrounds and for finite detector-field interaction time have been worked out in [36, 37].

In the vicinity of a radiating black hole, distinguishing between the Unruh and Hawking effects is not quite clear for different observers. However, there have been proposals to separate these two effects for a detector that is freely falling into a black hole [38, 39]. The contributions of Unruh and Hawking temperatures to the total effective temperature can be consistently separated by considering an asymptotic region. For such consistency we need the Unruh effect to be associated with the acceleration of an observer with respect to the asymptotic reference frame and not to the local free-fall one. This interpretation is the same as the standard one if one is calculating the observations of an observer in a specific vacuum state. However if one would like to consider the backreaction of the field on the trajectory of the observer, then the two interpretations do not have the same results [38].

Furthermore, comparing these two effects is a good example of a means for exploring the validity of the equivalence principle in the quantum regime, which has also been a topic of recent discussion [40, 41]. The equivalence principle forms the basis of general relativity, where it states that locally, a uniformly accelerating reference frame cannot be distinguished from a gravitational field. By the term 'locally' is meant the small region of spacetime where the tidal forces of the gravitational field are negligible. For such a comparison, one needs to choose a proper vacuum for each observer in different spacetimes since detection of radiation depends on both the spacetime and the type of vacuum. According to the paper [40], for an equivalent acceleration, a detector at rest in the Schwarzschild

spacetime with respect to Unruh vacuum registers a higher thermal radiation compared to an accelerating detector in the Rindler spacetime with respect to Minkowski vacuum, therefore it is possible to distinguish the two cases. The equivalence principle is restored as one approaches the horizon and the temperatures approach the same limit.

RQI is also concerned about foundational questions. There is perhaps nowhere in physics where this is more pertinent than in the relationship between classical and quantum systems. The as yet unrealized goal of obtaining a quantum theory of gravity has only served to further highlight the importance of understanding the classical/quantum boundary. Indeed, the need to quantize gravity is receiving increased attention. Here we take a small but important step in this direction by examining the consequences of coupling a classical system (as some postulate gravity may be) with a quantum system (which all other forces certainly are). We use harmonic oscillators for both, and examine the consequences of coupling the two together in a quantum/classical hybrid system.

The methods and results that are presented in the next chapters not only enlighten the fundamental features of the light-atom interaction in various physical settings of QFT in curved backgrounds, but also open a number of avenues with high potentials for future research.

1.2 Thesis outline

We will start in Ch.2 with a brief introduction to the basics of scalar quantum field theory and its quantization in both Minkowski and curved backgrounds to the extent that is important for the content of our work. We will continue with a review of Bogolyubov transformations and their importance in our work.

In Ch.3, we will introduce Unruh-DeWitt particle detectors and their interaction with the field in the cavity. We explore the Unruh effect in the framework of the cavity where the study is based on a perturbative approach to solve for the detector-field evolution. We also review the Hawking effect and its connection with the Unruh effect.

In Ch.4, we will introduce a method for determining what a particle detector would observe in general curved spacetimes within a specific range of curvature. Here we compare the transition probability of a particle detector traveling through a cavity in Minkowski and Schwarzschild backgrounds and show in which way and at what scales the equivalence principle is recovered.

In Ch.5, we will show that relativistic signatures of the transition probability of atoms moving through optical cavities are sensitive to perturbations in the kinematical param-

eters of their trajectories. We propose to use this sensitivity in metrology, both in the accelerometer and the alignment settings.

In Ch.6, we ask to what extent the Hawking spectrum can be modulated by a black hole's growth, and therefore to what extent such modulated Hawking radiation can carry away information about the infalling matter. Via the equivalence principle, this motivated us to determine the extent to which the Unruh spectrum of non-uniformly accelerated trajectories can be modulated. Depending on the extent to which the Unruh radiation is modulated, it can carry information about these trajectories. In this chapter we show that how what we call generalized concomitant frequencies are underlying the calculation of β coefficients of Bogolyubov transformations.

In Ch.7, we explore the difference between the behavior of a classical harmonic oscillator and that of a quantum harmonic oscillator which is in a Gaussian state. We seek to understand just how classical a quantum harmonic oscillator in a Gaussian state can be. This is an interesting question to study because Gaussian quantum mechanics (GQM) is a computational tool that can simplify intensive quantum mechanical calculations. Furthermore, it has been shown that Gaussian operations alone do not allow one to do universal quantum computing.

In Ch.8 we will conclude this thesis with the summary of our work and the outlook of future research.

Chapter 2

Quantum Field Theory

QFT is mainly a larger framework of quantum theory which is formed by applying the second quantization to the quantum mechanical wave functions. Therefore, amplitudes of the wave functions will be operators which are subject to the Heisenberg uncertainty relations. Quantum fluctuations of the wave function give us the annihilation and creation operators that obey the canonical commutation relations. After quantizing the field, one can try to find the eigenvalues and eigenstates of the Hamiltonian. That being said, when we are studying the relativistic dynamics of the field, the Lagrangian formulation of the field theory is more suitable because all expressions are Lorentz invariant. As long as one works with quantum field theory in a fixed background, renormalization procedure helps to resolve the infinities. However if one take into account the dynamics of general relativity, renormalization is not a effective procedure anymore. This could be another indication for the existence of a finite shortest length, ϵ, in the nature which could be the Planck scale. There are number of valuable resources on this topic including [42–44].

In this chapter, I will start with a brief review of the simplest case of quantum field theory (QFT), namely, scalar Klein-Gordon field and its quantization. I will also review the physics of QFT in curved spacetimes [17, 18] which I will refer to in the course of this thesis. I will also review the field theory in the cavity which is the main foundation of this thesis. The metric signature adopted in this work is $(+---)$, and natural units ($\hbar = c = k_B = 1$) are used unless otherwise specified.

2.1 Scalar quantum field theory

In field theory we are studying dynamics of fields which form a system with infinite degrees of freedom. A field is defined at every point of spacetime as

$$\phi(\mathbf{x}, t), \tag{2.1}$$

and its dynamics is governed by a Lagrangian which for a real scalar field is given by

$$\mathcal{L} = \frac{1}{2}\eta^{\mu\nu}\partial_\mu\partial_\nu\phi - \frac{1}{2}m^2\phi^2 \tag{2.2}$$

where $\eta^{\mu\nu} = \text{diag}(+1 - 1 - 1 - 1)$ is a Minkowski metric. The relativistic form of the Euler-Lagrange equation which is the Klein-Gordon (KG) equation is then given by

$$\Box\phi + m^2\phi = 0, \tag{2.3}$$

where $\Box = \partial_\mu\partial^\mu$ is the Laplacian in Minkowski space. There are two ways to link the Lagrangian formalism and the quantum theory. It is either by using the path integral methods or the canonical quantization which we describe here. For the latter approach we start with the Hamiltonian formalism of the field theory with the free Hamiltonian of the form

$$H = \int d^3\mathbf{x}\big(\pi(\mathbf{x}, t)\dot{\phi}(\mathbf{x}, t) - \mathcal{L}\big), \tag{2.4}$$

where $\pi(\mathbf{x}, t)$ is the momentum conjugate of the field $\phi(\mathbf{x}, t)$ computed as the functional derivatives

$$\begin{aligned} \pi(\mathbf{x}, t) &\equiv \frac{\delta L[\phi]}{\delta\dot{\phi}(\mathbf{x}, t)} = \dot{\phi}(\mathbf{x}, t), \\ L[\phi] &= \int \mathcal{L}d^3\mathbf{x}. \end{aligned} \tag{2.5}$$

2.2 Quantization of a scalar field

To quantize the field theory we follow a similar procedure to quantum mechanics where we use canonical quantization to upgrade the generalized position and momentum coordinates to operators. To have the quantum field theory using the second quantization, we promote

the field and its momentum conjugate to be operator valued functions obeying the canonical commutation relations at a given time t

$$\begin{aligned} [\hat{\phi}(\mathbf{x},t),\hat{\phi}(\mathbf{y},t)] &= 0, \\ [\hat{\pi}(\mathbf{x},t),\hat{\pi}(\mathbf{y},t)] &= 0, \\ [\hat{\phi}(\mathbf{x},t),\hat{\pi}(\mathbf{y},t)] &= \mathrm{i}\delta^3(\mathbf{x}-\mathbf{y}) \end{aligned} \tag{2.6}$$

Here we are working in the Heisenberg picture where the field operators are time dependent and they obey the Klein-Gordon equation,

$$\dot{\hat{\pi}}(\mathbf{x},t) = (\Delta - m^2)\hat{\phi}(\mathbf{x},t), \tag{2.7}$$

which is analogous to $\dot{\hat{p}}(t) = -k\hat{q}(t)$, namely, the equation of motion for a quantized Harmonic oscillator; however $(\Delta - m^2)$ is not a number like k. By taking a Fourier Transform of the field we can resolve this problem and replace the field ϕ with a collection of decoupled oscillators $\phi_{\mathbf{k}}(t)$ which are moving in the configuration space. The Fourier decomposition is given by

$$\hat{\phi}_{\mathbf{k}}(t) = \frac{1}{\sqrt{(2\pi)^{3/2}}}\int_{\mathbb{R}^3} d^3\mathbf{x}\mathrm{e}^{-\mathrm{i}\mathbf{k}\cdot\mathbf{x}}\hat{\phi}(\mathbf{x},t). \tag{2.8}$$

Each complex function $\phi_{\mathbf{k}}(t)$ is a k-mode of the field and satisfies the equation of motion for a quantum harmonic oscillator of frequency,

$$\omega_{\mathbf{k}} \equiv \sqrt{|\mathbf{k}|^2 + m^2}. \tag{2.9}$$

We can write these Hermitian field operators in terms of orthonormal field modes $\{u_k\}$ which are the plane wave solutions to the KG equation,

$$\hat{\phi}(\mathbf{x},t) = \int d\mathbf{k}\Big(u_{\mathbf{k}}(\mathbf{x},t)\hat{a}_{\mathbf{k}} + u^*_{\mathbf{k}}(\mathbf{x},t)\hat{a}^\dagger_{\mathbf{k}}\Big). \tag{2.10}$$

The solutions $\{u_k\}$ form a complete set of orthonormal basis with respect to the Klein-Gordon inner product evaluated at a fixed time,

$$(f,g) = \mathrm{i}\int dx(f^*\dot{g} - \dot{f}^*g). \tag{2.11}$$

As this product is preserved under KG evolution, we demand

$$\begin{aligned} (u_k, u_{k'}) &= \delta(k-k'), \\ (u^*_k, u^*_{k'}) &= -\delta(k-k'), \\ (u_k, u^*_{k'}) &= 0. \end{aligned} \tag{2.12}$$

Also $\{\hat{a}_k, \hat{a}_k^\dagger\}$ are annihilation and creation operators of a Fock basis which are respecting the canonical commutation relations equivalent to the field operators in Eq.(2.6),

$$\begin{aligned} [\hat{a}_{\mathbf{k}}, \hat{a}_{\mathbf{k}'}] &= 0, \\ [\hat{a}_{\mathbf{k}}^\dagger, \hat{a}_{\mathbf{k}'}^\dagger] &= 0, \\ [\hat{a}_{\mathbf{k}}, \hat{a}_{\mathbf{k}'}^\dagger] &= (2\pi)^3 \delta^3(\mathbf{k}-\mathbf{k}'). \end{aligned} \tag{2.13}$$

One way of checking this equivalency is by assuming to have $[\hat{a}_{\mathbf{k}}, \hat{a}_{\mathbf{k}'}^\dagger]$ and show

$$\begin{aligned} [\hat{\phi}(\mathbf{x},t), \hat{\pi}(\mathbf{y},t)] =& \int d\mathbf{k} d\mathbf{k}' \frac{-\mathrm{i}}{2(2\pi)^6} \sqrt{\frac{\omega_{\mathbf{k}'}}{\omega_{\mathbf{k}}}} \Big(- [\hat{a}_{\mathbf{k}}, \hat{a}_{\mathbf{k}'}^\dagger] \mathrm{e}^{\mathrm{i}(\mathbf{k}\cdot\mathbf{x} - \mathbf{k}'\cdot\mathbf{y})} + [\hat{a}_{\mathbf{k}}^\dagger, \hat{a}_{\mathbf{k}'}] \mathrm{e}^{\mathrm{i}(-\mathbf{k}\cdot\mathbf{x} + \mathbf{k}'\cdot\mathbf{y})} \Big) \\ =& \int d\mathbf{k} \frac{\mathrm{i}}{2(2\pi)^3} \Big(\mathrm{e}^{\mathrm{i}\mathbf{k}\cdot(\mathbf{x}-\mathbf{y})} + \mathrm{e}^{\mathrm{i}\mathbf{k}\cdot(\mathbf{y}-\mathbf{x})} \Big) \\ =& \ \mathrm{i}\delta^3(\mathbf{x}-\mathbf{y}). \end{aligned} \tag{2.14}$$

Based on the choice of mode basis that we have, the vacuum and excited states are respectively defined as

$$\hat{a}_{\mathbf{k}} |0\rangle = 0, \qquad \hat{a}_{\mathbf{k}}^\dagger |0\rangle = |1_{\mathbf{k}}\rangle . \tag{2.15}$$

In general, a state containing n particles is defined as

$$\left| n_{\mathbf{k_1}}^{(1)}, n_{\mathbf{k_2}}^{(2)}, ... \right\rangle = \frac{1}{\sqrt{n^{(1)}! n^{(2)}! ...}} \left(\hat{a}_{\mathbf{k_1}}^\dagger\right)^{n^{(1)}} \left(\hat{a}_{\mathbf{k_2}}^\dagger\right)^{n^{(2)}} ... |0\rangle , \tag{2.16}$$

where it represents $n^{(1)}$ in mode $\mathbf{k_1}$ and so on.

2.3 Infrared regularization: Field in the cavity

Now if we write the Hamiltonian in terms of creation and annihilation operators, we get

$$H = \int d\mathbf{k} \frac{1}{(2\pi)^3} \omega_{\mathbf{k}} \left[\hat{a}_{\mathbf{k}}^\dagger \hat{a}_{\mathbf{k}} + \frac{1}{2} (2\pi)^3 \delta^3(0) \right]. \tag{2.17}$$

According to our definition of the ground state, by applying this Hamiltonian to the ground state, $|0\rangle$, we find the energy eigenvalue to be infinity. This is the infinity that is referred to as an infra-red divergence and it arises because of the infinite size of space. We can resolve it by imposing a boundary condition in the field and study the field theory in a

cavity of volume $V = L^3$. Of course there is still an ultraviolet divergence due to an infinite number of field modes that can be dealt with by imposing a cutoff on the number of modes. Here L should be large enough so we do not have significant artificial effects because of the boundary conditions. Depending on the boundary conditions being Periodic, Dirichlet, or Neumann, the mode functions inside the cavity take different forms. In the case of a $(1+1)$-D Dirichlet cavity with boundary conditions, $\hat{\phi}(L,t), \hat{\phi}(0,t) = 0$, which is what we are considering in this thesis, the mode functions are the stationary waves

$$u_n(x,t) = \frac{1}{\sqrt{L\omega_n}} \mathrm{e}^{-\mathrm{i}\omega_n t} \sin(k_n x). \tag{2.18}$$

This boundary condition implies that the field operators are vanishing on the boundary which can be achieved by replacing the walls of the cavity with ideal mirrors. In this equation we have $k_n = n\pi/L$, n being natural positive number and ω_n is a field mode-k frequency given by Eq.(2.9). With this boundary condition, the field operator is given in terms of the field modes as

$$\hat{\phi}(x,t) = \sum_n \Big(u_n(x,t)\hat{a}_n + u_n^*(x,t)\hat{a}_n^\dagger \Big). \tag{2.19}$$

Similar to the case of the field in the continuum space in the absence of any boundary conditions, field operators satisfy the canonical commutation relation and we can show that the creation and annihilation operators satisfy the commutation relations,

$$[\hat{a}_n, \hat{a}_{n'}] = 0, \qquad [\hat{a}_n^\dagger, \hat{a}_{n'}^\dagger] = 0, \qquad [\hat{a}_n, \hat{a}_{n'}^\dagger] = \delta_{nn'}. \tag{2.20}$$

2.4 Bogolyubov transformation

So far we showed that the quantization of the field operator with respect to a set of orthonormal mode basis $\{u_k, u_k^*\}$. However this is not a unique choice and we can expand the field modes in terms of any orthonormal mode basis in the vector space. We can transform the mode functions that we found as solutions of the KG equation in one basis $\{u_k\}$ to any other basis $\{v_l\}$ using linear transformation which is called Bogolyubov transformation. In continuum spacetime this unitary transformation is given by

$$v_l = \int dk \big(\alpha_{lk} u_k + \beta_{lk} u_k^* \big) \tag{2.21}$$

where the coefficients are

$$\alpha_{lk} = (v_l, u_k), \qquad \beta_{lk} = -(v_l, u_k^*). \tag{2.22}$$

These coefficients are time independent because of the time independence of the Klein-Gordon inner product which is given in Eq.(2.11) with respect to Klein-Gordon evolution. We use this transformation of mode basis for example to bring all the observers to the same spacetime coordinates without modifying them. The field operator can be expanded equivalently in both basis as

$$\hat{\phi} = \int dk (u_k \hat{a}_k + u_k^* \hat{a}_k^\dagger) = \int dl (v_l \hat{b}_l + v_l^* \hat{b}_l^\dagger), \tag{2.23}$$

where $\{\hat{b_l}, {b_l}^\dagger\}$ are the creation and annihilation operators corresponding to the new basis $\{v_l, v_l^*\}$. The vacuum state that is defined in terms of one set of mode basis may not correspond to a vacuum state after the mode basis is evolved under a time-dependent Hamiltonian. Therefore, to study the particle content of a field state, we consider the Bogolyubov transformation. The linear transformation between the old and new operators is given by

$$\begin{aligned} \hat{b}_l &= \int dk (\alpha_{lk}^* \hat{a}_k - \beta_{lk}^* \hat{a}_k^\dagger), \\ \hat{a}_k &= \int dl (\alpha_{lk} \hat{b}_l + \beta_{lk}^* \hat{b}_l^\dagger). \end{aligned} \tag{2.24}$$

As we can see, only when the β coefficient is zero, $\hat{b}_l$ and $\hat{a}_k$ share the same vacuum state, $|0\rangle$. On the other hand, the nonzero β coefficient can provide us with information on the particle content of the vacuum state of the field in different basis. The average b-particle number is given by

$$\langle 0 | \hat{N}_l^{(b)} | 0 \rangle = \int dk \, |\beta_{lk}|^2, \tag{2.25}$$

where $\hat{N}_l^{(b)} = \hat{b}_l^\dagger \hat{b}_l$ is the b-particle number operator for a specific mode l. By calculating the expectation value of this number operator we can find the number of b-particles of mode v_l in the vacuum state of $\hat{a}_k$ operator.

$$\left\langle {}_{(a)}0 \right| \hat{N}_l^{(b)} \left| 0_{(a)} \right\rangle = |\beta_k|^2 \, \delta^3(0). \tag{2.26}$$

To resolve the divergent factor $\delta^3(0)$ which arises because of the infinite spatial volume, we replace it with a box of volume V and we find the mean density of particles to be $n_k = |\beta_k|^2$.

Similarly, when we have a confined field in a box where we have a discrete modes, we can perform a Bogolyubov transformation between the stationary and non-stationary

mode functions v_m as

$$\begin{aligned} v_m &= \sum_n \Big(\alpha_{mn} u_n + \beta_{mn} u_n^*\Big), \\ u_n &= \sum_m \Big(\alpha_{mn}^* v_m - \beta_{mn} v_m^*\Big). \end{aligned} \tag{2.27}$$

Chapter 3

Unruh-DeWitt particle detectors

In the last chapter we talked about how different observers in different coordinate systems may parametrize their spacetime differently and even expand the field operators in terms of different sets of modes and therefore perceive the particle content of the same quantum state differently. But how does an observer measure the perceived number of particles in a quantum state? To model the response of an accelerated probe measuring the quantum field, it is commonplace to use the so-called Unruh-DeWitt detector (UDW) [5, 17] which is an idealized model of a real particle detector that still encompasses all the fundamental features of the light-matter interaction when there is no angular momentum exchange involved [45]. This model consists of a two level quantum system such as a qubit with a energy gap Ω that couples to a scalar field via an interaction Hamiltonian along its worldline, $\hat{\phi}(x(\tau), t(\tau))$.

The Hamiltonian describing the whole system consists of three terms: $\hat{H}^{(\mathrm{d})}_{\mathrm{free}}$, the free Hamiltonian of the detector, $\hat{H}^{(\mathrm{f})}_{\mathrm{free}}$, the free Hamiltonian of the field, and the field-detector interaction Hamiltonian $\hat{H}_{\mathrm{int}}$ given we are working in the interaction picture:

$$\hat{H} = \hat{H}^{(\mathrm{d})}_{\mathrm{free}} + \hat{H}^{(\mathrm{f})}_{\mathrm{free}} + \hat{H}_{\mathrm{int}}. \tag{3.1}$$

The general form of the interaction Hamiltonian [5, 37] is given by

$$\hat{H}_{\mathrm{int}} = \lambda \chi(\tau) \hat{\mu}(\tau) \hat{\phi}\big(x(\tau)\big), \tag{3.2}$$

where the constant λ is the coupling strength, $\chi(\tau)$ is the *switching function* or *time window function* which is smooth and compactly supported function and it controls the well-defined behaviour of the interaction model to avoid the divergences [46–48]. This

function is a real-valued function ranging between 0 and 1. $\hat{\mu}(\tau)$ is the monopole moment of the detector and $\hat{\phi}\big(x(\tau)\big)$ is the massless scalar field in (1+1)-dimension to which the detector is coupling. We consider the coupling constant to be a small parameter so we can work with perturbation theory to second order in λ. The monopole moment operator of the detector has the usual form in the interaction picture,

$$\hat{\mu}(\tau) = (\sigma^{+}e^{i\Omega\tau} + \sigma^{-}e^{-i\Omega\tau}), \tag{3.3}$$

in which, Ω is the proper energy gap between the ground state, $|g\rangle$ and the excited state, $|e\rangle$ of the detector and σ^{-} and σ^{+} are Ladder operators.

3.1 Perturbative time evolution

The unitary time evolution operator generated by the interaction Hamiltonian in the time interval $[0, T]$ is given by the Dyson's perturbative expansion

$$\begin{aligned}\hat{U}(T,0) = \mathbb{I} \underbrace{-i\int_0^T d\tau \hat{H}_{\text{int}}(\tau)}_{\hat{U}^{(1)}} \\ \underbrace{+(-i)^2\int_0^T d\tau \int_0^{\tau} d\tau' \hat{H}_{\text{int}}(\tau)\hat{H}_{\text{int}}(\tau')}_{\hat{U}^{(2)}} + ... \\ \underbrace{+(-i)^n\int_0^T d\tau ... \int_0^{\tau^{(n-1)}} d\tau^{(n)} \hat{H}_{\text{int}}(\tau)...\hat{H}_{\text{int}}(\tau^{(n)})}_{\hat{U}^{(n)}} .\end{aligned} \tag{3.4}$$

In this model, we assume that the detector which is in its ground state is weakly coupled to the vacuum state of the field so that the initial state of the quantum system is $\rho_0 = |g\rangle\langle g| \otimes |0\rangle\langle 0|$ and keep the terms in the expansion (3.4) up to the second order of perturbation in λ. The system's density matrix at a time T would be evaluated as [49]

$$\rho_T = \big[\mathbb{I} + \hat{U}^{(1)} + \hat{U}^{(2)} + \mathcal{O}(\lambda^3)\big]\rho_0\big[\mathbb{I} + \hat{U}^{(1)} + \hat{U}^{(2)} + \mathcal{O}(\lambda^3)\big]^{\dagger} \tag{3.5}$$

which we write as

$$\rho_T = \rho_0 + \rho_T^{(1)} + \rho_T^{(2)} + \mathcal{O}(\lambda^3), \tag{3.6}$$

where

$$\rho_T^{(0)} = \rho_0, \tag{3.7}$$
$$\rho_T^{(1)} = \hat{U}^{(1)}\rho_0 + \rho_0\hat{U}^{(1)\dagger}, \tag{3.8}$$
$$\rho_T^{(2)} = \hat{U}^{(1)}\rho_0\hat{U}^{(1)\dagger} + \hat{U}^{(2)}\rho_0 + \rho_0\hat{U}^{(2)\dagger}. \tag{3.9}$$

We are interested to study the reduced state of the detector after the evolution which can be obtained by tracing out the field from each order contribution to the density matrix.

$$\begin{aligned} \mathrm{Tr}_F\rho_0 &= |g\rangle\langle g|, \\ \mathrm{Tr}_F\rho_1 &= \mathrm{Tr}_F(\hat{U}^{(1)}\rho_0 + \rho_0\hat{U}^{(1)\dagger}), \\ \mathrm{Tr}_F\rho_2 &= \mathrm{Tr}_F\Big(\hat{U}^{(1)}\rho_0\hat{U}^{(1)\dagger} + \hat{U}^{(2)}\rho_0 + \rho_0\hat{U}^{(2)\dagger}\Big). \end{aligned} \tag{3.10}$$

where

$$\langle e|\,\mathrm{Tr}_F\Big(\hat{U}^{(1)}\rho_0\hat{U}^{(1)\dagger}\Big)\,|e\rangle = \lambda^2\int_0^T d\tau\int_0^T d\tau'\chi(\tau)\chi(\tau')\,\mathrm{exp}^{-\mathrm{i}\Omega(\tau-\tau')}\,\langle 0|\,\phi(\tau)\phi(\tau')\,|0\rangle. \tag{3.11}$$

The partial tracing of $\hat{U}^{(2)}\rho_0$ and $\rho_0\hat{U}^{(2)\dagger}$ contributes two terms proportional to $|g\rangle\langle g|$ to the detector's density matrix and all other terms vanish. The $|g\rangle\langle g|$ term is the negative of Eq.(3.11) and therefore normalizes the state. Therefore, the only contribution to the reduced density matrix of the detector comes from the zeroth and second order terms in the expansion. The two-point function $\langle 0|\,\phi(\tau)\phi(\tau')\,|0\rangle$, which is also called the Wightmann function, depends on the trajectory of the detector. As we will see in the next chapters, computing the Wightmann function is the main part of evaluating the response function of particle detectors. Wightmann functions are the correlation functions of quantum fields which encode the relation between field operators in two different points of the field which are either timelike or spacelike separated. The properties of these functions are detailed in [17, 43]. For the theory to stay causal, commutators of the field are vanishing outside the lightcone. This is the property of both free and interacting theories.

We can write the Wightmann function in (3+1)-D Minkowski spacetime for a massless scalar field, in terms of the field modes $u_{\mathbf{k}}$ as

$$\langle 0|\,\phi\big(t(\tau),\mathbf{x}(\tau)\big)\phi\big(t(\tau'),\mathbf{x}(\tau')\big)\,|0\rangle = \int d^3\mathbf{k}\frac{1}{\sqrt{(2\pi)^3 2\omega_k}}\mathrm{e}^{-\mathrm{i}(\omega_k\Delta t-\mathbf{k}\cdot\Delta\mathbf{x})}, \tag{3.12}$$

where $\Delta t = t(\tau) - t(\tau')$ and $\Delta\mathbf{x} = \mathbf{x}(\tau) - \mathbf{x}(\tau')$.

3.2 Unruh effect

One of the renowned predictions of Quantum field theory in curved spacetime is called the 'Unruh effect' [17, 20, 50–53]. It was suggested by Unruh that uniformly accelerated observers in Minkowski spacetime detect a thermal distribution of particles (with a temperature proportional to their proper acceleration) when probing the vacuum state for an inertial observer. It is indeed a challenge to detect this effect using present technology, as it involves measuring low temperatures with 'thermometric probes' that move with extremely high accelerations. This effect also is mathematically related to the near horizon Hawking effect [17, 54] as we will explain in more details in Ch.6.

There are two equivalent ways for calculating the Unruh effect, either by finding the transition probability of a detector which is moving with a constant acceleration trajectory or by using the Bogolyubov transformation to relate the Minkowski frame operators to the Rindler frame operators and calculate the proper Bogolyubov coefficients.

In the first approach, consider a uniformly accelerated UDW detector with proper time τ and a constant proper acceleration $a = |\eta_{\mu\nu} a^\mu a^\nu|^{1/2}$ where $\eta_{\mu\nu}$ is the Minkowski metric and a^μ is the observer 4-acceleration. The worldline of this observer is a hyperbola in the inertial coordinates (t, x) with parametrization,

$$\begin{aligned} t(\tau,\xi) &= \frac{1}{a}\mathrm{e}^{a\xi}\sinh(a\tau), \\ x(\tau,\xi) &= \frac{1}{a}\mathrm{e}^{a\xi}\cosh(a\tau). \end{aligned} \tag{3.13}$$

where (τ, ξ) are the proper coordinates of the observer. We consider $\xi = 0$ for which the observer has acceleration a and perceives a horizon at proper distance $1/a$. In general the proper coordinates vary in the intervals of $-\infty < \tau < +\infty$ and $-\infty < \xi < +\infty$.

The transition amplitude for the detector to get excited is given by [17]

$$\psi(\Delta E) = \frac{\mathrm{i}\lambda \langle E_n | \hat{\mu} | E_0 \rangle}{(2\pi)^{3/2}\sqrt{2\omega_k}} \int_{-\infty}^{+\infty} \chi(\tau)\mathrm{e}^{\mathrm{i}(E_n - E_0)\tau}\mathrm{e}^{\mathrm{i}\left(\omega_k t(\tau) - \mathbf{k}\cdot\mathbf{x}(\tau)\right)} d\tau \tag{3.14}$$

where $(E_n - E_0)$ is the energy gap between the zeroth and n-th state of the detector. For our studies, considering a two level atom as our detector, we only have $n = 1$. This nonzero excitation probability gives us the Unruh effect.

In the second approach, we calculate the β coefficients, using the Bogolyubov transformation between the vacuum state of the Minkowski frame and the vacuum state of

the accelerated frame of the detector (proper frame). Since the mode expansion and the transformation has simpler forms in the lightcone coordinates, we are going to derive the Bogolyubov transformation in this coordinates. The inertial Minkowski frame and the accelerated (Rindler) frame in the lightcone coordinates are respectively given by (u, v) and $(\bar{u}, \bar{v})$ where

$$\begin{aligned} u &\equiv t - x, \qquad v \equiv t + x, \\ \bar{u} &\equiv \tau - \xi, \qquad \bar{v} \equiv \tau + \xi, \\ u &= -\tfrac{1}{a} \mathrm{e}^{-a\bar{u}}. \end{aligned} \tag{3.15}$$

In the Rindler frame, the quantum field mode in the Rindler wedge $x > |t|$ can be expanded in terms of the left and right moving modes as

$$\hat{\phi}(\bar{u}, \bar{v}) = \int_0^{+\infty} \frac{d\omega}{\sqrt{4\pi\omega}} \left[\mathrm{e}^{-\mathrm{i}\omega\bar{u}} \hat{b}^-_\omega + \mathrm{e}^{\mathrm{i}\omega\bar{u}} \hat{b}^+_\omega + \mathrm{e}^{-\mathrm{i}\omega\bar{v}} \hat{b}^-_{-\omega} + \mathrm{e}^{\mathrm{i}\omega\bar{v}} \hat{b}^+_{-\omega} \right] \tag{3.16}$$

where $\omega = |k|$ is the integration variable. Equivalently, we can write the lightcone mode expansion in the Minkowski frame as

$$\hat{\phi}(u, v) = \int_0^{+\infty} \frac{d\omega'}{\sqrt{4\pi\omega'}} \left[\mathrm{e}^{-\mathrm{i}\omega' u} \hat{a}^-_{\omega'} + \mathrm{e}^{\mathrm{i}\omega' u} \hat{a}^+_{\omega'} + \mathrm{e}^{-\mathrm{i}\omega' v} \hat{a}^-_{-\omega'} + \mathrm{e}^{\mathrm{i}\omega' v} \hat{a}^+_{-\omega'} \right] \tag{3.17}$$

where ω and ω' have both positive values. The relation between the $\hat{a}^\pm_{\pm\omega'}$ and $\hat{b}^\pm_{\pm\omega}$ is the more general form of the Bogolyubov transformation that we considered in Ch.2. The relation between $\hat{a}^\pm_{\omega'}$ and $\hat{b}^-_\omega$ is

$$\hat{b}^-_\omega = \int_0^\infty d\omega' [\alpha_{\omega'\omega} \hat{a}^-_{\omega'} + \beta_{\omega'\omega} \hat{a}^+_{\omega'}] \tag{3.18}$$

Unlike Eq. (2.24), since $\omega \neq \omega'$, this relation mixes the operators with different momenta. The reason for the domain of integration being only from $(0, +\infty)$ is that only Bogolyubov coefficients that relate momenta of the same sign are nonzero, therefore the left-moving (negative momenta) and right-moving (positive momenta) field modes do not mix. Then we can calculate the coefficients $\alpha_{\omega\omega'}$ and $\beta_{\omega\omega'}$ to be

$$\alpha_{\omega'\omega} = \sqrt{\frac{\omega}{\omega'}} F(\omega', \omega), \qquad \beta_{\omega'\omega} = \sqrt{\frac{\omega}{\omega'}} F(-\omega', \omega), \tag{3.19}$$

where $\omega,\ \omega' > 0$ and

$$F(\pm\omega', \omega) \equiv \int_{-\infty}^{\infty} \frac{d\bar{u}}{2\pi} \mathrm{e}^{\mathrm{i}(\mp\omega' u + \omega\bar{u})} = \int_{-\infty}^{0} \frac{du}{2\pi} \mathrm{e}^{\mp\mathrm{i}\omega' u} (-au)^{-\mathrm{i}\frac{\omega}{a} - 1}. \tag{3.20}$$

Given that, we find the mean density of particles with the frequency mode ω to be

$$n_\omega = \left\langle \hat{N}_\omega \right\rangle = \int_0^{+\infty} d\omega \, |\beta_{\omega'\omega}|^2 = \frac{1}{\mathrm{e}^{2\pi\omega/a} - 1}. \tag{3.21}$$

This is also equivalent to the Bose-Einstein distribution

$$n(E) = \frac{1}{\mathrm{e}^{E/T} - 1} \tag{3.22}$$

since for a massless particle $E = |\omega|$, therefore $T \equiv a/2\pi$ is the Unruh temperature. This approach also could help to clarify the mathematical analogy between the Unruh and Hawking effects. Eq.(3.21) can also be derived from Eq.(3.14) if we use the trajectory of a uniformly accelerated detector given by Eq.(3.13) for $\big(x(\tau), t(\tau)\big)$. This is derived in details in [17]. Using this parametrization, from Eq.(3.14) we can derive the transition probability per unit time to be

$$|\psi|^2 \propto \frac{\lambda^2}{2\pi} \sum_n \frac{\Delta E_n \, |\langle E_n| \, \mu_0 \, |E_0\rangle|^2}{\mathrm{e}^{2\pi\Delta E_n/a} - 1}. \tag{3.23}$$

The Plank factor that appeared here in the response of the accelerated particle detector interacting with the field is equivalent to Eq.(3.21) which describes an unaccelerated detector immersed in a thermal bath at the temparature T.

3.3 Hawking effect

Quantum theory predicts that vacuum fluctuations of quantum fields around the black holes create particles that are moving away from the horizon in the form of Hawking radiation. However, there is a limit as to how far the tunnelling picture can be extended because in the pair-creation of very low energy particles, the wavelength of particles would be much larger than the size of the black hole R, therefore they avoid falling through the event horizon [55]. Independent of how this radiation forms, we can compute the density of the emitted particles from a black hole registered by observers outside the horizon at different distances from it.

To study this effect and its comparison to the Unruh effect, we consider the simplest case of a non-rotating uncharged black hole which its stationary state is represented by the Schwarzschild solution to the Einstein equation,

$$ds^2 = g_{\mu\nu} dx^\mu dx^\nu = \left(1 - \frac{2M}{r}\right) dt^2 - \left(1 - \frac{2M}{r}\right)^{-1} dr^2 - r^2(d\theta^2 + d\phi^2 \sin^2\theta), \tag{3.24}$$

with the physical singularity at $r = 0$ and the singularity at $r = 2M$. We can resolve the coordinate singularity by a suitable change of coordinates in which the metric becomes regular at the BH horizon. To simplify the calculations, we consider a $(1+1)$-dimensional toy model where the quantum field ϕ is independent of the angular variables (θ, φ). In this toy model, we use the tortoise coordinates (t, r^*) to express the metric in a conformally flat form,

$$ds^2 = \left(1 - \frac{2M}{r}\right)(dt^2 - dr^{*2}), \tag{3.25}$$

where

$$r^*(r) = r - 2M + 2M \ln\left(\frac{r}{2M} - 1\right). \tag{3.26}$$

r^* ranges from $-\infty$ to $+\infty$. If we describe the tortoise frame in the lightcone coordinates using the relations $\bar{u} \equiv t - r^*$ and $\bar{v} \equiv t + r^*$, the metric will be

$$ds^2 = \left(1 - \frac{2M}{r}\right) d\bar{u}\, d\bar{v}. \tag{3.27}$$

This coordinates describes a locally accelerated observer. This metric is conformally flat everywhere and it asymptotes to the Minkowski metric as $r \to \infty$. However, it only covers the spacetime outside the horizon $r > 2M$, therefore we need another coordinate system to describe the entire spacetime, namely the Kruskal lightcone coordinates, (u, v). This frame which describes a locally inertial observer (free falling observer) relates to the tortoise lightcone coordinates by

$$u = -4M \exp\left(-\frac{\bar{u}}{4M}\right), \qquad v = -4M \exp\left(\frac{\bar{v}}{4M}\right). \tag{3.28}$$

Therefore the metric becomes

$$ds^2 = \frac{2M}{r} \exp\left(1 - \frac{2M}{r}\right) du dv, \tag{3.29}$$

where the parameters cover the intervals $-\infty < u < 0$ and $0 < v < +\infty$. If we compare Eq.(3.28) with Eq.(3.15), it seems that the relation between the tortoise and Kruskal coordinates is the same as the relation between the inertial and accelerated frames as we set $a \equiv 1/4M$. Therefore the observer sitting at rest frame far from the horizon is analog to the Unruh observer. It only sees a flux of outgoing (right-moving) modes with temperature

$$T_H = \frac{a}{2\pi} = \frac{1}{8\pi M}. \tag{3.30}$$

Another way of finding T_H is by calculating the Bogolyubov coefficients using the Bogolyubov transformation between the creation and annihilation operators of the tortoise and Kruskal coordinates. Respectively, by quantizing the field $\hat{\phi}$ in these coordinates, we get the solution to the corresponding KG equation as

$$\begin{aligned}\hat{\phi}(\bar{u},\bar{v}) &= \int_0^{+\infty} \frac{d\omega}{\sqrt{4\pi\omega}}\left[\mathrm{e}^{-\mathrm{i}\omega\bar{u}}\hat{b}^-_\omega + \mathrm{e}^{\mathrm{i}\omega\bar{u}}\hat{b}^+_\omega + \mathrm{e}^{-\mathrm{i}\omega\bar{v}}\hat{b}^-_{-\omega} + \mathrm{e}^{\mathrm{i}\omega\bar{v}}\hat{b}^+_{-\omega}\right], \\ \hat{\phi}(u,v) &= \int_0^{+\infty} \frac{d\omega}{\sqrt{4\pi\omega}}\left[\mathrm{e}^{-\mathrm{i}\omega u}\hat{a}^-_\omega + \mathrm{e}^{\mathrm{i}\omega u}\hat{a}^+_\omega + \mathrm{e}^{-\mathrm{i}\omega v}\hat{a}^-_{-\omega} + \mathrm{e}^{\mathrm{i}\omega v}\hat{a}^+_{-\omega}\right].\end{aligned} \tag{3.31}$$

Both solutions are Hermitian operators and obey the canonical commutation relation. The translation between the ladder operators from one coordinates to another follows what we did in sec.3.2. We need to stress that this precise analogy between the Schwarzschild and Rindler spacetimes only exists in 1+1 dimensions. If we consider the quantum field in 3+1 dimensions, the mode decomposition includes spherical harmonics $Y_{lm}(\theta,\phi)$ and the radial part of the KG equation that can be solved separately. In general the field equation is

$$\Box\phi(t,r,\varphi,\theta) = 0, \tag{3.32}$$

with its solution be written as

$$\frac{1}{r}\phi(r)Y_{lm}(\theta,\varphi)\mathrm{e}^{-\mathrm{i}\omega t}. \tag{3.33}$$

The angular part satisfies the equation

$$\hat{L}^2 Y_{lm}(\theta,\varphi) = -l(l+1)Y_{lm}(\theta,\varphi), \tag{3.34}$$

where $\hat{L}^2$ is the angular derivative operator. Therefore for the radial part we have

$$(\Box_r + V_l(r))\hat{\phi}(t,r) = 0, \tag{3.35}$$

where $\Box_r$ includes the radial derivatives [56]. This is the equation for a wave propagating in the effective potential of the form

$$V_l(r) \equiv \left(1-\frac{2M}{r}\right)\left(\frac{2M}{r^3}+\frac{l(l+1)}{r^2}\right). \tag{3.36}$$

The presence of this effective potential weakens the Hawking radiation, namely, the emissivity is less than a perfect black body. This effect is described as a greybody factor. The greybody factors of black holes can be calculated using a path-ordered-exponential

approach [57, 58]. The virtue of this method is that it provides a direct numerical evaluation of the intermediate frequency regime for the greybody factors where the Hawking flux and most of information are concentrated. This technique which is based on a "transfer matrix" formalism also provides semi-analytic expression for Bogolyubov coefficients which in general increases our understanding of transmission and reflection probabilities [59, 60].

One can also find the Hawking radiation and its temperature using a different formalism; for example, by calculating the stress-energy tensor $T_{\mu\nu}$ of the quantum field in the vicinity of black hole horizon. However this has only be explicitly done for $1+1$-dimensional spacetime. In general, when we get to curved spacetime, it is not possible to uniquely separate the solutions to the field equations into orthonormal sets of positive and negative frequencies because of the general coordinate invariance. Therefore, it is not possible to uniquely define the vacuum state. Another approach is by evaluating the asymptotic form of the Bogolyubov β_{ij} coefficient, which determines the number of emitted particles that are created by the gravitational field; it only depends on the surface gravity of the black hole in its stable stage when it has reached the equilibrium.

3.4 Black hole information paradox

In 1976, it was argued in [7] and further discussed in [6, 61] that in the process of formation and evaporation of black holes, information is destroyed. According to QM, for quantum information to escape from a black hole, the evaporation of the black hole should be unitary and the final state of the system after the black hole has evaporated is required to be pure, meaning that there is no information loss in the formation and decay of a black hole. On the other hand, in our current framework for physics, Local quantum field theory (LQFT) on the semiclassical black hole background predicts information loss [6], which means violating quantum mechanics. It has also been pointed out that the energy conservation can also be violated via virtual production of black holes if information is lost [62, 63]. Therefore for reconciling these two theories, it is suggested that by applying small corrections to LQFT in the vicinity of BH horizon, there is a hope for unitarizing the evolution [62, 64, 65].

We know that Hawking radiation originated from the vicinity of the Horizon and that black hole entropy can be derived from the degrees of freedom at the horizon. Therefore one might think that by perturbing the horizon we can get more information out of it. Perturbing the horizon creates quasinormal modes (QNMs), which we can study by applying the WKB approximation. Quasinormal frequencies of black holes encode information regarding the ringdown of the black hole after it is perturbed. These complex frequencies

and information they hold depend on the geometry of black holes and type of their perturbations. For example look at [66–68]. These studies have been pursued for vacuum black holes with an attempt to find a connection between the QNMs and possible quantization law for the horizon area. One can also study regular black holes, for which the gravity is coupled to some form of matter, and explore the possibility of finding such connections [69]. There are several reviews of all recent developments related to the topic of QNMs and their applications such as [70, 71].

One elegant way to describe the information transfer from BH interior to its surrounding is by entanglement transfer [72, 73]. This is either by the black hole absorption of matter already entangled with the surrounding or by pair particle production which will be entangled with the excited states inside the black hole. Unitarity demands that all the entanglement should be transferred out at the end so that the von Neumann entropy of the black hole does not change before and after complete evaporation. On the other hand, to have enough energy transformation to unitarize the BH evaporation, there should be a mechanism for transferring information from inside the black hole to the asymptotic observer outside so that the structure of the horizon stays untouched and there is no extra net flux in addition to the Hawking radiation. One candidate for such transformation channels can be described as metric perturbation couplings to the stress-energy tensor. These couplings need to be of order of unity for which the metric fluctuations can be soft. At linear order, the metric perturbations do not result in extra average energy flux and therefore do not violate BH thermodynamics. In the higher order in perturbations, we can keep the energy flux small by controlling the information-carrying coupling.

This was one of the various proposals to resolve the information problem. There are multiple reviews covering different approaches including [74, 75]. At the end of Ch.6 we will speculate on a possible way of addressing this paradox based on the method that we used to amplify the Unruh effect.

Chapter 4

Cavities in Curved Spacetimes: The Response of Particle Detectors

Note: The content presented in this chapter can be found in [1]. This work is in collaboration with Eduardo Martín-Martínez and Robert B. Mann.

We introduce a method to compute a particle detector transition probability in spacetime regions of general curved spacetimes provided that the curvature is not above a maximum threshold. In particular we use this method to compare the response of two detectors, one in a spherically symmetric gravitational field and the other one in Rindler spacetime to compare the Unruh and Hawking effects: We study the vacuum response of a detector freely falling through a stationary cavity in a Schwarzschild background as compared to the response of an equivalently accelerated detector traveling through an inertial cavity in the absence of curvature. We find that as we set the cavity at increasingly further radii from the black hole, the thermal radiation measured by the detector approaches the quantity recorded by the detector in Rindler background showing in which way and at what scales the equivalence principle is recovered in the Hawking-Unruh effect, i.e. when the Hawking effect in a Schwarzschild background becomes equivalent to the Unruh effect in Rindler spacetime.

We could have a vacuum of the BH which is in thermal equilibrium or we could have a vacuum of the black hole which is sitting in a zero temperature environment. The difference is if the BH is in thermal equilibrium you get heat radiation from all direction but if it is sitting in a zero temperature environment the radiation is only coming from the direction of the BH. There is a general expectation that the radiation provides a kind of buoyant force, that in principle could support the detector. It is therefore of interest to see what

the excitation rates of the detector near a black hole in situations that are not entirely in free fall [38].

4.1 Introduction

The response of a particle detector depends on the state of the field, the structure of spacetime and the detector's trajectory. Regarding different types of trajectories, a number of studies have been done in Minkowski spacetime and a variety of scenarios have been explored [46, 47, 76]. For example, the transition rate of a UDW detector coupled to a massless scalar field in Minkowski spacetime, regularized by the spatial profile, was analyzed in [47].

However, one faces technical difficulties when studying the response of detectors undergoing non-trivial trajectories in curved backgrounds. Notwithstanding simple two dimensional cases [40], in curved spacetimes the identification of the correct vacuum state of the theory, which provides a physical interpretation of the results, is difficult because of the lack of a global timelike Killing vector. Even when we can identify the relevant vacuum, obtaining the Wightmann function and its appropriate regularization in general backgrounds can also pose a challenging problem even for the simplest cases [77].

Given these difficulties it is interesting to explore some approximate regimes where it may be possible to find the response of a particle detector without running into the severe technical complications suffered by exact methods. In principle, approaches using cavity quantum field theory have been explored in order to answer questions regarding the particle content of the vacuum state of a field from the perspective of different observers [49,78,79]. In those approaches the treatment gets greatly simplified by the fact that the cavity field gets isolated from the rest of the free field in the spacetime and so an IR-cutoff is built into the theory. Futhermore, the problem of studying the response of particle detectors in optical cavities in relativistic regimes is a problem of intrinsic interest [78,79]; a recent result showed that an accelerated detector inside a cavity does very approximately thermalize to a temperature proportional to its acceleration [80].

Here we investigate the difference in the response of a detector when freely falling through a stationary cavity subjected to a spherically symmetric gravitational field as compared to the response of an equivalently accelerated detector that traverses an inertial cavity in the absence of curvature [1]. One might expect (via the equivalence principle) both

[1] Strictly speaking the proper comparison would be with an accelerated cavity and an inertial detector which is a subject of current investigation.

responses to be similar if the cavity is small compared to the distance from the source of the gravitational field. However, as we will see, as the cavity is placed closer to the region of strong gravity the detector responses increasingly differ.

With the help of some approximations that are applicable in the cavity scenario, we will be able to characterize the transition probability of particle detectors in a Schwarzschild background, circumventing the complexity involved in the calculation of the Wightmann function in such scenarios [37].

To this end, in this chapter, first in Sec.4.2 we introduce a physical model of our system including the methodology for investigating our cavity scenario. Then in Sec.4.3 and Sec. 4.4 we discuss our results and final remarks.

4.2 The setting

In order to investigate our method, we consider the following scenario to calculate and analyze the excitation probability of an UDW detector in the cavity. We consider a detector to be a two-level pointlike quantum system, which is a reasonable approximation for atomic-based particle detectors [45]. We will be working with three different coordinate systems. One is the coordinate system of the stationary observer at infinity, (r, t), the second one is the local coordinate system of the outermost wall of the cavity, (r', t') which is sitting at the radius $(r = R)$ and the third one is the proper frame of the detector, whose proper time we denote as τ.

The proper frame (r', t') of the outermost wall is related to the asymptotically stationary frame (r, t) by means of the following relationships:

$$r' = \left(1 - \frac{2m}{R}\right)^{-\frac{1}{2}} (R - r), \tag{4.1}$$

$$t' = \left(1 - \frac{2m}{R}\right)^{\frac{1}{2}} t. \tag{4.2}$$

Now, we want to parametrize the trajectory of a free-falling detector, which starts from rest at the beginning of the cavity ($r = R \Rightarrow r' = 0$), in terms of its own proper time τ. We would like to write the worldline of the detector in terms of a parametric curve in the cavity's frame coordinates, i.e. we want the detector's worldline $\big(r'(\tau), t'(\tau)\big)$. The

parametrization of the detector's trajectory in this frame is given by

$$r'\big(\theta(\tau)\big) = \left(1-\frac{2m}{R}\right)^{-\frac{1}{2}} R\sin^2\left(\frac{\theta(\tau)}{2}\right), \tag{4.3}$$

$$\begin{aligned} t'\big(\theta(\tau)\big) &= \left(1-\frac{2m}{R}\right)\left(\frac{R^3}{2m}\right)^{\frac{1}{2}}\left[\frac{1}{2}\Big(\theta(\tau)+\sin\left[\theta(\tau)\right]\Big)+\frac{2m}{R}\theta(\tau)\right] \\ &+ \left(1-\frac{2m}{R}\right)^{\frac{1}{2}} 2m\log\left[\frac{\tan\frac{\theta_H}{2}+\tan\frac{\theta(\tau)}{2}}{\tan\frac{\theta_H}{2}-\tan\frac{\theta(\tau)}{2}}\right], \end{aligned} \tag{4.4}$$

where θ is the following function of the proper time of the detector τ:

$$\theta(\tau) = 2\arccos\left(\frac{r(\tau)}{R}\right)^{\frac{1}{2}}. \tag{4.5}$$

and θ_H is the value of θ at the horizon [81]. We depict the scheme for this setting in Fig. 4.1.

The size of the cavity will be considered small enough so we can ignore any tidal effects. In this fashion we will assume that the reference frame of the outermost wall of the cavity will very approximately be the same frame as for all the rest of the points in the whole cavity. We will discuss the validity of this approximation later on; taking it as valid, the stationary cavity placed at $r = R$ has length L in its local coordinate system. Consequently, the length of the cavity as measured by a stationary observer at infinity, L_r, is related to L via $L_r = (1-2m/r)^{1/2} L$.

Now one would expect that a detector falling through the cavity, even if field and detector are in the ground state, would experience a Hawking-effect-like response. There are two main contributions to the distinct response of the detector in this regime. First, since the detector is freely falling, its proper time is different at each point in the cavity. Second, the solution to the Klein-Gordon equation would be different from the usual stationary waves in a flat-spacetime Dirichlet cavity.

In our model, we will carry out the following 'quasi-local' approximation. If the cavity is small enough and it is far enough from the strong gravity region, we can assume that the solutions of the Klein-Gordon (KG) equation inside the cavity can be very well approximated by plane waves in the locally flat tangent spacetime (corrections due to the effects of curvature can be incorporated via the Riemann normal coordinate expansion [82]). While moving through the cavity, the proper time of the detector will still experience a gravitational redshift, which will be responsible for its thermal response. We

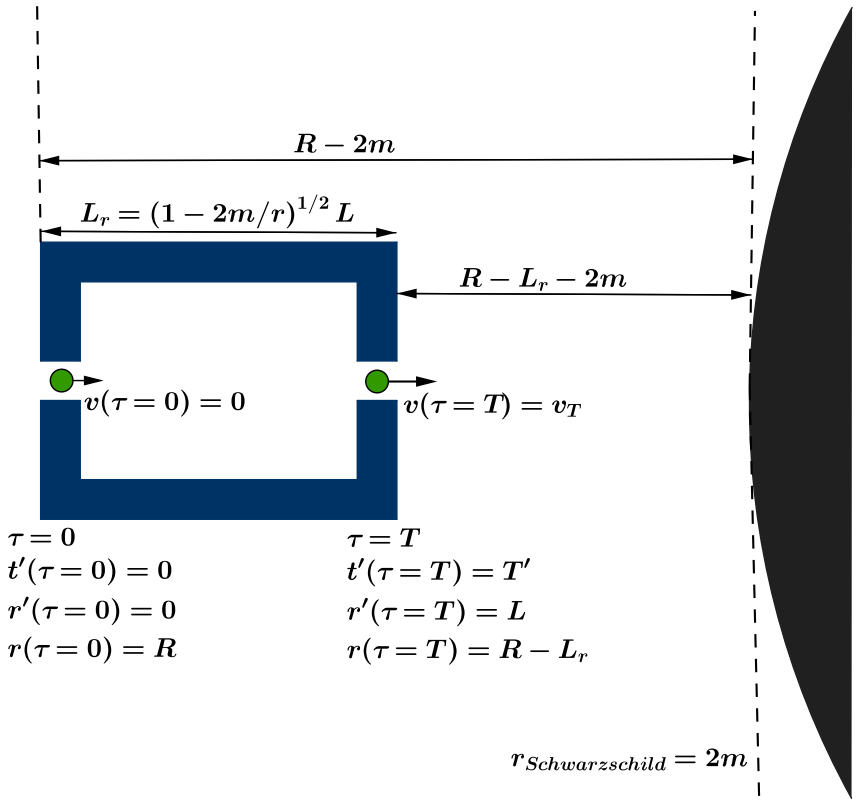

Figure 4.1: Scheme of a detector going through a cavity prepared in the vacuum state, in a curved background. The cavity, of proper length L (Length L_r in the asymptotically flat frame) is located at the arbitrary radius R in the asymptotically flat frame (r, t). The detector with zero initial velocity is falling through the cavity and it spends an amount of proper time of T (or equivalently T' from the cavity frame (r', t')) to travel through the cavity, exiting it with final proper speed v_T.

expect that departures in the KG solutions with respect to the flat spacetime scenario will introduce sub-leading corrections in the appropriate regimes; it is these corrections that we are neglecting.

To check the range of validity of this estimation we proceed as follows: the KG equation in a Schwarzschild background has the following form

$$\left[\partial_{\mathrm{t}}^2 - \frac{1}{r^2}\left(1-\frac{2m}{r}\right)\left(\partial_{\mathrm{r}}(r^2-2mr)\partial_{\mathrm{r}} + \Delta_S\right)\right]\psi(t,r) = 0$$

where r and t are the coordinates of the stationary observer in the asymptotically flat region and where Δ_S is the Laplacian on S^2. This expression can be written in a similar form as in flat spacetime if we write it in terms of the Regge-Wheeler coordinate (as introduced in Ch.3 to be $r^* = r + 2m\ln(r/2m-1)$) to be

$$\left[\partial_{\mathrm{t}}^2 - \partial_*^2 + V(r)\right]\psi(t,r) = 0 \tag{4.6}$$

where

$$V(r) = \left(1-\frac{2m}{r}\right)\left(\frac{2m}{r^3} - \frac{\Delta_S}{r^2}\right)$$

In two regimes $V(r)$ approaches zero: One is close to the horizon where $r \to 2m$ and the other one is far away from the horizon where $r \to \infty$. In these two ranges, the form of KG equation in the Regge-Wheeler frame would be effectively of the same form as the flat spacetime equation. Nevertheless, the KG equation in the cavity frame (r', t') (where we carry out the field quantization) will not be of that form. We need to find an estimator that tells us how precisely we can approximate the KG equation in a Schwarzschild background with the one in a locally flat background associated with the rest frame of the cavity. If the length of the cavity is small enough, the ratio between the length of the cavity in its own reference frame ($\Delta r' = L$) and the length of the cavity in the Regge-Wheeler frame ($\Delta r^* = L^*$) provides a physically meaningful estimator of the validity of the quasi-local approximation. Given the relationship between r^* and r' for the radially ingoing detector

$$r^* = -R + \left(1-\frac{2m}{R}\right)^{\frac{1}{2}} r' - 2m\ln\left[\frac{R-\left(1-\frac{2m}{R}\right)^{\frac{1}{2}} r'}{2m} - 1\right], \tag{4.7}$$

the estimator takes the following form

$$\frac{L^*}{L} = \frac{\Delta r^*}{\Delta r'} = \left(1-\frac{2m}{R}\right)^{\frac{1}{2}} - \frac{2m}{L}\ln\left[\frac{(R^2-2mR)^{\frac{1}{2}}}{(R^2-2mR)^{\frac{1}{2}} - L}\right]. \tag{4.8}$$

Figure 4.2 illustrates how this quantity changes as a function of R, the distance from the black hole and L, the length of the cavity. We see that $\Delta r^*/\Delta r'$ increases with both increasing cavity size and decreasing proximity to the Schwarzschild radius. Our approximation works well for the small cavities in the vicinity of the black hole. As we will see, the threshold size of the cavity is equal to the size of the black hole.

Note again that the estimator is reliable when we are very close to the event horizon, or far away from it, as discussed above. Nevertheless, and as an interesting remark, in a 1+1 dimensional Schwarzschild background, it is easy to prove that the Klein-Gordon equation in the Regge-Wheeler frame has the same form as (4.6) but with $V(r) = 0, \forall r$. In this case the estimator is reliable for any position of the cavity.

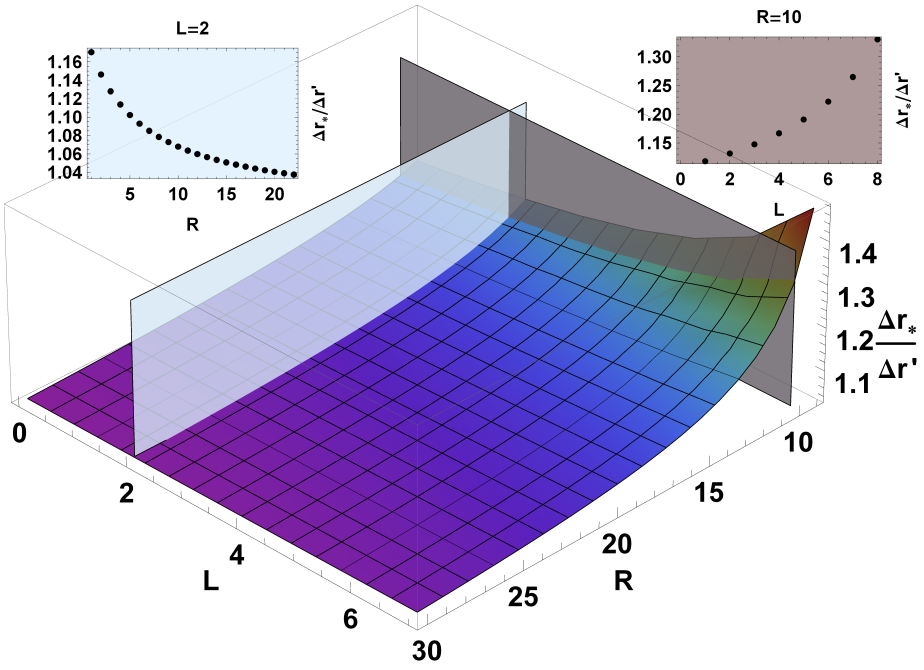

Figure 4.2: Estimator of the validity of the model: The closer to 1, the better the approximation. We see that, as expected, when we are far away from the horizon and when we consider small cavities, $\Delta r^*/\Delta r'$ approaches one. The inset located at the top right shows the behavior of the ratio vs. R for a fixed value of $L = 2$ and the top left one shows how ratio changes with L when the cavity is at $R = 10$ (all magnitudes are expressed in units of black hole mass).

Here we are using the same interaction Hamiltonian $\hat{H}_{int}$ as in Eq.(3.2). In our setting,

the switching function is nonvanishing only during the time the atom spends in the cavity, i.e., $\chi(\tau) = 1$ during $0 \leq \tau \leq T$.

Expanding the field in terms of an orthonormal set of solutions inside the cavity yields the Hamiltonian in the interaction picture [83]

$$\hat{H}_{\text{int}} = \lambda \frac{d\tau}{dt} \sum_{n=1}^{\infty} \frac{\hat{\mu}(t)}{\sqrt{\omega_n L}} \left(\hat{a}_n^\dagger u_n \left[r'(\tau), t'(\tau) \right] + \hat{a}_n u_n^* \left[r'(\tau), t'(\tau) \right] \right) \tag{4.9}$$

We will consider Dirichlet (reflective) boundary conditions for our cavity, (see Fig. 4.1)

$$\phi \left[0, t' \right] = \phi \left[L, t' \right] = 0 \tag{4.10}$$

and so under our quasi-local approximation the field modes take the form of the stationary waves

$$u_n \left[r'(\tau), t'(\tau) \right] = e^{i\omega_n t'(\tau)} \sin \left[k_n r'(\tau) \right]. \tag{4.11}$$

Note that $\omega_n = |k_n| = n\pi/L$, and $r'(\tau)$ and $t'(\tau)$ (given in equations (7.54) respectively) parameterize the trajectory of the detector freely falling from a cavity whose first wall is located at $r = R$ in the frame (r, t), proper to a stationary observer at infinity.

We want to characterize the vacuum response of a particle detector undergoing the trajectory in Eq.(7.54). For our purposes, we prepare the detector in its ground state and the cavity in the vacuum state

$$\rho_0 = |g\rangle\langle g| \otimes |0\rangle\langle 0| \tag{4.12}$$

To proceed, we let this detector start free falling through the cavity as shown in Fig. 4.1. The detector spends an amount of proper time T inside the cavity. The time evolution of the system is governed by the interaction Hamiltonian (4.9) in the time interval $0 < \tau < T$, whereas for the detector in the cavity it is given by Eq.(3.4).

Using (4.9) and (3.4), the first order term of the perturbative expansion takes the form

$$\hat{U}^{(1)} = \frac{\lambda}{i} \sum_{n=1}^{\infty} \left[\sigma^+ a_n^\dagger I_{+,n} + \sigma^- a_n I_{+,n}^* + \sigma^- a_n^\dagger I_{-,n} + \sigma^+ a_n I_{-,n}^* \right], \tag{4.13}$$

in which

$$I_{\pm,n} = \int_0^T d\tau \; e^{i[\pm\Omega\tau + \omega_n t'(\tau)]} \sin \left[k_n r'(\tau) \right]. \tag{4.14}$$

To compute the density matrix for the detector, $\rho_T^{(\mathrm{d})}$, we need to take the partial trace over the field degrees of freedom [49]. The first order contribution to the probability of transition vanishes, so the leading contribution comes from second order in the coupling strength, λ. The final form of the detector density matrix is

$$\rho_{T,(\mathrm{d})} = \mathrm{Tr}_{(\mathrm{f})}\Big[\rho_0 + \hat{U}^{(1)}\rho_0\hat{U}^{(1)\dagger} + \hat{U}^{(2)}\rho_0 + \rho_0\hat{U}^{(2)\dagger}\Big], \tag{4.15}$$

which yields

$$\rho_{T,(\mathrm{d})} = \mathrm{Tr}_{\mathrm{f}}\,\rho_T = \begin{bmatrix} 1-P_2 & 0 \\ 0 & P_1 \end{bmatrix}, \tag{4.16}$$

where $P_1 = P_2$ is given by

$$\begin{aligned} P_1 &= \lambda^2 \sum_{n=1}^{\infty} |I_{+,n}|^2 \\ &= \lambda^2 \sum_{n=1}^{\infty} \int_0^T d\tau \int_0^\tau d\tau_1 \Big[e^{-i[\Omega\tau+\omega_n t'(\tau)]} \sin\left[k_n r'(\tau)\right] \times e^{i[\Omega\tau_1+\omega_n t'(\tau_1)]} \sin\left[k_n r'(\tau_1)\right] \Big]. \end{aligned} \tag{4.17}$$

P_1 gives the transition probability of the detector from the ground state to the first excited state to the leading order in perturbation theory.

Note that we have decided to compute the probability of transition rather than the transition rate. Given the time translational invariance of our setting, there is no formal or computational advantage in computing the rate over the probability, and both magnitudes contain the same information.

We furthermore note that the transition probability of a suddenly switched detector becomes logarithmically divergent in the 3+1 dimensional case, but it is finite in lower dimensional scenarios [37, 84], effectively rendering our calculation in the relevant radial coordinate (where we assume the cavity is longer) divergence-free. A repetition of the same calculation in 3 spatial dimensions would entail making the switching function of the detector continuous. Alternatively one can compute differences between transition probabilities as in [37, 85]. Since in this article we are comparing the Rindler with the Schwarzschild detector response the fundamental results reported here would not be modified by these effects.

4.3 Transition probability of the detector

Applying the formalism of section 4.2, we proceed to present and compare our results for the response of the detector freely falling in Schwarzschild spacetime to that of an accelerated one in a Minkowski background.

For the Schwarzschild case, we consider a free-falling detector passing through a cavity. It starts falling with zero initial velocity at at $r = R$, the entrance of the cavity. We assume that the detector enters the cavity in the ground state (of the free Hamiltonian) and that the field in the cavity is prepared in the local vacuum state. This set up is shown schematically in Fig. 4.1. The detector gets excited due to the difference between its proper time and the proper time in the cavity frame, which induces an effective time dependence in the interaction Hamiltonian.

Using equation (4.17), we find the transition probability. We select an arbitrary value (of $\lambda = 0.01$) for the coupling strength and set $\Omega = 6\pi/L$ so the detector resonates with the 6th mode of the field in the cavity. This somewhat arbitrary choice is convenient in that by coupling the detector to a higher harmonic of the cavity we avoid its decoupling from the cavity field by being taken off-resonance through the blueshift the field modes experience in the detector's frame [80].

Now, to compare these results with the Rindler scenario, we set a cavity of the same proper length in a Minkowski background, traversed by an accelerated detector (of proper acceleration a equal to the gravitational field intensity in the spherically symmetric Schwarzschild background at a radius $r = R$) and with the same energy gap as above. The detector's worldline, parametrized in terms of its proper time is

$$x(\tau) = \frac{1}{a}\left(\cosh(a\tau) - 1\right), \tag{4.18}$$

$$t(\tau) = \frac{1}{a}\sinh(a\tau) \tag{4.19}$$

so that the detector is at $x = 0$ (the cavity entrance) at time $t = \tau = 0$. By inserting these functions in the interaction Hamiltonian (4.9) (substituting r' and t' by x and t) and following the same calculation that we did for the Schwarzschild case, we find the transition probability for the detector in Rindler spacetime. The behavior of the response of the accelerated detector while it is passing through the cavity is shown in Fig. 4.3 (green squared curve). As noted above, to compare the excitation probability of the detector in Rindler spacetime with those at different radii in the Schwarzschild background, the

detector's proper accelerations in the Rindler scenario will be taken to be

$$a = \frac{m}{R^2 \left(1 - \frac{2m}{R}\right)^{\frac{1}{2}}} \tag{4.20}$$

so that they are equivalent to the real acceleration measured by the detector at the specific radii considered in the curved background (i.e. the local strength of the gravitational field).

Plotting all quantities in units of the black hole mass m, Fig. 4.3 shows the behaviour of the excitation probability of the detector while it is traveling from the beginning to the end of a cavity of size $L = 5$ located at radius $R = 10$ for both the Schwarzschild and Rindler cases.

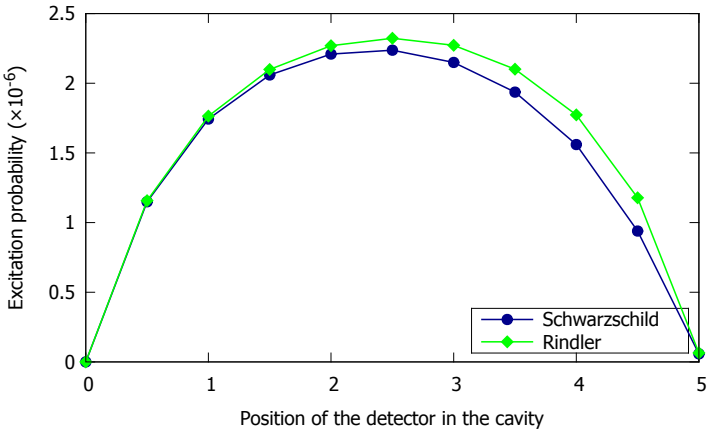

Figure 4.3: Excitation probability of the detector while it is traveling from the beginning to the end of the cavity of size $L = 5$. The green (squared) curve indicates the transition probability in the Rindler background and the blue (circled) curve is for the case of Schwarzschild spacetime. The coupling strength set to be $\lambda = 0.01$.

Figure 4.4 shows how the transition probability changes as we set the cavity at different distances from the black hole for the cavity of fixed length and the consistent change in the atom's acceleration for the Rindler cavity.

To compare our results in the presence and absence of curvature, we present the ratio of the probabilities of the two scenarios in Fig. 4.5. Each curve represents the behaviour of the ratio for a specific length of the cavity as it is located at different R. According to the approximation estimator we considered, the longer L cases are less accurate. However for all radii above $R = 40$, the estimator (4.8) remains less than 3% above 1 even when the cavity proper length is $L = 6$, which is the largest cavity length considered.

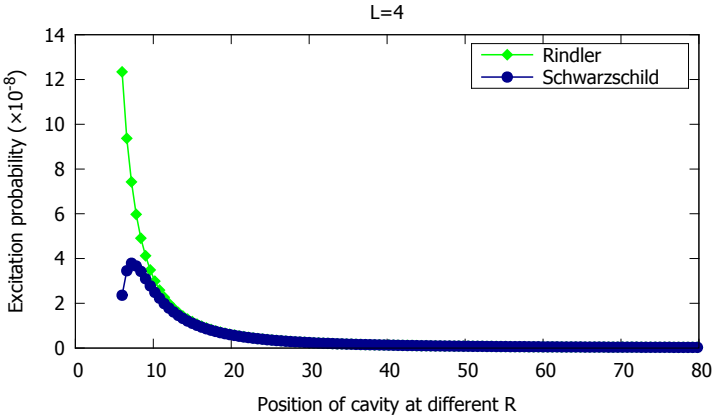

Figure 4.4: Behavior of the detector transition probability as it starts falling through the cavity of length $L = 4$ from different radii R for Schwarzschild (circled curve) and Rindler (squared curve) spacetimes.

We see from Fig. 4.5 that the larger the cavity, the greater the difference in excitation probability as the cavity is placed close to the horizon. As expected from the equivalence principle, very small cavities ($L = 10^{-3}$) are virtually indistinguishable from the Rindlerian case, therefore to see any distinction one would have to place the cavity much closer to the horizon than our present computational resolution admits. However departures from the Rindlerian case can be seen even for moderately small cavities ($L = 0.3$), and these departures rapidly increase with cavity size provided one is within the vicinity of about 20 horizon radii.

A better comparison is given in Fig.4.5b, in which we compute the ratio of the probabilities of the two scenarios where the constant acceleration for the Rindlerian case is taken to be the Schwarzschild acceleration in the middle of the cavity. We see that the Schwarzschild case is consistently smaller than the Rindler case, with the discrepancy increasing with both increasing cavity size and closer proximity to the horizon.

4.4 Conclusions

We have introduced a cavity model in which we can find the transition probability of a Unruh-DeWitt detector in a curved spacetime without facing the difficulties of solving the wave equations, regularizations and defining the notion of vacuum state for different

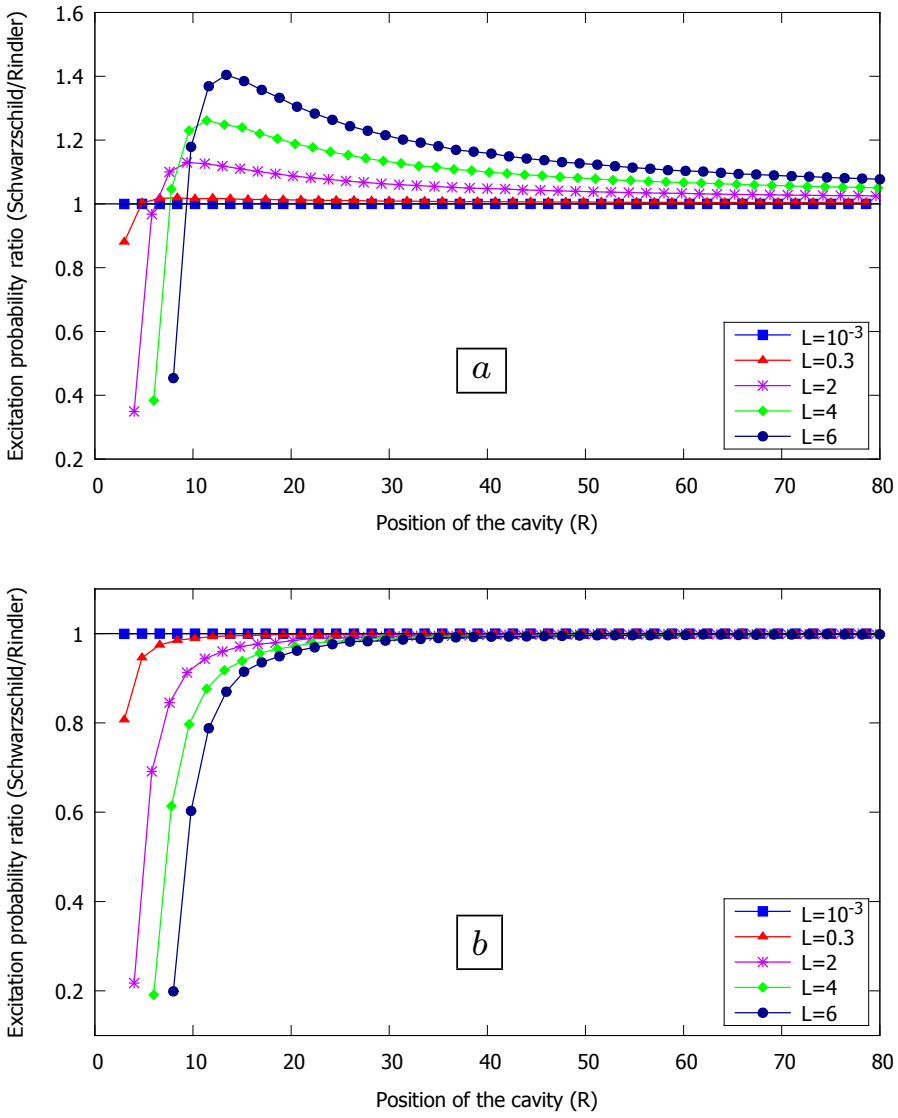

Figure 4.5: The ratio of the transition probability of an Unruh-DeWitt detector in a Schwarzschild background to the equivalent quantity in Rindler spacetime. Each curve shows the behaviour of the ratio for a different cavity length as it gets placed at different R from the Schwarzschild black hole and equivalently gets assigned with different constant accelerations equal to the Schwarzschild acceleration at the a) entrance to the cavity and b) middle of the cavity.

observers in a curved background. Our model works well where the interplay of the size of the cavity and strength of the curvature provides an environment in which a quasi-local approximation to the wave equation is valid.

We studied the cavity setting in two scenarios: that of a freely falling detector in Schwarzschild and that of a uniformly accelerated detector in flat space-time crossing a stationary cavity. We found near-identical transition rates for both scenarios in the limit of small cavities, with increasing departures from this situation as the cavity size increases.

Consequently, in the limit of small cavity and large R we are studying a particular case of the equivalence principle: the Schwarzschild scenario is completely equivalent to a Rindler scenario consisting of a cavity accelerating toward a stationary detector. We have shown that this scenario coincides exactly with a setup where we have a uniformly accelerated detector crossing an inertial cavity. Our work stands in contrast to that in which transition rates of detectors are computed for scalar fields in free space (for a review see [21]). It would be desirable in future work to go beyond the quasi-local approximation to better understand the effect of curvature in the excitation probability.

More generally, comparing the Schwarzschild scenario to the Rindler scenario in which the uniform acceleration is taken to be the Schwarzschild acceleration (average of the field strength) in the middle of the cavity, we find that the latter case is consistently larger than the former, the discrepancy increasing with both closer proximity to the horizon and increasing cavity size. Our results show that the amounts of thermal radiation recorded by a detector in a Rindler space and the Hawking-like radiation that the detector observes in a Schwarzschild background approach the same quantity.

For larger cavities, the quasi-local approximation breaks down for distances closer to the black hole where the curvature is large. To find the transition probability of the detector in this case, one must solve for the response function of the detector using the Wightmann function in free space.

Note that the response of our detector is independent of the global vacuum choice outside the cavity since, in our idealized setting, the detector is 'shielded' by the cavity walls. For non-ideal cavities the outside field could leak inside the cavity, which would indeed have an effect on the response of the detector, particularly when the cavity is placed close to the event horizon. In those situations the choice of vacuum outside the cavity would become important. Considering these effects remains a subject of study for further research.

The methods we present in this chapter should be applicable to a much broader class of situations. Inclusion of mass is straightforward, and it would be interesting to study the

effects of curvature relative to those previously obtained for uniform acceleration [86]. Of particular interest is to understand the effects of an ergoregion on transition probabilities.

Chapter 5

Measuring motion through relativistic quantum effects

Note: The content presented in this chapter can be found in [2]. This work is in collaboration with Eduardo Martín-Martínez and Robert B. Mann.

Quantum metrology provides techniques to make precise measurements which are not possible with purely classical approaches. In quantum metrology protocols such as quantum-positioning and clock-synchronization [87, 88], the exploitation of quantum effects such as quantum entanglement has allowed for a significant enhancement of the precision in estimating unknown parameters as compared to classical techniques [89].

On the other hand, there exist metrology settings where general relativistic effects play an important role in establishing the ultimate accuracy of the measurement of physical parameters [90]. It is thus pertinent to introduce a framework where relativistic effects are considered even in quantum metrology schemes [91], where it is relevant to study how (or if) incorporating relativistic approaches to quantum metrology may increase the precision and accuracy of the estimation and measurement of physical parameters.

In this chapter we focus on finding suitable quantum optical regimes where the response of particle detectors becomes sensitive to small variations of the parameters governing their motion, incorporating relativistic effects. Our goal is to assess the sensitivity of the response of particle detectors to such variations, in turn allowing for the precise measurement of such parameters.

In particular, we consider a setting in which an atomic detector crosses a stationary optical cavity while undergoing constant acceleration. Relativistic accelerating atoms in

optical cavities have been considered before in the context of an enhancement of Unruh-like radiation effect [92–94], and later, in this context, to analyze the subtleties of the Unruh effect in the presence of boundary conditions [80]. The suitability of such settings as theoretical accelerometers was studied in [86], where it was shown that a detector's response is sensitive to variations of its proper acceleration. In this chapter, we will show that near the relativistic regimes, but still, much below the accelerations required for the Unruh effect to be detectable, the detectors' response becomes sensitive to small (and maybe time-dependent) perturbations in either the parameters that govern their trajectory or in the alignment of the optical cavity. We will study this sensitivity to determine to what extent it is possible to exploit it for quantum metrological effects.

We consider two different scenarios of metrological interest. In the first, we study the sensitivity of the response of the detector to time-dependent variations of its proper acceleration. Specifically, we consider a uniformly accelerated atomic detector crossing an optical cavity with constant proper acceleration that undergoes a small harmonic time-dependent perturbation. If the system alignment is tuned, we might wonder how sensitive it is to the amplitude and frequency of the perturbation.

In the second scenario we study the sensitivity of the detector's response to variations of its trajectory. To accomplish this, we consider small harmonic perturbations of the spatial trajectory of a uniformly accelerated observer. We explore how sensitive this setting is to the amplitude and frequency of the perturbation, thus providing a setting to measure the wellness of the atom's trajectory alignment with respect to the cavity frame.

In the next section, we start by introducing two physical settings including the methodology for investigating our two scenarios.

5.1 The setting

In this section we consider two different scenarios in which we want to precisely measure different parameters of the trajectory of an atomic probe. For the first scenario, which we will call the *accelerometer setting*, we consider an atomic probe following a constantly accelerated trajectory, but whose proper acceleration undergoes a harmonically time-dependent perturbation. In the second scenario, which we will refer to as the *alignment metrology setting*, we consider that the atomic probe's trajectory undergoes small harmonic perturbations as seen from the lab frame, so as to be able to measure the precision of the alignment of a cavity with a beam of atomic detectors.

In both scenarios we model the light-atom interaction by means of the Unruh-DeWitt

model. Although simple, this model captures the fundamental features of the coupling between atomic electrons and the EM field involving no exchange of orbital angular momentum [45, 95].

5.1.1 A quantum accelerometer

Particle detectors with time dependent accelerations have been previously studied in [96, 97], where the response of an Unruh-DeWitt detector with time dependent acceleration in the long time regimes has been considered in a flat spacetime with no boundary conditions. We would like to study how sensitive the detector response is to time-dependent perturbations of its proper accelerations in the short-time regime and in optical cavity settings.

In order to analyze this accelerometer setting, let us first consider the parametrization of the trajectory of an atomic probe for a general time dependent trajectory in terms of the probe's proper time τ [98]:

$$x(\tau) = x_0 + \int_{\tau_0}^{\tau} d\tau' \sinh\big[\xi(\tau')\big], \tag{5.1}$$

$$t(\tau) = t_0 + \int_{\tau_0}^{\tau} d\tau' \cosh\big[\xi(\tau')\big], \tag{5.2}$$

where

$$\xi(\tau') = \xi_0 + \int_{\tau_0}^{\tau} d\tau' a(\tau') \tag{5.3}$$

represents the atom's instantaneous speed, and $a(\tau)$ is the instantaneous proper acceleration of the probe.

For our purposes, we consider that the probe undergoes a constant acceleration, which is disturbed by a small harmonic perturbation:

$$a(\tau) = a_0\big[1 + \epsilon \sin(\gamma\tau)\big]. \tag{5.4}$$

ϵ and γ are the respective relative amplitude and frequency of the harmonic perturbation.

The general form of the trajectories for both perturbed and constant accelerations is shown in Fig. 5.1.

In our setting, to find the transition probability of the detector, we let it cross a cavity of length L with an initial velocity ξ_0 and we measure its excitation probability for the

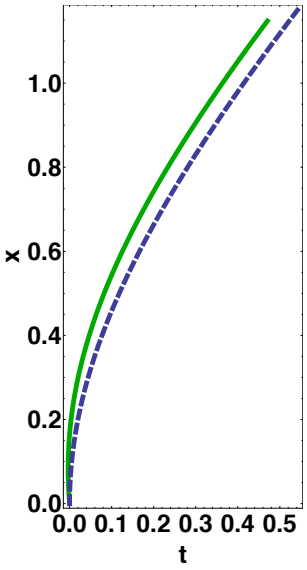

Figure 5.1: (Color online) The non-perturbed (blue-dashed curve) and perturbed (green-solid curve) trajectory for the accelerometer scenario. The trajectory is parameterized in terms of the proper time, τ of the detector.

period of time T that it spends traveling the full length of the cavity. The Hamiltonian that describes our system generates translations with respect to time τ in the detector's proper frame. As in the last chapter, we model the detector-field interaction Hamiltonian with (3.2). The Hamiltonian in the interaction picture that we apply here is

$$\hat{H}_{\rm int}(t) = \lambda \sum_{n=1}^{\infty} \frac{\hat{\mu}_{\rm d}(\tau)}{\sqrt{\omega_n L}} \Big(\hat{a}_n^{\dagger} u_n \left[x(\tau), t(\tau)\right] + \hat{a}_n u_n^{*} \left[x(\tau), t(\tau)\right] \Big). \tag{5.5}$$

We still consider Dirichlet (reflective) boundary conditions for our cavity as in the last chapter, $\phi\big(0,t\big) = \phi\big(L,t\big) = 0$. Working in the Minkowski background, the field modes take the form of stationary waves

$$u_n \left[x(\tau), t(\tau)\right] = e^{{\rm i}\omega_n t(\tau)} \sin\left[k_n x(\tau)\right]. \tag{5.6}$$

To characterize the vacuum response of the particle detector undergoing trajectory (5.1), we initially prepare the detector in the ground state and the field in the optical cavity in a coherent state $|\alpha\rangle$. We choose the coherent state to be in the j-th cavity mode with frequency $\omega_j = j\pi/L$, while the rest of the cavity modes are in the ground state. This

way the main effects will not come from vacuum fluctuations but will instead be amplified by the stimulated emission and absorption of photons by the atom coupled to the coherent state [49, 99]. Therefore the initial state of the system will be

$$\rho_0 = |g\rangle\langle g| \otimes |\alpha_j\rangle\langle\alpha_j| \bigotimes_{n\neq j} |0_n\rangle\langle 0_n| \,. \tag{5.7}$$

While passing through the cavity, the detector spends a period of proper time T inside the cavity. Time evolution of the system is governed by the interaction Hamiltonian (3.2) in the proper frame of the detector. Time evolution operator for the detector inside the cavity and the system density matrix are given by (3.4) and (3.5), respectively.

Using the interaction Hamiltonian and the time evolution operator, the first order term of the perturbative expansion will be

$$\hat{U}^{(1)} = \frac{\lambda}{\mathrm{i}} \sum_{n=1}^{\infty} \left[\sigma^+ a_n^\dagger I_{+,n} + \sigma^- a_n I^*_{+,n} + \sigma^- a_n^\dagger I_{-,n} + \sigma^+ a_n I^*_{-,n}\right], \tag{5.8}$$

where $I_{\pm,n}$ is

$$I_{\pm,n} = \int_0^T d\tau \; e^{\mathrm{i}[\pm\Omega\tau + \omega_n t(\tau)]} \sin\left[k_n x(\tau)\right] . \tag{5.9}$$

As in Eqs. (5.10), to compute the density matrix for the detector, $\rho_T^{(\mathrm{d})}$, we need to take the partial trace over the field degrees of freedom [49]. The leading contribution comes from second order in the coupling strength, λ and the final form of the detector density matrix will be [1]

$$\rho_{T,(\mathrm{d})} = \mathrm{Tr}_{(\mathrm{f})}\Big[\rho_0 + \hat{U}^{(1)}\rho_0\hat{U}^{(1)\dagger} + \hat{U}^{(2)}\rho_0 + \rho_0\hat{U}^{(2)\dagger}\Big], \tag{5.10}$$

which yields

$$\rho_{T,(\mathrm{d})} = \mathrm{Tr}_{\mathrm{f}}\,\rho_T = \begin{bmatrix} 1-P_\alpha & 0 \\ 0 & P_\alpha \end{bmatrix} . \tag{5.11}$$

P_α is the transition probability of the detector from the ground state to the first excited state to leading order in perturbation theory, given by [99]

$$P_\alpha(\epsilon,\gamma) = \frac{\lambda^2}{L}\left[\frac{\alpha_j^2}{k_{\alpha_j}}\left(|I_{+,j}|^2 + |I_{-,j}|^2\right) + \sum_{n=1}^{\infty}\frac{|I_{+,n}|^2}{k_n}\right], \tag{5.12}$$

where α_j is the amplitude of a coherent state in a cavity mode j of frequency k_{α_j}. Notice that the probabilities $P_\alpha(\epsilon,\gamma)$ depend on γ and ϵ through the integrals $I_{\pm,n}$, given in (5.9) as functions of $x(\tau)$ and $t(\tau)$. $x(\tau)$ and $t(\tau)$ dependence on a_0,γ,ϵ is obtained by substituting (5.3) and (5.4) into (5.1).

5.1.2 Alignment metrology

In the alignment metrology setting, we study the sensitivity of the response of a detector to small harmonic spatial perturbations of its otherwise constantly accelerated trajectory, and analyze its possible use as a witness of the relative alignment of an optical cavity with a beam of atomic detectors. In this setting, the atomic probes move along a constantly accelerated trajectory which undergoes a spatial perturbation that is harmonic in the cavity's reference frame, (x,t):

$$x(t) \;=\; \frac{1}{a}\left[\sqrt{1+a^2t^2}-1\right]+\epsilon\sin(\gamma t), \tag{5.13}$$

where ϵ and γ are characterizing the amplitude and frequency of the perturbation, respectively. In this case, since the motion is analyzed from the lab's frame, we need to find the (rather non-trivial) relationship between the proper time of the accelerated atom and the cavity frame. The relationship between the cavity frame's proper time and the atomic probe's proper time can be worked out from

$$\left(\frac{d\tau}{dt}\right)^2 = 1-\left(\frac{dx}{dt}\right)^2. \tag{5.14}$$

Solving this differential equation for $d\tau/dt$ together with (5.13) yields

$$\tau(t)=\frac{\operatorname{arcsinh}(at)}{a}-\frac{a\epsilon\Big(\cos(\gamma t)+t\gamma\sin(\gamma t)\Big)}{\gamma}+\mathcal{O}(\epsilon^2). \tag{5.15}$$

The general form of this trajectory is shown in Fig. 5.2 for both the perturbed and the non-perturbed cases.

While crossing the cavity, the detector spends a period of time T in traversing the full length along its trajectory. In order to find the time evolution of the system, we first need to find the form of the atom-field Hamiltonian that generates evolution for the entire system with respect to the time coordinate of the lab frame, t. The way to obtain this

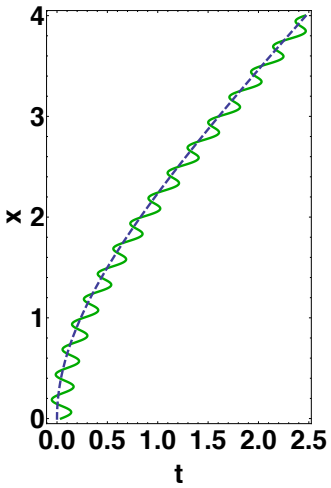

Figure 5.2: (Color online) The non-perturbed (blue-dashed curve) and perturbed (green-solid curve) trajectory for the alignment metrology setting. The trajectory is parameterized in the lab's frame (x, t).

is explained in detail in [78]. The correct time-reparametrization of (3.1) in terms of t is given by

$$\hat{H}(t) = \frac{d\tau}{dt}\hat{H}^{(\mathrm{d})}_{\mathrm{free}}[\tau(t)] + \hat{H}^{(\mathrm{f})}_{\mathrm{free}}(t) + \frac{d\tau}{dt}\hat{H}_{\mathrm{int}}[\tau(t)]. \tag{5.16}$$

The monopole moment operator takes the usual form

$$\hat{\mu}(t) = \left(\sigma^{+}e^{\mathrm{i}\Omega\tau(t)} + \sigma^{-}e^{-\mathrm{i}\Omega\tau(t)}\right), \tag{5.17}$$

and interaction Hamiltonian becomes

$$\hat{H}_{\mathrm{int}}(t) = \lambda\frac{d\tau}{dt}\sum_{n=1}^{\infty}\frac{\hat{\mu}(t)}{\sqrt{\omega_n L}}\left(\hat{a}^{\dagger}_n u_n\left[x(t), t\right] + \hat{a}_n u^{*}_n\left[x(t), t\right]\right), \tag{5.18}$$

with

$$u_n\left[x(t), t\right] = e^{\mathrm{i}\omega_n t}\sin\left[k_n x(t)\right]. \tag{5.19}$$

Working in this frame, the form of the function $I_{\pm,n}$ in the time evolution operator (5.8) turns into

$$I_{\pm,n} = \int_0^T dt\; e^{\mathrm{i}[\pm\Omega\tau(t)+\omega_n t]}\sin\left[k_n x(t)\right]. \tag{5.20}$$

Using the same approach as in the accelerometer setting, for characterizing the vacuum response of the particle detector undergoing trajectory (5.13), we prepare a coherent state (5.7) for the scalar field to which the ground state of the detector is coupled and find the transition probabilities from (5.12).

5.2 Results

The transition probabilities of atomic detectors crossing the cavity contain information about the parameters characterizing the detectors' motion. Of course, we would not want to use perturbations of the Unruh temperature as a means to characterize the the trajectory of the detector. This would be a rather futile endeavour since the the Unruh temperature itself is something extremely difficult to measure, let alone small perturbations of it. Instead, we will operate in a non-equillibrium regime where the detector will not have enough time to thermalize with the 'modified' Unruh radiation. Therefore, we let the detector spend a small amount of time inside the cavity such that it does not thermalize with its environment. On top of that, and as discussed above, we consider a coherent state background which helps amplify the signal. This is the reason why we may expect our system to show more sensitivity to the atom's trajectory. In this section, we analyze the sensitivity of the response of the detectors to perturbations in the kinematical parameters of the detectors' trajectory that we want to measure, both in the accelerometer and the alignment settings.

We pause to remark that our choice of switching function $\chi(t)$ (shown above equation (6.2)) removes the interaction between the field and the atom is off when the atom is outside of the cavity. This assumption needs some justification since one cannot just 'switch off' the interaction of the atom with the electromagnetic field when it is outside the cavity. The rationale of this assumption is twofold. On one hand we assume that the atomic state preparation happens at the entrance of the cavity, when the atom's speed is zero. Equivalently, we are considering a situation in which the atom is post-selected to be in its ground state prior to entering the cavity, and so pre-existing excitations as may be present outside of the cavity are not relevant. On the other hand, the main effects on the atomic state responsible for the results reported here are provoked by the variation of the boundary conditions and the perturbation of the atomic trajectory, which are amplified by the fact that the trajectory is relativistic. As we discussed above, the signature of the Unruh effect itself is small as compared to the non-equilibrium effects coming from the time dependence of the trajectory perturbations. Therefore if the flight of the atom includes some small segments of free flight (outside the cavity), since the Unruh noise would be in

these cases arguably negligible it should not modify our results.

5.2.1 A quantum accelerometer

We focus first on the accelerometer setting, in which there might be small fluctuations of the probe's acceleration of the detector in its own proper frame. We will model this by assuming that the proper acceleration of a set of uniformly accelerated detectors is perturbed by a small harmonic function. One possible way to think about these time dependent oscillations is to associate them with possible inexactnesses in the measure of the acceleration in the proper frame of the detector, so that through relativistic quantum effects we may expect to be able to use the internal degree of freedom of the atomic probe to increase the accuracy in exactly determining this proper acceleration.

With this aim, we study the sensitivity of the transition probability of the detector to the amplitude of the harmonic perturbations and characterize the spectral response of the setting to the specific frequency range of the perturbations. The detector's trajectory (with a harmonically perturbed acceleration) is given by inserting (5.4) in (5.1).

To study how sensitive the setting is to the parameters of the perturbation, we will analyze the following sensitivity estimator:

$$S(\epsilon,\gamma)=\frac{|P_\alpha(\epsilon,\gamma)-P_\alpha(0,\gamma_0)|}{P_\alpha(0,\gamma_0)} \tag{5.21}$$

where $P(\epsilon,\gamma)$ is the transition probability of the detector with a perturbed acceleration given by (5.4), and $P(0,\gamma_0)$ is the transition probability for a constantly accelerated detector whose trajectory is unperturbed.

Fig.5.3 shows the explicit dependence of the sensitivity estimator (5.21) on the parameters characterizing the perturbation. Namely, it shows the sensitivity of the response of the detector to the amplitude ϵ of the perturbations for different values of acceleration, whereas the spectral response of the sensitivity to different values of the perturbation frequency (γ) is shown in Fig.5.4.

As one can observe in Fig.5.3, for small accelerations, closer to the regimes where the atom does not attain relativistic speeds while crossing the cavity, the sensitivity (to acceleration perturbations) of the detector's transition probability is monotonic on the amplitude of the perturbations. However, for large accelerations the sensitivity does not behave monotonically, and there appear specific amplitudes for which the sensitivity dips. The spectral response displayed in Fig.5.4 shows that the response of the detector is always

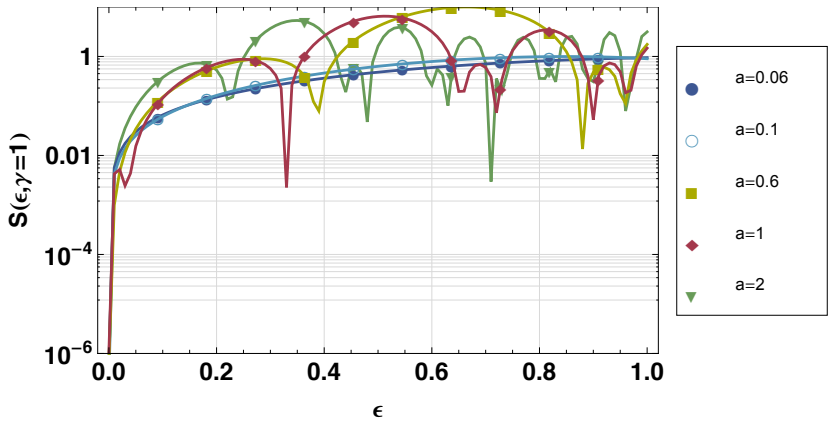

Figure 5.3: (Color online) Behaviour of the sensitivity of the detector's transition probability as a function of the amplitude of a perturbed proper acceleration for different initial accelerations.

more sensitive to the lower frequencies. The behaviour for higher frequencies depends on the energy gap of the atomic probe. For a fixed gap, the sensitivity of the probe seems to be exponentially suppressed as the frequency of the perturbations grows. One possible way to understand this is that when the frequency of the harmonic acceleration perturbation is much higher than the frequency associated with the transition of the atom, the the atomic probe is primarily responsive to its average constant acceleration; the perturbations are much faster than the dynamics of the atom and so become invisible to it. However, as we see in Fig. 5.4b), it is possible to adjust the gap of the atomic transition used as a probe to tune out to a specific frequency range of the perturbations.

In Fig. 5.4c), we show how sensitive the response of the atomic probes is to the length of the cavity they're traversing. This in turns also determines how much relativistic the probes are when existing the cavity for constant acceleration. These curves also suggest that it may be possible to use similar settings as a means to determine the length of an optical cavity.

Of course, the sensitivity estimator we studied only gives us an idea of the potentiality of these settings for the measurement of the parameters of the perturbation. A more realistic practical implementation of such settings would require considerable effort. For example this might be implemented by comparing one setting where all the parameters are known with another setting where the parameters are not known. The comparison of the transition rates of beams of atoms in these two settings may reveal the information about the parameters to be determined. In such a comparison the estimator built here becomes

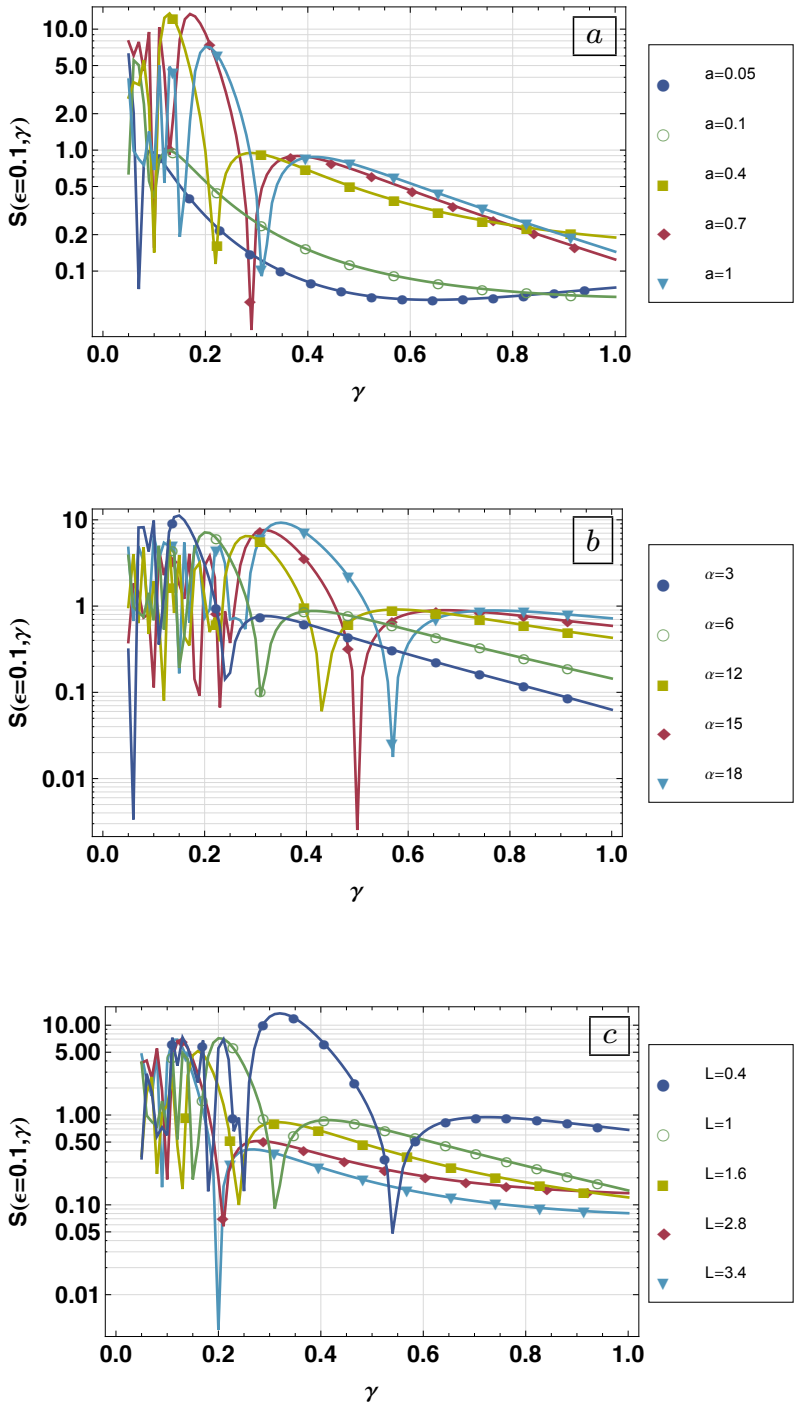

Figure 5.4: (Color online) Spectral response of the detector for a) both relativistic and nonrelativistic accelerations, b) different modes of the field which are in coherent states and coupled to the ground state of the detector and c) different lengths of the cavity.

relevant.

5.2.2 Alignment metrology

In the alignment setting we assume that the trajectory of uniformly accelerated detectors is perturbed by a small harmonic motion, that we could, for instance, ascribe to oscillations of the trajectory of the detector in the cavity frame. These can be understood as time dependent imprecisions in the alignment of the setting with the optical cavity.

Here we study the sensitivity of the detector's response to the amplitude of the harmonic perturbations and characterize the spectral response of the setting to the frequency of perturbations. We consider the spatial perturbation as expressed in equation (5.13). Since in the derivation of the parametrization of the detector's world line (5.15) we linearized in the amplitude of the perturbation ϵ, we only consider small amplitudes $0 < \epsilon < 0.1$ in our study. The sensitivity of the response of the detector as a function of the amplitude ϵ for different values of acceleration and different frequencies are shown in Fig. 5.5a) and b) respectively. We estimate this sensitivity by using the same quantity (5.21) as in the accelerometer setting with the only difference that $P(\epsilon, \gamma)$ represents transition probability of the detector with a spatially perturbed trajectory which is otherwise constantly accelerated.

As shown in Fig. 5.5a) for small accelerations where the system is closer to nonrelativistic regimes, the detector's response shows more sensitivity to the perturbation of its trajectory than in the case of higher accelerations (relativistic regimes). In contrast to the previous case of perturbations in the probe's proper acceleration, we see from Fig. 5.5b) that the detector's response is less sensitive to low frequency perturbations of its spatial trajectory. This is again reasonable, considering that the higher the frequency of perturbations of the spatial trajectory in the lab frame, the more of an effective change they will have on the detector's proper acceleration; a high frequency spatial perturbation in the lab frame corresponds to a large instantaneous change of the proper acceleration of the detector. This in turn affects the response of the detector more dramatically than if the perturbation of the spatial trajectory is slow. As expected, the sensitivity increases monotonically as the amplitude of fluctuations grows, as seen in the figures.

We display in Fig. 5.6 the spectral response of the sensitivity of the probe's excitation probability for a fixed amplitude of the perturbation for different values of the setting parameters: proper accelerations Fig. 5.6a), cavity lengths Fig. 5.6b) and detector gaps Fig. 5.6c).

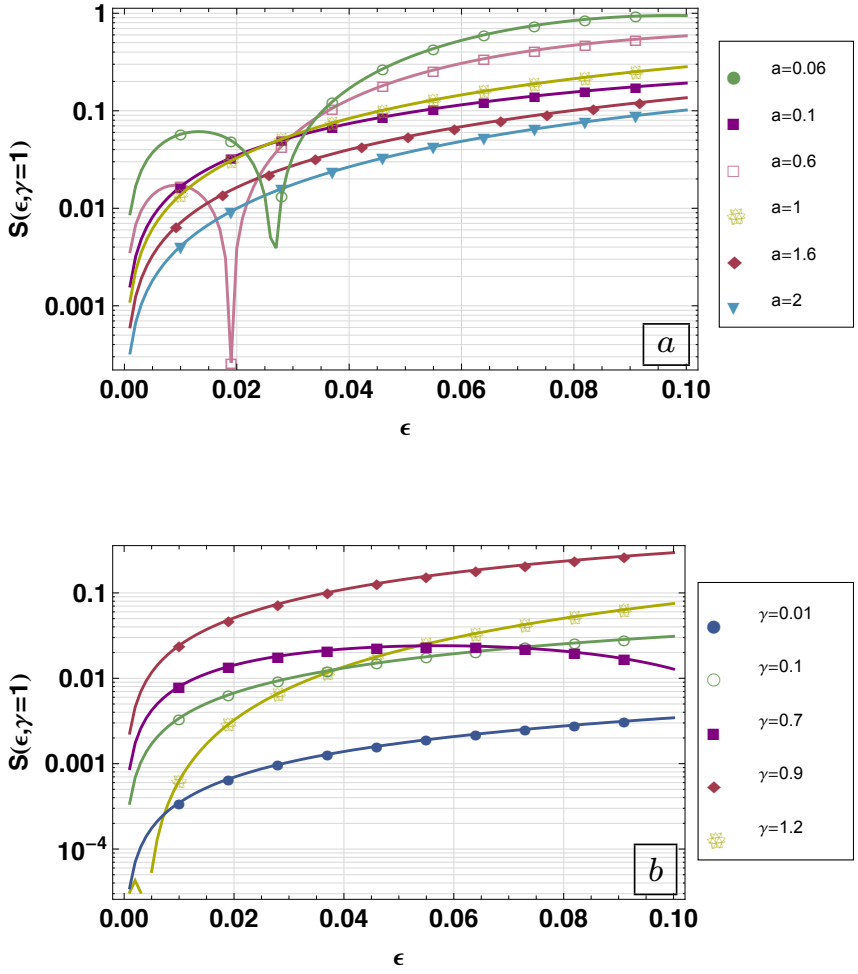

Figure 5.5: (Color online) The sensitivity of the excitation probability of the detector to the amplitude ϵ of the trajectory perturbations for a) different constant accelerations and for b) different frequencies of perturbation.

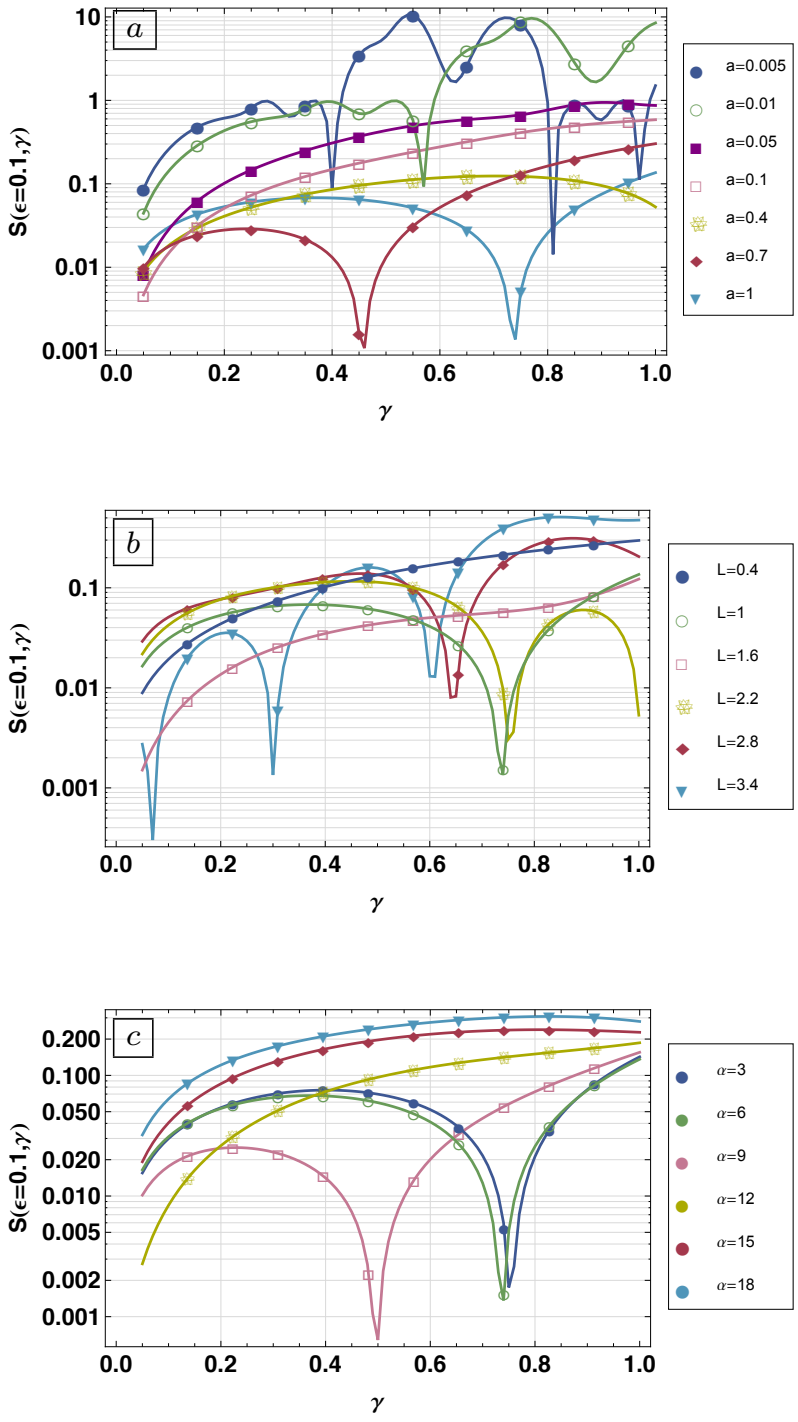

Figure 5.6: (Color online) Spectral response of the detector for a) different accelerations from nonrelativistic regimes ($a = 0.005, 0.01, 0.05$) to relativistic regimes ($a = 0.1, 0.4, 0.7, 1$), b) different lengths of the optical cavity and c) different modes of the field which are in coherent states and coupled to the state of the detector.

The general trend in all cases is that the transition probability of the detector presents dips for specific values of the perturbation frequency γ. In other words, there are some specific perturbation frequencies for which the sensitivity of the setting goes down abruptly, being the position of these dips is a function of the system parameters. This resonance-like effect may be related with the spatial distribution of the cavity modes as seen from the reference frame of the atom whose trajectory is perturbed, but it seems to depend non-trivially on the system parameters and we have not been able to identify its exact origin through numerical analysis.

5.3 Conclusions

We have analyzed the sensitivity of the response of a constantly accelerated atomic probe, traversing an optical cavity, when its trajectory is perturbed. We showed that the probe's transition probability is, in principle, sensitive to small deviations from constant acceleration. We conclude that the transition rate of a beam of atoms transversing optical cavity can provide information about its past spatial trajectory.

We have theoretically studied the potential of the use of an atomic internal quantum degree of freedom to design novel quantum metrology settings. In particular we considered two scenarios: one where the probe undergoes small time-dependent perturbations of its proper acceleration, and another one when the probe's trajectory experiences small spatial time-dependent perturbations as seen from the laboratory's frame.

The first scenario could correspond to an accelerometer setting where we use the internal degree of freedom of the atom to identify small time-dependent forces acting on the probe that will cause it to deviate from constant proper acceleration. The second scenario could correspond to an alignment measurement setting where we use the internal atomic degree of freedom to characterize small vibrations or imperfections of the alignment of an optical cavity with a beam of atoms transversing it.

While an analysis of a proper experimental implementation goes beyond the scope of this chapter, these findings have a potential use in quantum metrology of optical setups. For instance one could compare one setting where all the parameters are known with another setting where they are not known.

In practice, however, the ratio of the probabilities will be subject to significant statistical fluctuations that could mask the effects we have obtained. To achieve the sensitivity levels that are potentially available, the implementation of our scheme will require accumulation of statistics over a number of identical experiments by sending a large number of atomic

probes through the cavity. Thus, by analyzing the transition rates of different atomic beams, one could in principle deduce the specific form of the trajectory of such beams or infer the parameters of the optical cavities they are traversing.

Chapter 6

Strong transient modulation of horizon radiation

Note: The content presented in this chapter can be found in [4]. This work is in collaboration with Achim Kempf.

The spectrum of the Unruh radiation of non-uniformly accelerated trajectories is not thermal and, depending on the extent to which the Unruh radiation is modulated, it can carry information about the trajectory. Analogously, via the equivalence principle, as a black hole accretes matter, its Hawking radiation is not thermal and, depending on the extent to which the Hawking spectrum is modulated, it may carry classical and possibly quantum information about the infalling matter. With this motivation, we here focus on the Unruh effect, answering the long-standing question of to what extent Unruh spectra can be modulated through non-uniform acceleration and, correspondingly, what the optimal trajectories are. Our findings should be of interest also for experimental efforts to detect the Unruh effect.

6.1 Introduction

Our aim here is to answer a long-standing question regarding the Unruh effect, see [5, 20, 37, 47, 51, 97], namely the question of to what extent Unruh spectra can be modulated through non-uniform acceleration and, correspondingly, which trajectories between given initial and final velocities optimize the magnitude of the Unruh effect.

On one hand, our findings should be useful for designing experiments to detect the Unruh effect. On the other hand, our findings should be of interest because the Unruh and Hawking effects [6, 61] are closely related via the equivalence principle: a particle detector stationed close to the horizon of a black hole behaves in many ways similar to a detector in Minkowski space with corresponding acceleration, see [17, 39, 40, 55, 100, 101]. This connects our study here to a long-standing question regarding the Hawking effect: while a black hole accretes matter its Hawking radiation may not be thermal, i.e., it may not be of maximum entropy for the given energy, which means that it may carry classical and potentially quantum information away. In the context of the black hole information loss problem [62, 73, 102–104], a key question is, therefore, to what extent the transient Hawking radiation can be modulated.

From the perspective of the Unruh effect that we will focus on here, there is indeed reason to expect that horizon radiation can be modulated significantly by variations in the acceleration (or, as far as the equivalence principle applies, by variations in a black hole's surface gravity). To see this, we begin by recalling the mechanism behind the Unruh effect. First, any quantum system that can act as a detector of field quanta must contain a charge in order to couple to the field. As the detector is accelerated so is its charge and it will, therefore, radiate, i.e, it will excite the quantum field. The quantum field backreacts by exciting the detector, which is then interpreted as the detector registering Unruh radiation. The formation of a horizon is not strictly necessary for the Unruh effect to occur.

For accelerated classical charges, backreaction effects, such as the Abraham Lorentz force [105] or Feynman and Wheeler's radiation resistance [106], are known to be sensitive to variations in acceleration. It is, therefore, plausible that the Unruh effect can also be significantly modulated by variations in a particle detector's acceleration, i.e., by higher-than-second derivatives in the detector's trajectory. For prior work on detectors with non-uniform acceleration, see, in particular, [2, 41, 49, 97, 107–111]. In the chapter, our main goal is to determine to what extent the Unruh effect can be enhanced or suppressed by a suitable choice of non-uniformly accelerated trajectory, as compared to the uniformly accelerated trajectory with the same initial and final velocities.

6.2 The Setting

While we will not carry out an information theoretic analysis here, the underlying motivation is ultimately information theoretic. Therefore, we will not calculate the magnitude of the overall Unruh effect. Instead, we will calculate for each elementary Unruh process separately how its probability amplitude is affected by non-uniformity of the acceleration.

By an elementary Unruh process we mean a process in which the accelerated detector creates a field quantum of momentum $\boldsymbol{k}$ while transitioning from its ground state of energy E_0 into an excited state of energy E_1.

For simplicity, we consider a free scalar field and we model particle detectors as localized first-quantized two-level systems, so-called Unruh-DeWitt (UDW) detectors with interaction Hamiltonian [5, 17, 24, 37, 45, 95, 112]:

$$\hat{H}_{\rm I} = \lambda\chi(\tau)\hat{\mu}(\tau)\hat{\phi}\left(\mathbf{x}(\tau), t(\tau)\right). \tag{6.1}$$

Here, τ is the proper time of the UDW detector, $(t(\tau), \boldsymbol{x}(\tau))$ is its trajectory, and $\hat{\phi}\left(x(\tau)\right)$ is the field along the trajectory. λ is a small coupling constant and $\chi(\tau) \geq 0$ is a window function to switch the detector. $\hat{\mu}(\tau)$ is the detector's monopole moment operator:

$$\hat{\mu}(\tau) = (\hat{\sigma}^{+} e^{{\rm i}\tau\Delta E} + \hat{\sigma}^{-} e^{-{\rm i}\tau\Delta E}). \tag{6.2}$$

Here, $\Delta E = E_1 - E_0$ is the proper energy gap between the ground state, $|E_0\rangle$, and the excited state, $|E_1\rangle$, of the detector. In Minkowski space, the first-order probability amplitude for an UDW detector to register a particle, i.e., to transition from its ground to its excited state, $|E_0\rangle \to |E_1\rangle$ while creating a particle of momentum $\boldsymbol{k} \in \mathbb{R}^3$ from the vacuum is given by [17],

$$\psi_k(\Delta E) = \eta \int_{-\infty}^{\infty} {\rm e}^{{\rm i}\Delta E\, \tau} {\rm e}^{{\rm i}(\omega_k t(\tau) - \boldsymbol{k}.\boldsymbol{x}(\tau))} \chi(\tau) d\tau, \tag{6.3}$$

where

$$\eta = \frac{{\rm i}\lambda \left\langle E_1 \right| \hat{\mu}_0 \left| E_0 \right\rangle}{(16\pi^3\omega_k)^{1/2}}. \tag{6.4}$$

Apart from a constant prefactor, $\psi_k(\Delta E)$ is the Fourier transform of the τ-dependent function ${\rm e}^{{\rm i}(\omega_k t(\tau) - \boldsymbol{k}.\boldsymbol{x}(\tau))}$. Since the interaction Hamiltonian is time-dependent (as a result of time-dependent trajectory), energy is not conserved. One source of energy here is coming from the agent who transfers energy to the detector to accelerate it and also to the field.

If an always-on detector, $\chi(\tau) \equiv 1$, is on an inertial trajectory through the origin with a velocity $\boldsymbol{v}$, then

$${\rm e}^{{\rm i}(\omega_k t(\tau) - \boldsymbol{k}.\boldsymbol{x}(\tau))} = e^{{\rm i}\tau(\omega_k - \boldsymbol{k}.\boldsymbol{v})(1-\boldsymbol{v}^2)^{-1/2}} = e^{{\rm i}\bar{\omega}\tau}, \tag{6.5}$$

yielding

$$\psi_k(\Delta E) = 2\pi\eta\delta(\Delta E + \bar{\omega}). \tag{6.6}$$

Since $\Delta E \geq 0$ and $\bar{\omega} = (\omega_k - \boldsymbol{k}.\boldsymbol{v})(1-\boldsymbol{v}^2)^{-1/2} > 0$, we have $\psi_k(\Delta E) = 0$, i.e., an always-on inertial detector will not get excited. $\psi_k(\Delta E)$ is non-vanishing for a suitable $\Delta E < 0$. This is the case of an initially excited detector that decays while emitting a field quantum of momentum $\boldsymbol{k}$.

Here, we are interested in the amplitude, $\psi_k(\Delta E)$, for an Unruh process to occur, i.e., for an accelerated detector that starts in the ground state (i.e., $\Delta E > 0$) to get excited in the Minkowski vacuum. This amplitude can be nonzero because of the mathematical phenomenon that a wave that monotonically changes its frequency within a certain (e.g., negative) frequency interval will have a Fourier transform which contains also frequencies outside that interval, including positive frequencies. The mathematical machinery underlying the Fourier Transform (FT) has been widely used in both science and engineering areas such as quantum mechanics, imaging, signal processing and communication. The Fourier transform reveals the frequency composition of a signal (function of time) by transforming it from the time domain into the frequency domain while its inverse combines the contribution of all the frequencies to recover the original signal. There is a mathematical phenomenon that when a wave generator has its frequency vary over time from frequency ω_1 to ω_2, then the Fourier transform of the resulting signal includes not only plateau, namely, the frequencies in the interval from ω_1 to ω_2 but also significantly includes the highly oscillatory frequencies outside that interval on the tail of the FT both in positive and negative frequencies as shown in Fig.6.1.

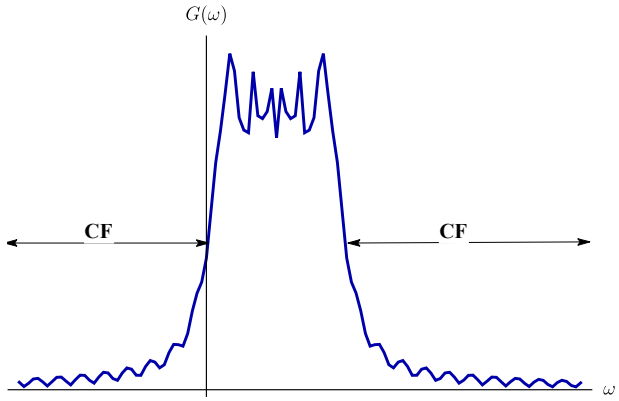

Figure 6.1: Fourier transform of a monotonically increasing function which includes the concomitant frequencies (CF).

The occurrence of such *concomitant frequencies,* is at the heart of the Unruh effect: Intuitively, $e^{i(\omega_k t(\tau) - \boldsymbol{k}.\boldsymbol{x}(\tau))}$ runs through a set of positive values for $\bar{\omega}$, which should prevent

excitation. The Fourier transform, $\psi_k(\Delta E)$, generally shows, however, the presence of both positive and negative frequencies in $\mathrm{e}^{\mathrm{i}(\omega_k t(\tau)-\boldsymbol{k}.\boldsymbol{x}(\tau))}$, i.e., the probability amplitude $\psi_k(\Delta E)$ is nonzero also for $\Delta E > 0$.

A simple example is a detector with constant acceleration, a, and trajectory $(t(\tau), x(\tau)) = (\sinh(a\tau)/a, \cosh(a\tau)/a, 0, 0)$ with $\boldsymbol{k} = (1, 1, 0, 0)$ and $\chi(\tau) \equiv 1$. The Fourier integral Eq.6.3 can be solved using the Gamma function:

$$\psi_k(\Delta E) = \frac{\mu}{a}\sqrt{\frac{\Delta E}{\omega_k}} e^{-\frac{\pi\Delta E}{2a}} e^{\mathrm{i}\frac{\Delta E}{a}\ln(\frac{\omega_k}{a})}\Gamma(-\mathrm{i}\Delta E/a). \tag{6.7}$$

Another example is an always-on detector which, for a finite amount of time, is accelerated so that the frequency increases linearly, preceded and followed by inertial motion. Fig.6.2 shows the Fourier transforms $\psi_k(\Delta E)$ for this trajectory and for a trajectory of uniform acceleration. Both exhibit the presence of concomitant frequencies, including finite amplitudes for positive ΔE which cause the Unruh effect: We expect the Fourier transform for the trajectory of temporary acceleration to contain frequencies within the interval from the initial to the final frequency (on the negative half axis), as well as a peak at either end of the interval because the initial and final velocities are maintained for an infinite amount of time. The Fourier transform contains these features as well as concomitant frequencies on the negative and positive ΔE axes. Similarly the case of the trajectory of uniform acceleration is expected to contain frequencies on the negative ΔE half axis but it also has support on the positive half axis.

Our aim now is to study the origin of the phenomenon of concomitant frequencies in order to determine how strong and how weak the phenomenon can be made, i.e., to what extent $\psi_k(\Delta E)$ can be modulated by choosing trajectories with suitable non-uniform accelerations.

Before we do so, we need to separate off another effect which can also lead to detector excitations in the vacuum, namely the effect of a switching of the detector through a nontrivial function $\chi(\tau)$. Assume that the detector is inertial, which means that in Eq.6.3 the complete integrand, $u(\tau) = \mathrm{e}^{\mathrm{i}\Delta E\tau}\mathrm{e}^{\mathrm{i}(\omega_k t(\tau)-\boldsymbol{k}.\boldsymbol{x}(\tau))}$, takes the form $u(\tau) = e^{\mathrm{i}\int_0^\tau \omega(\tau')\ d\tau'}$ with $\omega(\tau') \equiv \omega$ and $\omega > 0$. Then if the detector is switched on for an integer number of cycles of the integrand, its integral $\psi_k(\Delta E)$ vanishes, $\int_0^{2\pi N/\omega} e^{\mathrm{i}\omega\tau} d\tau = 0$.

However, if the detector is kept on for a non-integer number of cycles (or if $\chi(\tau)$ is a generic smooth switching function), then $\psi_k(\Delta E)$ is finite. The effect is maximal for a half integer number of cycles, in which case $|\psi_k(\Delta E)| = 2/\omega$. Physically, the finite probability for an inertial detector to click due to this truncation effect expresses the time-energy uncertainty principle. Our interest here, however, is not in the time-energy uncertainty

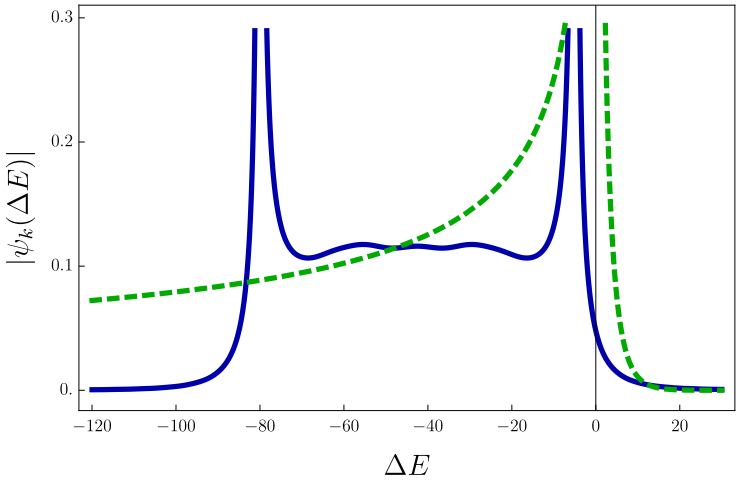

Figure 6.2: The Fourier transform, $|\psi_k(\Delta E)|$, for a trajectory of uniform acceleration (dashed) and a trajectory of temporary acceleration (solid) with the frequencies running through the interval $(5, 80)$. The finite amplitudes on the positive axis show the concomitant frequencies that cause the Unruh effect.

principle but in the phenomenon of concomitant frequencies. Therefore, we now investigate the contribution, $\psi_k^{(N)}(\Delta E)$, of an integer number, N, of complete cycles of the integrand in Eq.6.3, to the $\psi_k(\Delta E)$ of an always-on detector.

We can thereby trace the origin of concomitant frequencies (and acceleration-induced detector clicks in the vacuum) to the fact that the integral over N complete cycles does not need to be zero if the frequency changes during the N cycles. Consider an always-on detector with a trajectory with an integer number, N, of cycles completed in the time interval $[0, \tau_f]$, i.e., $u(0) = u(\tau_f) = 1$. In the integrand $u(\tau) = e^{\mathrm{i}\int_0^\tau \omega(\tau')\ d\tau'}$, when the detector accelerates (or decelerates), $\omega(\tau') > 0$ is a monotonically increasing (or decreasing) function.

We arrive at the extremization problem to find those monotonic functions, $\omega(\tau')$, obeying $0 < \omega(0) < \omega(\tau_f)$ which extremize

$$|\psi_k^{(N)}(\Delta E)| = \left| \int_0^{\tau_f} e^{\mathrm{i}\int_0^\tau \omega(\tau')d\tau'} d\tau \right| \tag{6.8}$$

while completing N cycles. Given $\omega(\tau)$, corresponding trajectories, differing by directions, can then be reconstructed straightforwardly. The question is which $\omega(\tau)$ and corresponding trajectories, i.e., which accelerations as a function of time, contribute maximally or minimally to $\psi_k(\Delta E)$ for fixed $\boldsymbol{k}, \Delta E$, N and for fixed initial and final velocities.

We can solve the corresponding constrained variational problem by using symmetry considerations. To this end, we change the integration variable in Eq.(6.8) by defining $v(\tau) := \int_0^\tau \omega(\tau')d\tau'$, so that $d\tau/dv = 1/\omega(\tau(v))$:

$$\psi_k^{(N)}(\Delta E) = \int_0^{2\pi N} e^{\mathrm{i}v} \frac{1}{\omega(\tau(v))}\, dv. \tag{6.9}$$

The extremization problem is now to find those monotonic functions $\omega(\tau(v))$ which extremize $|\psi_k^{(N)}(\Delta E)|$. The integral is equivalent to calculating the center of mass of a wire of length $2\pi N$ coiled up N times on the unit circle in the complex plane with the wire's mass density at length v being $1/\omega(\tau(v))$. The problem of maximizing $|\psi_k^{(N)}(\Delta E)|$ is now to monotonically vary the mass density of the wire between its prescribed initial and final values $1/\omega(0)$ and $1/\omega(\tau(2\pi N))$ such that the center of mass of the coiled-up wire is as much as possible off center.

For $N = 1$, the answer is clearly to put as much mass as possible on one half circle and as little as possible on the other half. This means that $|\psi_k^{(1)}(\Delta E)|$ is maximal if the initial ω is maintained, $\omega(\tau(\nu)) \equiv \omega(0)$, in the first half of the cycle and then the frequency is abruptly changed to the final frequency which is then maintained, $\omega(\tau(\nu)) \equiv \omega(2\pi)$, for the second half of the cycle. All acceleration happens abruptly mid cycle. The maximum is, therefore:

$$|\psi_k^{(1)}(\Delta E)| = \left| \int_0^{2\pi} \frac{e^{\mathrm{i}v}}{\omega(\tau(v))}\, dv \right| = 2 \left| \frac{1}{\omega(0)} - \frac{1}{\omega(\tau_f)} \right|. \tag{6.10}$$

For $N > 1$, by the same argument, it is optimal to pursue this acceleration regime in one of the cycles and to have all prior and subsequent cycles at constant velocity. Eq.6.10 also shows that the effect of concomitant frequencies can grow as large as

$$2 \max(1/\omega(0), 1/\omega(\tau(2\pi))), \tag{6.11}$$

which is the maximal size of the truncation effect due to the time-energy uncertainty principle.

Conversely, there are trajectories over N cycles that contribute minimally to $|\psi_k(\Delta E)|$. These are the trajectories where all accelerations are abrupt and occur only at the beginnings (or ends) of cycles. In this way, all cycles are individually monochromatic and do not contribute. The minimum is, therefore, $|\psi_k^{(N)}(\Delta E)| = 0$.

We conclude that suitable non-uniform acceleration over N cycles is able to modulate the amplitude, $|\psi_k^{(N)}(\Delta E)|$, for individual Unruh processes within the range $(0, 2\,|1/\omega(0) - 1/\omega(\tau_f)|)$.

This confirms our expectation that suitable nonzero higher-than-second derivatives in trajectories can significantly modulate the Unruh amplitudes $|\psi_k^{(N)}(\Delta E)|$. However, these trajectories are unrealistic in the sense that they are distributional by requiring a sudden contribution of arbitrarily large higher derivatives. The question arises to what extent $|\psi_k^{(N)}(\Delta E)|$ can be modulated by trajectories that are regular in the sense that they possess only a few nonzero higher derivatives and to what extent such trajectories can enhance the Unruh effect compared to trajectories of uniform acceleration with the same initial and final velocities.

In order to calculate those trajectories that optimize $|\psi_k^{(N)}(\Delta E)|$ when allowing only finitely many derivatives to be nonzero, we solved the problem of constrained optimization of $|\psi_k^{(N)}(\Delta E)|$ by finding a suitable trajectory numerically. The trajectory is indirectly represented by a polynomial function, $\omega(\tau)$, of a pre-determined maximal degree, which is monotonically increasing between set initial and final values, within a fixed integer number, N, of cycles.

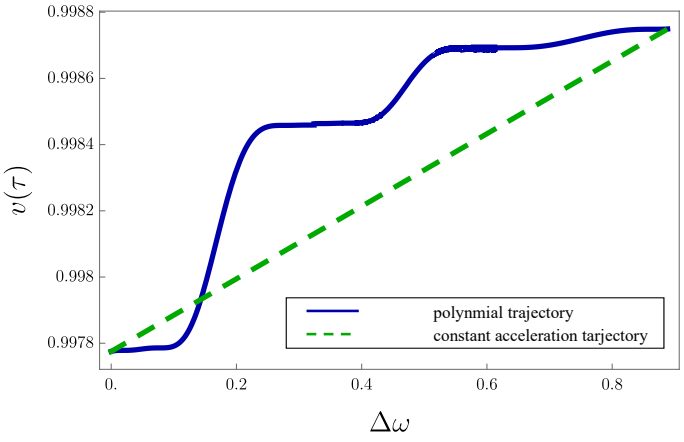

Figure 6.3: The velocity, $v(\tau)$, for a straight line trajectory of uniform acceleration (dashed), and the velocity $v(\tau)$ of a polynomial straight line trajectory that is orthogonal to $\boldsymbol{k}$, of degree 13 and optimizes $|\psi_k^{(3)}(\Delta E)|$ over three cycles (solid).

We remark that since $\omega(\tau)$ is not the trajectory itself, its polynomial expansion is not the same as the standard expansion of a trajectory in terms of acceleration, jerk, snap and higher derivatives, which was used, for example, in the analysis of non-uniform trajectories in [97]. Fig.6.3 compares a trajectory of constant acceleration with the trajectory that maximizes $|\psi_k^{(N)}(\Delta E)|$ among all trajectories of polynomial degree $n \leq 13$ for $N = 3$ cycles and the same overall change in velocity. We notice that the latter trajectory involves

alternating periods of diminished and enhanced acceleration. We can now address to what extent a trajectory with non-uniform acceleration can increase the probability for an elementary Unruh process to occur.

To this end we compare, in Fig.6.4, the moduli of the probability amplitudes $|\psi_k^{(N)}(\Delta E)|$ for elementary Unruh processes for an optimal trajectory (which is of distributional acceleration), for a regular trajectory of non-uniform acceleration that is polynomial of a given degree, and for a trajectory of uniform acceleration, all with the same initial and final velocities. We see that the larger the difference between the initial and final velocities, the more $|\psi_k^{(N)}(\Delta E)|$ can be enhanced by a trajectory of non-uniform acceleration.

We asked to what extent the Hawking spectrum can be modulated by a black hole's growth, and therefore to what extent the modulated Hawking radiation can carry away information about the infalling matter. Via the equivalence principle, this motivated us to determine the extent to which the Unruh spectrum of non-uniformly accelerated trajectories can be modulated.

Technically, we asked how much the probability for an individual Unruh process can be enhanced by choosing a trajectory of suitable non-uniform acceleration while holding fixed the initial and final velocities and the number of cycles. We found that the probability for an Unruh process can be enhanced strongly over its probability for a trajectory of uniform acceleration. $|\psi_k^{(N)}(\Delta E)|$ can reach as high as $2\,|1/\omega(0) - 1/\omega(\tau_f)|$, whose magnitude is comparable to $\max(2/\omega(0), 2/\omega(\tau_f))$, which is the maximal size of the effect due to a sudden switching of the detector. The effect of sudden switching of an UDW detector is known to be very large in the sense that in 3+1 dimensional Minkowski space the cumulative excitation probability obtained by integrating $|\psi_k(\Delta E)|^2$ over all modes $\boldsymbol{k}$, diverges [37, 47, 113].

Further, we determined the condition for the modulation of $|\psi_k(\Delta E)|$ to be strong by analysing the origin of concomitant frequencies. We found that the condition is that there is a significant change in frequency within one cycle, i.e, that the trajectory is non-adiabatic in this sense. Let us now estimate if this condition can realistically be met in the cases of the Unruh and Hawking effects. The Unruh temperature for a trajectory of uniform acceleration, a, is $T = a/2\pi$, with the dominant radiation at a wavelength of $\lambda \approx 1/a$, in natural units. Therefore, to significantly modulate the dominant Unruh processes, the acceleration needs to significantly change at or below the time scale $\lambda \approx 1/a$.

To the extent that the equivalence principle applies, this indicates that for the dominant modes of Hawking radiation to be modulated significantly by an infalling body, the time scale for the black hole to settle after accreting the body should be at or below the oscillation time scale of the dominant wavelength of the Hawking radiation. Since these time scales are of the same order, namely of the order of the formal light crossing time of

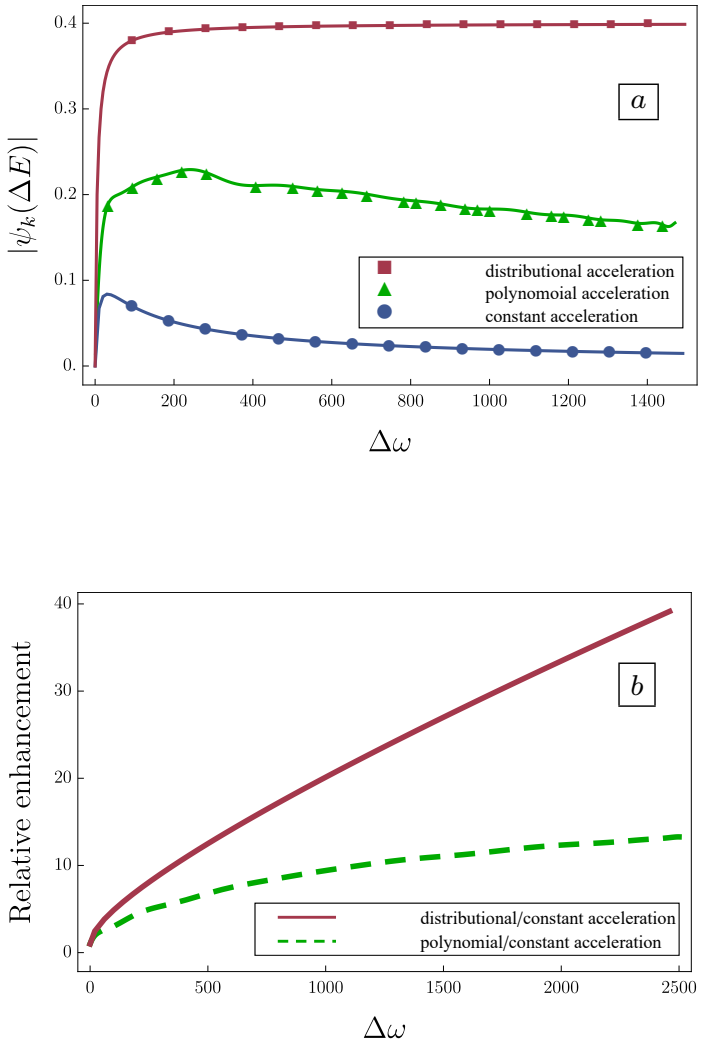

Figure 6.4: (a) Contribution to $|\psi_k(\Delta E)|$ by one cycle, as a function of $\Delta\omega$ for a trajectory of constant acceleration (circles), for a polynomial trajectory (triangles), and for a trajectory with a distributional acceleration (squares). (b) Relative enhancement of elementary Unruh processes: the two curves show the ratio of the two upper curves by the lowest curve of Fig.6.4a. Here, the initial frequency is $\omega(0) = 5$ and the energy gap of the detector is $\Omega = 3$.

the Schwarzschild radius, our results indicate that the spectrum of Hawking radiation may indeed be significantly modulated by the transient non-adiabaticity caused by infalling matter.

Going forward, it may not be necessary to continue to invoke the equivalence principle to transfer results about the Unruh effect to the Hawking effect. Instead, our new approach to concomitant frequencies may be useful directly in any study of the modulation of Hawking radiation and the amount of classical and quantum information it can carry away. This is because any such calculation should in some regime yield a modulation of Bogolyubov β coefficients and these are in effect concomitant frequencies: to choose a definition of the vacuum state is to choose a definition of what constitutes positive frequencies in mode functions. The Bogolyubov β coefficients that arise with a change of vacuum are then the amplitudes of negative frequencies that arise from the varying of positive frequencies. For example, in the case of uniform acceleration, the same integral as that leading to Eq.6.7 arises in the calculation of the Bogolyubov β coefficients, see, e.g., [55]. It should, therefore, be of interest to try to adapt and apply the new method of concomitant frequencies directly in any of the various models for how Hawking radiation could be modulated by infalling matter, models such as those discussed in [62, 64, 65, 72, 73].

Chapter 7

Classicality of a Quantum Oscillator

Note: The content presented in this chapter can be found in [3]. This work is in collaboration with Robert B. Mann, and Daniel R. Terno.

Gaussian quantum systems exhibit many explicitly quantum effects, but can be simulated classically. Using both the Hilbert space (Koopman) and the phase-space (Moyal) formalisms we investigate how robust this classicality is. We find failures of consistency of the dynamics of hybrid classical-quantum systems from both perspectives. By demanding that no unobservable operators couple to the quantum sector in the Koopmanian formalism, we show that the classical equations of motion act on their quantum counterparts without experiencing any back-reaction, resulting in non-conservation of energy in the quantum system. Using the phase-space formalism we study the short time evolution of the moment equations of a hybrid classical-Gaussian quantum system, and observe violations of the Heisenberg Uncertainty Relation in the quantum sector for a broad range of initial conditions. We estimate the time scale for these violations, which is generically rather short. This inconsistency indicates that while many explicitly quantum effects can be represented classically, quantum aspects of the system cannot be fully masked. We comment on the implications of our results for quantum gravity.

7.1 Concise review of Gaussian quantum mechanics

In this section we give a brief introduction to the formalism of Gaussian quantum mechanics (GQM), including the definition of Gaussian states, operations, and measurements. There are a number of complete introductions and reviews to the topic such as [114, 115],

and specifically in the context of particle detectors in [78]. Gaussian continuous variable quantum information processes are mainly of interest in quantum communication, quantum teleportation, relativistic quantum field theory, and quantum optics. Gaussian framework provides applicable theoretical and experimental tools for a wide variety of tasks and applications in the field of quantum information.

Consider a continuous-variable quantum system such as N quantum harmonic oscillators which could be N bosonic modes. These N modes are corresponding to N pairs of annihilation and creation operators $\{\hat{a}_i, \hat{a}_i^\dagger\}$. This system can also be described by the quadrature field operators, $\{\hat{q}_i, \hat{p}_i\}$ arranged in the form of the vector

$$\hat{\mathbf{x}} = (\hat{q}_1, \hat{p}_1, ..., \hat{q}_N, \hat{p}_N)^T \tag{7.1}$$

The field operators are dimensionless canonical observables of the system which satisfy the canonical commutation relations

$$[\hat{x}_i, \hat{x}_j] = \mathrm{i}\Omega_{ij}, \tag{7.2}$$

where Ω_{ij} are the entries of a symplectic form matrix given by

$$\mathbf{\Omega} = \bigoplus_{i=1}^{N} \begin{pmatrix} 0 & 1 \\ -1 & 0 \end{pmatrix}. \tag{7.3}$$

The relation between the quadrature operators and creation and annihilation operators of each mode is given by

$$\hat{q}_i = \frac{1}{\sqrt{2}}(\hat{a}_i + \hat{a}_i^\dagger), \qquad \hat{p}_i = \frac{\mathrm{i}}{\sqrt{2}}(\hat{a}_i^\dagger - \hat{a}_i). \tag{7.4}$$

In general, the quantum state of a system of N-bosonic modes can be presented by a density matrix $\hat{\rho}$ which is a trace-one positive operator acting on the corresponding Hilbert space. This density operator can also be represented in terms of a quasi-probability distribution or Wigner function in the phase space. The Wigner function is a Fourier transform of a Wigner characteristic function $\chi(\xi)$ and has the form

$$W(\mathbf{x}) = \int_{\mathbb{R}^{2N}} \frac{d^{2N}\xi}{(2\pi)^{2N}} \exp\left(-\mathrm{i}\mathbf{x}^T\Omega\xi\right)\chi(\xi). \tag{7.5}$$

The Wigner functions are characterized by the statistical moments of a quantum state. The first moment is the mean value and the second moment is the covariance matrix σ given by

$$\begin{aligned} \langle \hat{\mathbf{x}} \rangle &= Tr(\hat{\mathbf{x}}\hat{\rho}), \\ \sigma_{ij} &= \frac{1}{2} \langle \{\Delta\hat{x}_i, \Delta\hat{x}_j\} \rangle = \frac{1}{2}(\langle \hat{\mathbf{x}}_i\hat{\mathbf{x}}_j + \hat{\mathbf{x}}_j\hat{\mathbf{x}}_i \rangle - 2 \langle \hat{\mathbf{x}}_i \rangle \langle \hat{\mathbf{x}}_j \rangle). \end{aligned} \tag{7.6}$$

In the case of a Gaussian state, the first two moments characterize the Wigner function fully. There are a number of important classes of pure, Gaussian states including the vacuum state with covariance matrix $\sigma_{vac} = I_{2N}$. Note that Gaussian states are pure iff its Wigner function is non-negative. Single-mode squeezed vacuum states are pure states with a covariance matrix of the form

$$\sigma_{sq} = \begin{pmatrix} \mathrm{e}^{-r} & 0 \\ 0 & \mathrm{e}^{r} \end{pmatrix}, \tag{7.7}$$

where r is the squeezing parameter. Squeezed states share the minimum uncertainty principle. Thermal states are another group of Gaussian states with the covariance matrix of the form

$$\sigma_T = \bigoplus_{i=1}^{N} \begin{pmatrix} \nu_i & 0 \\ 0 & \nu_i \end{pmatrix}, \tag{7.8}$$

where

$$\nu_i = \frac{\exp(\omega_i/T) + 1}{\exp(\omega_i/T) - 1}, \tag{7.9}$$

and T is temperature of the thermal state.

7.2 Introduction to hybrid classical-quantum systems

The shifting boundary between quantum and classical regimes [116,117] is a long-standing subject of scrutiny, both for its foundational and technical aspects. Indeed, the emergence of classical behaviour from the underlying quantum structure is still a controversial subject with several attempts aiming to address and resolve it such as [118]. To this end, semi-classical methods play an important role both in quantum mechanics and quantum field theory.

From a purely pragmatic viewpoint, it often happens that some degrees of freedom can be much easier described classically, commonly to an excellent degree of approximation. However either for consistency (e.g., in semiclassical quantum gravity, [119]), or for practical purposes (e.g., study of chemical reactions) it becomes necessary to follow their interaction with other degrees of freedom that must be described by quantum mechanics. Indeed, there have been several attempts to formulate a consistent hybrid classical-quantum (CQ) theory [120–126], each with varying results [126, 127].

Both fundamental and practical aspects were explored in recent efforts investigating the equivalence of Gaussian Quantum Mechanics (GQM) and classical statistical mechanics (more precisely, epistemically-restricted Liouville mechanics (ERL)) [128, 129]. GQM [115, 130] restricts allowed states only to the so-called Gaussian states that have Gaussian Wigner quasiprobability distribution [131], and transformations and measurements that preserve this property. A positive Wigner distribution can be interpreted as a probability density on the phase space of a corresponding classical system. By imposing epistemic restrictions on Liouville classical mechanics — postulating that conjugate quantities cannot be known with precision better than the fundamental quantum uncertainty — one can assign classical statistical interpretations (probability distributions) to those Gaussian procedures, allowing a phenomenon to be described equivalently in both languages [128,129]. Remarkably, ERL captures many phenomena that are usually considered explicitly quantum, including entanglement (though not the ability to violate Bell-type inequalities), while being describable by local hidden variable theory.

These results indicate that a Gaussian quantum system behaves classically in some important respects. An interesting complementary question is then to what extent GQM can be regarded as fully classical, or alternatively, whether or not GQM inevitably displays tell-tale signs of quantum physics. For an isolated Gaussian system a specific question along these lines concerns the behaviour of the expectation values of reasonable classical observables (to be defined precisely in Sec. 7.4). Another is that of the dynamics of interacting Gaussian and classical systems, and the pre-requisites for a consistent description of such dynamics. Such mixed dynamics is used to treat a variety of phenomena that range from gas kinetics and dynamics of chemical reactions to one-loop quantum gravity. Indeed, this latter question is of particular importance in the ongoing discussion as to whether or not gravity should be quantized.

Motivated by the above, our goal in this chapter is to investigate the consistency of combined classical and Gaussian quantum systems, or CGQ. If a Gaussian quantum system is indeed equivalent (under certain criteria) to a classical system, then its coupling to another classical system should be consistent with this equivalence whilst retaining the intrinsic quantum characteristics of the former. In particular, can CGQ ensure that quantum

sector of the system respects the uncertainty principle?

A Gaussian Hamiltonian is at most quadratic in canonical variables and, as a result, perfectly satisfies the correspondence principle: equations of motion for quantum dynamical variables are the same as their classical counterparts. Thus it is natural to investigate if the different mathematical structures used to describe classical and quantum systems can be made fully compatible.

We first investigate this question from the perspective of the Koopmanian formalism of mechanics in Sec. 7.3. In this approach, both quantum and classical systems are described by wave functions on their respective Hilbert spaces. It is known that the Hilbert space description of a classical system is fully consistent and sometimes advantageous. We consider one quantum and one classical harmonic oscillator and the most general Gaussian interaction coupling the two. We find that various inconsistencies appear for any non-trivial bilinear interaction.

The phase-space description of a combined quantum-classical system that we use in Sec. 7.4 is based on the opposite approach. It is possible to describe the evolution of a quantum system on its classical phase space if Moyal brackets replace Poisson brackets. The two coincide for a harmonic oscillator, giving an additional interpretation to the results of [128]. If again the classical and quantum oscillators are linearly coupled, preservation of the Heisenberg uncertainty relation for the quantum oscillator requires introduction of a minimal uncertainty in the classical one. This is again consistent with a view that effectively replaces classical mechanics (that allows, in principle, for infinite precision) with a statistical description that evolves according to the classical dynamical laws. In Sec. 7.4 we show how prior correlations between classical and quantum systems and/or different non-quadratic classical potentials lead to violation of the uncertainty relation for the quantum initially Gaussian system.

We discuss the implication of these results and the connection to the logical necessity to quantize gravity in the concluding section.

7.3 Hilbert space picture

We start with a brief discussion of the Koopmanian formalism, followed by applying it to the most general interacting Gaussian system with two degrees of freedom, one treated classically and the other quantum-mechanically. A more detailed presentation of the mathematical aspects of this approach can be found in [132,133], while applications to measurement theory, entanglement, and mixed states were discussed in [116, 126]. For simplicity

we consider a single degree of freedom and denote the canonical variables as x and k (we reserve the symbols p and q for the momentum and position (operators) of a quantum system, to be introduced later). Consider the Liouville equation for a system with the phase space variables (x, k), the Hamiltonian $H(x, k)$, and the probability density $f(x, k)$,

$$\mathrm{i}\,\partial f/\partial t = Lf, \tag{7.10}$$

where L is the Liouville operator, or Liouvillian,

$$L = \left(\frac{\partial H}{\partial k}\right)\left(-\mathrm{i}\frac{\partial}{\partial x}\right) - \left(\frac{\partial H}{\partial x}\right)\left(-\mathrm{i}\frac{\partial}{\partial k}\right). \tag{7.11}$$

Since the Liouville density f is never negative it is possible to introduce likewise a function

$$\psi_c \equiv \sqrt{f}, \tag{7.12}$$

which in this case satisfies the same equation of motion as f,

$$\mathrm{i}\,\partial\psi_c/\partial t = L\psi_c. \tag{7.13}$$

It has the structure of the Schrödinger equation with the Liouvillian taking the role of the generator of time translations, and its self-adjointness can be established under mild conditions of the potential [132, 133]. Hence we can interpret ψ_c as "classical wave function."

We shall now consider ψ as the basic object. However, for our classical system only $f = |\psi|^2$ has a direct physical meaning. It can be proven that, under reasonable assumptions about the Hamiltonian, the Liouvillian is an essentially self-adjoint operator and generates a unitary evolution [132, 133]:

$$\langle\psi_c|\phi_c\rangle := \int \psi_c(x,k,t)^*\,\phi_c(x,k,t)\,dxdk = \text{const.} \tag{7.14}$$

Note that while the classical wave function of Eq. (7.12) is real, complex-valued functions naturally appear in this space, which can be extended to a Hilbert space with inner product given by (7.14) above [116]. It is possible to further mimic quantum theory by introducing *commuting* position and momentum operators $\hat{x}$ and $\hat{k}$, defined by

$$\hat{x}\,\psi_c = x\,\psi_c(x,k,t) \qquad \text{and} \qquad \hat{k}\,\psi_c = k\,\psi_c(x,k,t), \tag{7.15}$$

respectively. Note that the momentum $\hat{k}$ is not the shift operator (the latter is $\hat{p}_x = -\mathrm{i}\partial/\partial x$). Likewise the boost operator is $\hat{p}_k = -\mathrm{i}\partial/\partial k$. These two operators are not observable. We shall henceforth omit the hats over the classical operators when there is

no danger of confusion. The physical quantities are represented by x and k. The operators $\hat{p}_x$ and $\hat{p}_k$ generate translations in the variables x and k, respectively.

What we have above is a "Schrödinger picture" (operators are constant, wave functions evolve in time as $\psi(t) = U(t)\psi(0)$, where the unitary operator $U(t) = e^{-\mathrm{i}Lt}$ if the Hamiltonian is time-independent). We can also define a "Heisenberg picture" [126] where wavefunctions are fixed and operators evolve:

$$X_H(t) = U^\dagger X U. \tag{7.16}$$

The Heisenberg equation of motion

$$\mathrm{i}\, dX_H/dt = [X_H, L_H] = U^\dagger [X, L]\, U, \tag{7.17}$$

together with the Liouvillian (7.11), readily give Hamilton's equations

$$\frac{dx}{dt} = \frac{\partial H}{\partial k}, \qquad \frac{dk}{dt} = -\frac{\partial H}{\partial x}. \tag{7.18}$$

This formalism allows one to describe the states of classical and quantum systems in a single mathematical framework, namely in the joint Hilbert space $\mathcal{H} = \mathcal{H}_q \otimes \mathcal{H}_c$. Since we are dealing with the Hilbert spaces, the concepts of a partial trace and entanglement (including the one between classical and quantum states) are naturally defined.

In the following we discuss coupled classical and quantum harmonic oscillators with the frequencies ω_c and ω_q, respectively. To simplify the analysis we use dimensionless canonical variables. For a quantum oscillator we set the position and the momentum scales as l and $l_p = \hbar/l$, by defining $\bar{q} := q/l$ and $\bar{p} := p/l_p$, respectively. For a classical oscillator the scales are set by λ and $\lambda_k = \kappa/\lambda$, where κ is a parameter with the units of action. The scales are set as

$$l = \sqrt{\frac{\hbar}{m\omega_q}}, \qquad l_p = \frac{\hbar}{l} = \sqrt{\hbar m \omega_q}, \tag{7.19}$$

$$\lambda = \sqrt{\frac{\kappa}{m\omega_c}}, \qquad \lambda_k = \frac{\kappa}{\lambda} = \sqrt{\kappa m \omega_c}, \tag{7.20}$$

so

$$[\bar{q}, \bar{p}] = [\bar{x}, \bar{p}_x] = [\bar{k}, \bar{p}_k] = 1 \tag{7.21}$$

and the Hamiltonians can be expressed as

$$H_q = \tfrac{1}{2}\hbar\omega_q\big(\bar{q}^2 + \bar{p}^2\big), \qquad H_c = \tfrac{1}{2}\kappa\omega_c\big(\bar{x}^2 + \bar{k}^2\big). \tag{7.22}$$

In terms of creation and annihilation operators, the most general bilinear Hermitian term coupling the quantum and classical systems is

$$K_i = \mathrm{i}\left(\beta^*_{0x} a b_x - \beta_{0x} b^\dagger_x a^\dagger + \beta^*_{0k} a b_k - \beta_{0k} b^\dagger_k a^\dagger\right) + \alpha_{0x} a^\dagger b_x + \alpha^*_{0x} b^\dagger_x a + \alpha_{0k} a^\dagger b_k + \alpha^*_{0k} b^\dagger_k a. \quad (7.23)$$

Using the relations $\alpha_{0x} = \alpha^{(1)}_{0x} + \mathrm{i}\alpha^{(2)}_{0x}$ and $\beta_{0x} = \beta^{(1)}_{0x} + \mathrm{i}\beta^{(2)}_{0x}$, and similar ones for α_{0k} and β_{0k}, and demanding that no unobservable operators are coupled to the quantum sector, we obtain the following form for the equations of motion

$$\begin{aligned} \dot{\bar{q}} &= \omega_q \bar{p} + 2\alpha^{(2)}_{0x}\bar{x} + 2\alpha^{(2)}_{0k}\bar{k}, & \dot{\bar{p}} &= -\omega_q \bar{q} - 2\alpha^{(1)}_{0x}\bar{x} - 2\alpha^{(1)}_{0k}\bar{k}, \\ \dot{\bar{x}} &= \omega_c \bar{k}, & \dot{\bar{k}} &= -\omega_c \bar{x}, \\ \dot{\bar{p}}_x &= \omega_c \bar{p}_k - 2\beta^{(2)}_{0x}\bar{q} + 2\beta^{(1)}_{0x}\bar{p}, & \dot{\bar{p}}_k &= -\omega_c \bar{p}_x - 2\beta^{(2)}_{0k}\bar{q} + 2\beta^{(1)}_{0k}\bar{p}. \end{aligned} \quad (7.24)$$

See Appendix A for a detailed derivation of these results.

Providing an alternative derivation of the results in [125, 126], we observe that the classical position and momentum act on their quantum counterparts as external forces without experiencing any backreaction. This bizarre state of affairs also brings the system to resonance when $\omega_c = \omega_q$, describing an unlimited increase of energy of the quantum oscillator, similar to [125, 126].

7.4 Phase space picture

The phase-space formulation of quantum mechanics provides us with an alternative way of analyzing hybrid quantum-classical systems. In this formulation, which is based on the Wigner function, the quantum mechanical operators are associated with c-number functions in the phase space using Weyl's ordering rule [131]. The quantum mechanical features of operators in Hilbert space, such as their noncommutativity, represents itself in the noncommutative multiplication of c-number functions through the Moyal $\star$-product in the phase space, which corresponds to the Hilbert space operator product.

In classical mechanics the evolution of a dynamical variable, represented by an arbitrary function of the form $f(x, k, t)$ in a phase space whose conjugate variables are (x, k), is described by Hamilton's equations of motion. These equations are

$$\frac{d}{dt} f(x, k, t) = \{f, H\} + \frac{\partial}{\partial t} f(x, k, t), \quad (7.25)$$

where $\{\cdot\,,\cdot\}$ is the Poisson bracket and H is a classical Hamiltonian. In quantum mechanics one can obtain an analogous phase space description by replacing the Poisson with the Moyal bracket, and the Liouville function with the Wigner function $W(x,k,t)$. The Moyal evolution equation is given by [134, 135]

$$\frac{\partial}{\partial t}W(x,k,t) = \frac{H\star W - W\star H}{\mathrm{i}\hbar} \equiv \{\!\{W,H\}\!\}, \tag{7.26}$$

where $\{\!\{\cdot\,,\cdot\}\!\}$ represents the Moyal bracket and the $\star$-product is defined as

$$\star \equiv \mathrm{e}^{\frac{\mathrm{i}\hbar}{2}\left(\overleftarrow{\partial_x}\overrightarrow{\partial_k} - \overleftarrow{\partial_k}\overrightarrow{\partial_x}\right)}, \tag{7.27}$$

where $\overleftarrow{\partial}$ means that the derivative acts on the function to its left and $\overrightarrow{\partial}$ acts on the function to its right. One can represent the Moyal bracket with a Poisson bracket plus correction terms

$$\{\!\{W,H\}\!\} = \{W,H\} + \mathcal{O}(\hbar). \tag{7.28}$$

It is also important to note that for quadratic Hamiltonians the Moyal bracket reduces to the Poisson bracket.

The question of equivalence of quantum and classical descriptions makes sense in the following context. A positive initial Wigner function $W(x,k,t=0)$ that corresponds to the quantum state $\hat{\rho}(t=0)$ can be identified with the Liouville function, $f(t=0) \leftarrow W(t=0)$. This function is evolved classically by Eq. (7.25), and then the reverse identification is made: $W(t) \leftarrow f(t)$. If this represents a valid quantum state ρ_f the procedure is consistent. If, furthermore, the phase space expectation values, calculated with $f(t)$ or, equivalently, the quantum expectations calculated with $\hat{\rho}_f(t)$ are the same as the expectations that are obtained with the quantum-evolved state $\hat{\rho}(t)$, the two descriptions are equivalent.

This is the context of the statement of equivalence of GQM and classical statistical mechanics. Already at this stage, however, we point a minor issue that directly follows from properties of the Wigner function [131]. The phase space expectation with W_ρ is equivalent to the Weyl-ordered expectation with the state ρ. If the expectation of a different combination of operators needs to be evaluated, it cannot be done directly in the phase space; rather the Liouville/Wigner function needs first to be converted to the corresponding quantum state.

Let us consider a system with two degrees of freedom with the Hamiltonian

$$H = \frac{1}{2}\left(p^2 + k^2\right) + V(q,x), \tag{7.29}$$

where (q, p) and (x, k) are the canonical pairs for the first and the second subsystems, respectively. As before, we use the dimensionless canonical variables and $\hbar \to 1$.

We consider the most general form of the potential given by

$$V(q, x) = U_1(q) + U_2(x) + U(q, x). \tag{7.30}$$

Mixed quantum-classical dynamics, with substitution of Moyal brackets for Poisson brackets in the quantum subsystem, may be either a good approximation or produce unphysical results. A clear signature of the latter would be violation of the Heisenberg uncertainty relation for the presumably quantum subsystem.

The subsequent analysis can be thought as an investigation of the consistency of the phase-space based mixed quantum-classical dynamics, where the first pair (q, p) is a quantum system, that unless specified otherwise is a harmonic oscillator ($U_1(q) = \alpha q^2/2$), whilst the classical potential $U_2(x)$ and the interaction term $U(q, x)$ are general. Alternatively, it can be viewed as an investigation of how the phase-space description of the quantum dynamics breaks down. From either perspective, since Gaussian states are particularly well-behaved, we assume that the initial Wigner functions and/or Liouville distributions are of Gaussian form.

To observe the violation of uncertainty relations we must trace the evolution of statistical moments in time. Here we briefly review their basic properties and the role in characterization of Gaussian states.

The quantum moments are defined as

$$M^{a,b} \equiv \left\langle \delta\hat{q}^a \delta\hat{p}^b \right\rangle_{\text{ord}}, \tag{7.31}$$

where the subscript 'ord' refers to a particular ordering, e.g. symmetric or Weyl, and the expectation value of an operator $\hat{A}$ is given by the trace formula

$$\left\langle \hat{A} \right\rangle = \text{tr}(\hat{\rho}\hat{A}). \tag{7.32}$$

The quantities $\delta\hat{q} = \hat{q} - \langle\hat{q}\rangle$ and $\delta\hat{p} = \hat{p} - \langle\hat{p}\rangle$ are the operators for deviations from the mean (expectation) values, and the sum of the indices $(a + b)$ is the order of the moment $M^{a,b}$.

Analogously, we define the classical moments as

$$M_C^{a,b} \equiv \left\langle \delta x^a \delta k^b \right\rangle, \tag{7.33}$$

where $\delta x = x - \langle x \rangle$ and $\delta k = k - \langle k \rangle$ are deviations from the mean values of position and momentum respectively in the classical system. The mean (average) value of a function $A(x,k)$ is obtained by using the Liouville density $f(x,k,t)$,

$$\langle A(t) \rangle = \int_{-\infty}^{\infty} \int_{-\infty}^{\infty} A(x,k) f(x,k,t) dx\, dk. \tag{7.34}$$

We shall use angle brackets for both classical means and quantum expectation values, employing (7.32) and (7.34) as appropriate.

A Gaussian state $\hat{\rho}$ has a Gaussian characteristic function which its Fourier transform gives us a (Gaussian) Wigner function [115, 130],

$$W(\boldsymbol{X}) = \frac{\exp\left[-1/2(\boldsymbol{X}-\boldsymbol{\mu})^T \boldsymbol{\sigma}^{-1}(\boldsymbol{X}-\boldsymbol{\mu})\right]}{(2\pi)^N \sqrt{\det \boldsymbol{\sigma}}}, \tag{7.35}$$

where $\boldsymbol{\mu} \equiv \langle \boldsymbol{X} \rangle$ and where σ is a covariance matrix, namely, the second moment of the state $\hat{\rho}$. By definition, a Gaussian probability distribution can be completely described by its first and second moments; all higher moments can be derived from the first two using the following method

$$\left\langle (\boldsymbol{X}-\boldsymbol{\mu})^k \right\rangle = 0 \qquad \text{for odd } k, \tag{7.36}$$

$$\left\langle (\boldsymbol{X}-\boldsymbol{\mu})^k \right\rangle = \sum (c_{ij}...c_{xz}) \qquad \text{for even } k \tag{7.37}$$

also known as Wick's theorem [136]. The sum is taken over all the different permutations of k indices. Therefore we will have $(k-1)!/(2^{k/2-1}(k/2-1)!)$ terms where each consists of the product of $k/2$ covariances $c_{ij} \equiv \langle (X_i - \mu_i)(X_j - \mu_j) \rangle$.

Epistemically-restricted Liouville mechanics (ERL) [128] is obtained by adding a restriction on classical phase-space distributions, which are the allowed epistemic states of Liouville mechanics. These restrictions are *the classical uncertainty relation (CUP)* and *the maximum entropy principle (MEP)*. CUP implies that the covariance matrix of the probability distribution $\boldsymbol{\chi}$ must satisfy the inequality

$$\boldsymbol{\chi} + \mathrm{i}\epsilon \boldsymbol{\Omega}/2 \geq 0, \tag{7.38}$$

where ϵ is a free parameter of ERL theory and $\boldsymbol{\Omega}$ is known as the symplectic form [115, 130]. To reproduce GCM we must set $\epsilon = \hbar$. The MEP condition requires that the phase-space distribution of the covariance matrix $\boldsymbol{\chi}$ has the maximum entropy compared to all the distributions with the same covariance matrix. Any distribution that satisfies these two conditions is a valid epistemic state and can be equivalently described by a Gaussian state.

Now consider a system of two interacting degrees of freedom. Its initial state (quantum, classical or mixed) is Gaussian, i.e. fully described by the first two statistical moments. If the system is in a valid quantum or ERL state, its covariance matrix $\boldsymbol{\sigma}$ is non-negative, namely,

$$\boldsymbol{\sigma} + \mathrm{i}\boldsymbol{\Omega}/2 \geq 0, \tag{7.39}$$

This condition requires that all the symplectic eigenvalues of the covariance matrix be non-negative or equivalently, its leading principal minors be all non-negative. Having the symplectic matrix organized in pairs of coordinates for each oscillator as (q, p, x, k), the covariance matrix $\boldsymbol{\sigma}$ describing the state of the entire system can be decomposed as

$$\boldsymbol{\sigma} = \begin{pmatrix} \boldsymbol{\sigma}_Q & \boldsymbol{\gamma}_{QC} \\ \boldsymbol{\gamma}_{QC}^T & \boldsymbol{\sigma}_C \end{pmatrix}, \tag{7.40}$$

where $\boldsymbol{\sigma}_Q$, $\boldsymbol{\sigma}_C$ are 2×2 covariance matrices that describe the reduced states of respective subsystems Q and C. The 2×2 matrix $\boldsymbol{\gamma}_{QC}$ encodes the correlations between the two subsystems.

As discussed above we take the initial state of the entire system to be Gaussian. The first moments at the time $t = 0$ are

$$\langle \hat{q}(0) \rangle = q_0, \qquad \langle \hat{p}(0) \rangle = p_0, \qquad \langle x(0) \rangle = x_0, \qquad \langle k(0) \rangle = k_0, \tag{7.41}$$

and the reduced correlation matrices are

$$\boldsymbol{\sigma}_Q = \begin{pmatrix} 1/2 + z_1 & \langle \delta p \delta q \rangle \\ \langle \delta p \delta q \rangle & 1/2 + z_2 \end{pmatrix}, \quad \boldsymbol{\sigma}_C = \begin{pmatrix} 1/2 + y_1 & 0 \\ 0 & 1/2 + y_2 \end{pmatrix}. \tag{7.42}$$

where to simplify the exposition we assume a diagonal correlation matrix for the system C.

Up to now these are simply two distinct systems. Anticipating the uncertainty relation, we consider the first system Q to be quantum-mechanical and the second system C to be classical, and parametrize

$$\langle \delta q^2 \rangle \equiv \tfrac{1}{2} + z_1, \qquad \langle \delta p^2 \rangle \equiv \tfrac{1}{2} + z_2, \tag{7.43}$$

with analogous meanings for y_1 and y_2 for the system C. By definition z_1, z_2, y_1, and y_2 can take any value from $(-1/2, \infty)$. The classical-classical correlations (CC) are assumed to be zero for simplicity. Depending on how squeezed the state can get and how two systems are interacting with each other through correlation matrices, one can determine a

specific range for these free parameters while satisfying the positivity condition (7.39) of the covariance matrix of the whole ensemble.

It is straightforward to show that for the Gaussian quantum subsystem alone the Heisenberg Uncertainty Relation (UR) is

$$f(t) = \left\langle \delta p^2 \right\rangle \left\langle \delta q^2 \right\rangle - \left\langle \delta q \delta p \right\rangle^2 - \frac{1}{4} \geq 0. \tag{7.44}$$

The same requirement holds for the classical subsystem only if it is in a valid ERL state.

Instead of evolving the quantum state or the Liouville density, it is possible to follow the (generally infinite) hierarchy of statistical moments [137, 138]. To find the moment equations we use the general formula for the time derivatives of the classical moments [137], as detailed in Appendix A.2. As we are not looking for numerical solutions to these equations but rather wish only to probe for (lack of) consistency, we study their short-term temporal behaviour via series expansions. We therefore write

$$\left\langle \delta p^2 \right\rangle \equiv \sum_{n=0}^{N} \frac{\langle \delta p^2 \rangle_0^{(n)}}{n!} t^n, \qquad \left\langle \delta q^2 \right\rangle \equiv \sum_{n=0}^{N} \frac{\langle \delta q^2 \rangle_0^{(n)}}{n!} t^n, \qquad \left\langle \delta q \delta p \right\rangle \equiv \sum_{n=0}^{N} \frac{\langle \delta q \delta p \rangle_0^{(n)}}{n!} t^n, \tag{7.45}$$

truncating the series at $N = 3$, which is sufficient for our purposes.

Our goal is to study the behaviour of $f(t)$ in CGQ. In particular, we investigate under what circumstances (if any) $f(t) < 0$, signifying violation of uncertainty relations. For non-Gaussian states it is easy to see the violation even in the first order term since not all the odd moments are zero. We can observe this by considering an arbitrary potential with a single degree of freedom, $V(q)$, as in the following example. For such potential without any initial QQ and CQ correlations we have

$$\begin{aligned} f(t) &= \frac{1}{2}\Big(z_1 + z_2 + 2z_1 z_2\Big) - \frac{1}{120}\Big[(1+2z_1)\Big(60 \left\langle \delta p\, \delta q^2 \right\rangle V^{(3)}(q) \\ &+ 20 \left\langle \delta p\, \delta q^3 \right\rangle V^{(4)}(q) + 5 \left\langle \delta p\, \delta q^4 \right\rangle V^{(5)}(q) + \left\langle \delta p\, \delta q^5 \right\rangle V^{(6)}(q)\Big)\Big] t + \mathcal{O}(t^2). \end{aligned} \tag{7.46}$$

where $V^{(n)}(q) = \partial_q^n V(q)$ and the first term (the uncertainty at $t = 0$ can be zero and the overall sign of the first order term is negative. Hence for a generic state that initially saturates the uncertainty relation, $f(0) = 0$, the time evolution with any potential immediately violates it. However, Gaussian states are quite robust against the violation of Heisenberg uncertainty relation. If $f(t = 0) = 0$, then any potential of the form $V(q)$ will lead to a violation only in the third order term.

Next we consider the most general form of the potential (7.30). By including both initial QQ $\langle \delta q \delta p \rangle_0$ and, e.g., QC $\langle \delta q \delta x \rangle_0$ correlations, while setting other correlations to zero, the general form of (7.44) becomes

$$\begin{aligned} f(t) &= \frac{1}{2}\Big(z_1 + z_2 + 2z_1 z_2 - 2\langle \delta q \delta p \rangle_0^2\Big) \\ &+ \frac{1}{16}\langle \delta q \delta p \rangle_0 \langle \delta q \delta x \rangle_0 \Big[32U^{(1,1)} + 8(1+2y_2)U^{(1,3)} + \big(1 + 4y_2 + 4y_2^2\big)U^{(1,5)} \\ &+ 32\langle \delta q \delta x \rangle_0 U^{(2,2)} + 8\langle \delta q \delta x \rangle_0 U^{(2,4)}(1+2y_2) + (8+16z_1)U^{(3,1)}\Big(2 + 16\langle \delta q \delta x \rangle_0^2 + 4y_2 \\ &+ 4z_1 + 8y_2 z_1\Big)U^{(3,3)} + 8\langle \delta q \delta x \rangle_0 U^{(4,2)}(1+2z_1) + (1 + 4z_1 + 4z_1^2)U^{(5,1)}\Big]t + \mathcal{O}(t^2), \end{aligned} \tag{7.47}$$

up to the leading order in time. Here we used the short form for $U^{(i,j)}(q,x) = \partial_q^i \partial_x^j U(q,x)$ to be $U^{(i,j)}$. The first term of this relation, which describes UR at $t = 0$, cannot be initially saturated (namely $f(0) \neq 0$) since inclusion of the QC correlation implies the reduced state of the quantum subsystem will no longer be pure (the only case where UR saturates). In this case the quantum system has some positive initial value $f(0)$ that can be minimized whilst satisfying the positivity condition (7.39) of the covariance matrix of the whole system.

We can establish the inconsistency if the linear term is negative and the second order term is either negative or sufficiently small as to enable $f(t_*) < 0$ for some time t_*. We therefore observe that a necessary condition for violation of UR in the linear term is that neither of $\langle \delta q \delta p \rangle_0$, $\langle \delta q \delta x \rangle_0$ vanish, and at least one of the $U^{(i,j)}(q,x)$ is nonzero. Otherwise terms of higher order in t must be included in (7.47) for any possibility of observing a violation of UR. For example if we consider no QC or QQ correlations, the first term in (7.47) saturates at $t = 0$ and the first order term disappears. If the second order term can be made negative then a violation of UR follows immediately. Similar considerations hold for higher-order terms if the second-order term is positive. In the following examples we will analyze the behaviour of each term.

Consider a specific form of an interaction potential given by

$$U(q,x) = \beta_1 q g(x) + \beta_2 q^2 g(x), \tag{7.48}$$

where

$$g(x) = \gamma_1 x + \gamma_2 x^2. \tag{7.49}$$

For the case with no QQ or QC correlations, equation (7.44) takes the following form up

to the third order in time

$$
\begin{aligned}
f(t) &= \frac{1}{2}\Big(z_1+z_2+2z_1z_2\Big) \qquad (7.50)\\
&+ \frac{1}{4}(1+2y_2)(1+2z_1)\Big(\beta_1^2+4q_0\beta_1\beta_2+2\beta_2^2\big(1+2q_0^2+2z_1\big)\Big)\Big(\gamma_1^2+2x_0\gamma_1\gamma_2\\
&+ \big(1+4x_0^2+2y_2\big)\gamma_2^2\Big)t^2+2k_0\left(\frac{1}{2}+z_1\right)\times\beta_2(\gamma_1+2x_0\gamma_2)\Bigg[\frac{1}{2}+z_2-\left(\frac{1}{2}+z_1\right)\alpha\\
&- 2\left(\frac{1}{2}+y_2\right)\left(\frac{1}{2}+z_1\right)\beta_2\gamma_2-x_0(1+2z_1)\beta_2(\gamma_1+x_0\gamma_2)\Bigg]t^3+\mathcal{O}(t^4).
\end{aligned}
$$

In this example, the quadratic term is always positive; we can minimize its effect by choosing $y_2 \to -1/2$. This is the case of the extreme squeezing, namely, the Gaussian distribution in phase space is squeezed in one dimension and elongated in the other. Violations of UR will occur if the coefficient of the t^3 term is negative, which can be arranged by setting $\beta_2, \alpha > 0$, with all other variables also being positive. Three out of five terms in the square bracket are negative, and so the entire coefficient can be made negative by choosing large positive values for α and β_2. The fourth-order order term included both negative and positive terms and one can strengthen the negative terms by choosing the initial values arbitrarily large while diminishing the positive terms by choosing $y_2 \to -1/2$. For quadratic potentials the implications of these results remain to be understood, since previous work has indicated that a valid classical epistemic state can be equivalently described by a Gaussian state [128]. Therefore, in our case of study, the evolution should be identical to that of two coupled quantum systems.

In the second example we consider an interaction potential of the form

$$U(q,x) = \beta_1 q x^2 + \beta_2 q^2 x, \qquad (7.51)$$

for which the equation (7.44) takes the form

$$
\begin{aligned}
f(t) &= \frac{1}{2}\Big(z_1+z_2+2z_1z_2\Big) \qquad (7.52)\\
&+ \frac{1}{4}(1+2y_2)(1+2z_1)\Big(\big(1+4x_0^2+2y_2\big)\beta_1^2+8q_0x_0\beta_1\beta_2+2\beta_2^2\big(1+2q_0^2+2z_1\big)\Big)t^2\\
&- \frac{1}{2}\Big(k_0(1+2z_1)\beta_2(-1-2z_2+\alpha+2z_1\alpha+2x_0\beta_2+4x_0z_1\beta_2)\Big)t^3+\mathcal{O}(t^4).
\end{aligned}
$$

Like the previous example, the second order term can be minimized by choosing $y_2 \to -1/2$. Violation of the UR will be manifest in the third and fourth order terms provided the free

parameters x_0, k_0, α, and β_2 are chosen to be large enough to make the quantity in the brackets positive.

For a potential of the form (7.51), by introducing non-zero cross correlations (QC) between the classical and quantum subsystems (for example by considering $\langle \delta q \delta x \rangle_0$ in the correlation matrix γ_{QC}) and also taking $\langle \delta q \delta p \rangle_0 \neq 0$, we have

$$\begin{aligned} f(t) &= \frac{1}{2}\Big(z_1 + z_2 + 2z_1 z_2 - 2\langle \delta q \delta p \rangle_0^2\Big) + 2\langle \delta q \delta p \rangle_0 \langle \delta q \delta x \rangle_0 (\beta_1 x_0 + \beta_2 q_0) t \\ &+ \frac{1}{4}\Bigg[\beta_1\Big(8k_0 \langle \delta q \delta x \rangle_0 \langle \delta q \delta p \rangle_0 + 4x_0(\langle \delta q \delta x \rangle_0 + 2\langle \delta q \delta x \rangle_0 z_2) + (1+2y_2)^2(1+2z_1)\beta_1 \\ &+ 4x_0^2\beta_1\big(1 - 4\langle \delta q \delta x \rangle_0^2 + 2y_2 + 2z_1 + 4y_2 z_1\big)\Big) + 4\beta_2\Big(2p_0 \langle \delta q \delta p \rangle_0 \langle \delta q \delta x \rangle_0 \\ &+ 2\beta_1 \langle \delta q \delta x \rangle_0 (1+2y_2)(1+2z_1) + q_0\big(\langle \delta q \delta x \rangle_0 + 2z_2 \langle \delta q \delta x \rangle_0 - 8x_0\beta_1 \langle \delta q \delta x \rangle_0^2 \\ &+ 2x_0\beta_1(1+2y_2)(1+2z_1)\big)\Big) + 2\beta_2^2\Big(q_0^2\big(2 - 8\langle \delta q \delta x \rangle_0^2 + 4y_2 + 4z_1 + 8y_2 z_1\big) \\ &+ (1+2z_1)\big(4\langle \delta q \delta x \rangle_0^2 + (1+2y_2)(1+2z_1)\big)\Big)\Bigg] t^2 + \mathcal{O}(t^3). \end{aligned} \tag{7.53}$$

In this case we cannot saturate the first term since by including the QC correlation terms the reduced state of the quantum subsystem will not be pure anymore which is the only case where UR saturates. So we shall begin with some positive initial value that we can minimize while satisfying the positivity condition (7.39) of the covariance matrix of the whole system. However, we can make the first and second derivative negative by satisfying the following conditions,

- $q_0 < 0$, $p_0 < 0$, $k_0 < 0$, and $\beta_1 < 0$. p_0 can be as large as it is needed to make the whole second order term negative and rest of the parameters need to be positive.

Applying these conditions keeps both linear and quadratic terms negative and the upper limit for the time scale during which $f(t)$ crosses zero can be obtain from

$$t_* \leq \left| -\frac{z_1 + z_2 + 2z_1 z_2 - 2\langle \delta q \delta p \rangle_0^2}{4\langle \delta q \delta p \rangle_0 \langle \delta q \delta x \rangle_0 (\beta_1 x_0 + \beta_2 q_0)} \right|. \tag{7.54}$$

7.5 Conclusions

Our investigation has produced a result that is complementary to that of Bartlett, Rudolph and Spekkens [128]: while a stand-alone Gaussian quantum system can be treated classi-

cally, it exhibits telltale quantum features that are revealed when it is coupled to a classical system.

The results of Sec.7.3 show that Koopmanian formalism distinguishes between quantum and classical descriptions even if the interaction between the two systems is Gaussian. The correspondence principle cannot be enforced, and exclusion of the non-observable operators from the equations of motion eliminates the very possibility for the quantum subsystem to influence the classical one. In addition, since the classical Liouvillian operator is unbounded from below, a resonance leading to an infinite flow of energy from the classical to quantum system is possible.

The phase space quantum-classical picture is, as expected, consistent if the statistical moments satisfy the ERL restrictions and the Hamiltonian is Gaussian. However, if the interaction term is $U(x, q)$ is not bilinear, the mixed evolution quickly becomes inconsistent (after a time given in (7.54)) even if the initial state is Gaussian.

Chapter 8

Conclusions and Future Directions

In this thesis we addressed several questions of interest in RQI, the field that elegantly forms a framework encompassing three main fields of theoretical physics: general theory of relativity, quantum theory and information theory. Our aim was to pave the way toward a better understanding of fundamental features of light-matter interaction and the notion of particle creation in relativistic quantum fields. For our investigations we used one of the well-studied tools in RQI, the Unruh-DeWitt particle detector. Along the way, in Ch.4 we introduced a method for computing particle detector transition probabilities in localized regions of general curved spacetimes provided that the curvature is not above a maximum threshold. With the help of some approximations that are applicable in the cavity scenario we employed, we were able to circumvent the complexity involved in the calculation of the Wightmann function in the transition probability of the detector in such scenarios [37]. In Ch.5 we exhibited the sensitivity of the relativistic signatures on the transition probability of atoms that are moving through optical cavities. We have studied the potential of the use of an atomic internal quantum degree of freedom to design novel quantum metrology settings. In particular we considered two scenarios: one where the probe undergoes small time-dependent perturbations of its proper acceleration, and another one when the probe's trajectory experiences small spatial time-dependent perturbations as seen from the laboratory's frame.

The results that are stated in Ch.6 settle a long-standing question regarding the Unruh effect: which trajectories will maximize the Unruh effect, and exactly how strong can the Unruh effect be made? By introducing the new method of analyzing concomitant frequencies, we established the exact answers nonperturbatively and fully generally for each field mode and for each choice of detector gap. In particular, our new results show that the usually-considered paths of uniform acceleration are sub-optimal and how they

can be improved upon. This is also of interest regarding the great challenge of developing experiments that probe the Unruh effect.

And finally in Ch.7 we studied the dynamics of a hybrid classical-quantum system using both Hilbert space and the Moyal formalism. We showed that while many explicitly quantum effects can be represented classically, quantum aspects of the system cannot be fully masked. Our results have implications for the no-cloning theorem, quantum teleportation, and the EPR thought experiment, insofar as the lack of consistency of the hybrid models we describe render them unable to properly account for these phenomena. In addition, our result has a bearing on the question of the logical necessity of quantizing linearized gravity [139–142]. Consider a scalar field minimally coupled to a linearized gravitational field. Expanding both systems into normal modes we have two families of non-linearly coupled oscillators. In a consistent mixed description a family of quantum oscillators (scalar field) non-linearly interacts with classical oscillators (gravity). Assuming that the results of [127] can be extended to a setting with infinite degrees of freedom, it is necessary to introduce uncertainty into the state of classical oscillators, thus indicating that a consistent mixed dynamics should involve at least a stochastic gravity. Moreover, the presence of the nonlinear interaction as in the examples above should eventually lead to the violation of uncertainty relations for quantum oscillators, making the entire scheme untenable. We will make a rigorous analysis along these lines in a future work.

In this final chapter, we address several directions for future research based on the ground work and results of this thesis. For advancing these ideas, further developments in theoretical methods will be required. In principle, these ideas are not only important in the fundamental theoretical aspects, but they have potentially great impact on real-world quantum technologies and specifically on quantum communications.

8.1 Transition probability: Trajectories with non-uniform accelerations

One largely unexplored aspect of RQI is the physics of detectors that are non-uniformly accelerating. It is essential to study such non-idealized cases since these offer realistic physically realizable setups, in contrast to the forever uniformly accelerating observers that are typically investigated. Often in experimental proposals to test the Unruh effect [92, 143–146], it is required for a detector to have non-uniform [76, 96, 97] or finite-time acceleration [47, 147, 148]. Therefore, there are no past/future horizons for such detectors; to check the robustness of the Unruh effect in these non-ideal cases one needs to apply

concepts and techniques in non-equilibrium quantum field theory [149].

Interesting related work along these lines was considered by Good [150], who generalized the moving mirror model of Davies and Fulling [151, 152] to a variety of non-uniformly accelerated trajectories. The motivation of his work was to find trajectories along which the particle creation from the initial non-thermal phase of the mirror till its late time thermal distribution resembles the entire history of black hole Hawking radiation from initial formation of a black hole. It would be interesting to examine the response of detectors following the same kinds of trajectories as those employed by Good for mirrors. In particular, we are interested to compare the class of mirror trajectories that model the radiation from a black hole. For this class, the number of created particles and the finite energy flux asymptotes in time to the thermal distribution of black hole radiation.

8.2 Modulation of Hawking radiation: Black hole information paradox

We developed the results in Ch.6 with a view to their eventual application to the black hole information loss problem. Indeed, having shown how Unruh radiation can be modulated very strongly, we invoke the equivalence principle to argue that this indicates that Hawking radiation could also be correspondingly strongly modulated and could, therefore, be carrying away significant amounts of information. The applicability of the equivalence principle in this context is discussed in a key paper by Candelas [39], a paper by Singleton and Willburn [40] and the subsequent discussion [100, 101]. They discuss how the equivalence principle relates the Unruh effect to the Hawking effect close to the horizon. Even without invoking the equivalence principle, our new approach to concomitant frequencies could be directly useful in studies of the modulation of Hawking radiation. This is because any such calculation should ultimately yield a modulation of Bogolyubov β coefficients (or it can be re-formulated in this way, e.g., when working in the path integral formalism). And Bogolyubov β coefficients are amplitudes of concomitant frequencies: to choose a definition of the vacuum state is to choose a definition of what constitutes positive frequencies in mode functions. The Bogolyubov β coefficients are then the amplitudes of negative frequencies that arise from the varying of positive frequencies. This suggests trying to adapt and apply the new method of concomitant frequencies directly in any of the various models for how Hawking radiation could be modulated by infalling matter.

In Ch.6 we demonstrated a general method for analyzing how concomitant frequencies arise when they are maximally modulated, and what the magnitude of this maximal

modulation is. We worked this out in full detail only for the case of the Bogolyubov transformations of the Unruh effect, but the approach should work more generally. In particular, we used the new techniques to determine the exact circumstances when strong modulation of Bogolyubov β coefficients is possible. This circumstance is a particular kind of non-adiabaticity, which is sufficient and necessary for strong modulation of the horizon radiation. For the Unruh effect, we determined when this non-adiabaticity condition holds: namely when the acceleration changes on a time scale that is comparable to the time scale of the dominant frequency of the Unruh radiation. This non-adiabaticity condition is likely to also hold in the case of matter falling into a black hole because the time scale of the ringdown after a black hole consumes an infalling object is roughly comparable to the time scale of the peak frequency of the Hawking spectrum, namely the light crossing time of the black hole.

Another question that one may explore is how purified the outgoing radiation is, or how much quantum information can be carried out of the black hole. Here the challenge is to determine how infalling matter (which may be modeled using massive UDW detectors) is deforming the black hole, by using techniques of quasinormal modes, and then to apply the mathematical analysis of concomitant frequencies to establish the modulation of the Hawking spectrum. This should provide us with a channel that maps the entropy of the infalling matter to changes in the entropy of the outgoing Hawking radiation. The challenge is to find the maximum quantum channel capacity. In order to determine this channel capacity, the infalling matter needs to be assumed to be entangled with matter that remains outside the black hole. The task then would be to calculate to what extent this preexisting entanglement can be transferred into entanglement with the outgoing Hawking radiation. So far, in Ch.6, we have studied the phenomenon of concomitant frequencies only for the purpose of determining the overall size of the possible modulation of the horizon radiation. We can extend the present analysis of concomitant frequencies to include a careful tracking not only of the magnitudes but also of the phases of concomitant frequencies. Then we would expect that such a complete picture could enable us to draw general conclusions about the possible magnitude of quantum channel capacities and therefore about the purity of the final state. While any calculations with a similar purpose are generally very difficult, a key advantage of the new approach that focuses on the generic phenomenon of concomitant frequencies, is that it is independent of the assumption of any particular mechanism for how the classical and quantum information gets transferred into the outgoing Hawking radiation.

8.3 Closing remarks

One of the key lessons of this thesis is that the incorporation of quantum information in our understanding of gravity and quantum physics appears to be essential in achieving our ultimate goal of uncovering the fundamental principles of quantum gravity. The methods and results presented have, through several examples, demonstrated the applicability of effective information-theoretic approaches of RQI in studying foundational ideas and issues in physics. The tools developed should find application in confronting a broad range of theoretical and experimental aspects of physics, and perhaps will make useful and important contributions to quantum technologies.

References

[1] Aida Ahmadzadegan, Eduardo Martín-Martínez, and R. B. Mann. Cavities in curved spacetimes: the response of particle detectors. *Phys. Rev. D*, 89:024013, 2014.

[2] Aida Ahmadzadegan, Robert B. Mann, and Eduardo Martín-Martínez. Measuring motion through relativistic quantum effects. *Phys. Rev. A*, 90:062107, Dec 2014.

[3] Aida Ahmadzadegan, Robert B. Mann, and Daniel R. Terno. Classicality of a quantum oscillator. *Phys. Rev. A*, 93:032122, Mar 2016.

[4] Aida Ahmadzadegan and Achim Kempf. Strong transient modulation of horizon radiation. *(Submitted to Phys. Rev. Lett.) arXiv:1702.00472*, 2017.

[5] B. DeWitt. *General Relativity; an Einstein Centenary Survey*. Cambridge University Press, Cambridge, UK, 1980.

[6] S. Hawking. Particle creation by black holes. *Comm. Math. Phys.*, 43:199–220, 1975.

[7] S. W. Hawking. Breakdown of predictability in gravitational collapse. *Phys. Rev. D*, 14:2460–2473, Nov 1976.

[8] I. Fuentes-Schuller and R. B. Mann. Alice falls into a black hole: Entanglement in noninertial frames. *Phys. Rev. Lett.*, 95:120404, Sep 2005.

[9] Paul M. Alsing and G. J. Milburn. Teleportation with a uniformly accelerated partner. *Phys. Rev. Lett.*, 91:180404, Oct 2003.

[10] Paul M. Alsing and Ivette Fuentes. Observer dependent entanglement. *Class. Quantum Grav.*, 29, October 2012.

[11] F. Kiałka A. Dragan P. T. Grochowski, G. Rajchel. Effect of relativistic acceleration on continuous variable quantum teleportation and dense coding. *arXiv:1701.02251*, 2017.

[12] ATLAS collaboration. Evidence for the spin-0 nature of the Higgs boson using ATLAS data. *Phys. Lett. B*, 726(13):120 – 144, 2013.

[13] David J. Gross and Frank Wilczek. Ultraviolet behavior of non-abelian gauge theories. *Phys. Rev. Lett.*, 30:1343–1346, Jun 1973.

[14] Julian Schwinger. On quantum-electrodynamics and the magnetic moment of the electron. *Phys. Rev.*, 73:416–417, Feb 1948.

[15] C. J. Isham. An introduction to quantum gravity. In *Quantum gravity; Proceedings of the Oxford Symposium, Harwell, Berks., England, February 15, 16, 1974. (A76-11051 01-90) Oxford.*, pages 1–77. Clarendon Press, 1975.

[16] C. J. Isham. Quantum Field Theory in Curved Space Times: An Overview. In *8th Texas Symposium on Relativistic Astrophysics Boston, Mass.*, page 114, December 1976.

[17] N.D. Birrell and P.C.W. Davies. *Quantum fields in curved space*. Cambridge university press. England., 1984.

[18] S.A. Fulling. *Aspects of Quantum Field Theory in Curved Spacetime*. London Mathematical Society Student Texts. Cambridge University Press, 1989.

[19] Achim Kempf. Quantum field theory for cosmology (course notes), 2017.

[20] W.G. Unruh. Notes on black-hole evaporation. *Physical Review D*, 14(4):870, 1976.

[21] B.L. Hu, Shih-Yuin Lin, and Jorma Louko. Relativistic Quantum Information in Detectors-Field Interactions. *Class.Quant.Grav.*, 29:224005, 2012.

[22] Masahiro Hotta. Quantum measurement information as a key to energy extraction from local vacuums. *Phys. Rev. D*, 78:045006, Aug 2008.

[23] Masahiro Hotta. Controlled hawking process by quantum energy teleportation. *Phys. Rev. D*, 81:044025, Feb 2010.

[24] Alejandro Pozas-Kerstjens and Eduardo Martín-Martínez. Entanglement harvesting from the electromagnetic vacuum with hydrogenlike atoms. *Phys. Rev. D*, 94:064074, Sep 2016.

[25] Benni Reznik, Alex Retzker, and Jonathan Silman. Violating Bell's inequalities in vacuum. *Phys. Rev. A*, 71:042104, 2005.

[26] Daniel Braun. Entanglement from thermal blackbody radiation. *Phys. Rev. A*, 72:062324, Dec 2005.

[27] Juan León and Carlos Sabín. Generation of atom-atom correlations inside and outside the mutual light cone. *Phys. Rev. A*, 79:012304, Jan 2009.

[28] Eric G. Brown. Thermal amplification of field-correlation harvesting. *Phys. Rev. A*, 88:062336, Dec 2013.

[29] S. J. Summers and R. F. Werner. The vacuum violates Bell's inequalities. *Phys. Lett. A*, 110:257, 1985.

[30] A. Peres and D. R. Terno. Quantum information and relativity theory. 76:93–123, 2004.

[31] E. Martin-Martinez and N. C. Menicucci. Cosmological quantum entanglement. *Classical and Quantum Gravity*, 29(22), 2012.

[32] Eduardo Martn-Martnez and Nicolas C Menicucci. Entanglement in curved spacetimes and cosmology. *Classical and Quantum Gravity*, 31(21):214001, 2014.

[33] Grant Salton, Robert B Mann, and Nicolas C Menicucci. Acceleration-assisted entanglement harvesting and rangefinding. *New Journal of Physics*, 17(3):035001, 2015.

[34] Stephen Fulling. Nonuniqueness of Canonical Field Quantization in Riemannian Space-Time. *Physical Review D*, 7(10):2850–2862, May 1973.

[35] P. C. W. Davies. Scalar particle production in schwarzschild and rindler metrics. *J. Phys. A*, 8(4):609–616, 1975.

[36] A. Higuchi, G. E. A. Matsas, and C. B. Peres. Uniformly accelerated finite-time detectors. *Phys. Rev. D*, 48:3731–3734, Oct 1993.

[37] Jorma Louko and Alejandro Satz. Transition rate of the unruh-dewitt detector in curved spacetime. *Class.Quant.Grav.*, 25:055012, October 2008.

[38] Luis C. Barbado, Carlos Barceló, Luis J. Garay, and Gil Jannes. Hawking versus unruh effects, or the difficulty of slowly crossing a black hole horizon. *Journal of High Energy Physics*, 2016(10):161, 2016.

[39] P. Candelas. Vacuum polarization in schwarzschild spacetime. *Phys. Rev. D*, 21:2185–2202, Apr 1980.

[40] Douglas Singleton and Steve Wilburn. Hawking radiation, unruh radiation and the equivalence principle. *Phys.Rev.Lett.*, 107:081102, February 2011.

[41] Matteo Smerlak and Suprit Singh. New perspectives on hawking radiation. *Phys. Rev. D*, 88:104023, Nov 2013.

[42] P.A.M. Dirac. *Lectures on Quantum Field Theory*. Bekfer Graduate School of Science. Monographs Series. Belfer Graduate School of Science, 1966.

[43] Michael E Peskin and Daniel V Schroeder. *An Introduction to Quantum Field Theory*. Westview Press, 1995.

[44] S. Weinberg. *The Quantum Theory of Fields*, volume 1. Cambrigde Univeristy Press, Cambrigde, 1995.

[45] Eduardo Martín-Martínez, Miguel Montero, and Marco del Rey. Wavepacket detection with the unruh-dewitt model. *Phys. Rev. D*, 87:064038, Mar 2013.

[46] Lee Hodgkinson and Jorma Louko. How often does the unruh-dewitt detector click beyond four dimensions? *J. Math. Phys.*, 63:082301, June 2012.

[47] Jorma Louko and Alejandro Satz. How often does the unruh-dewitt detector click? regularisation by a spatial profile. *Class.Quant.Grav.*, 23:6321, 2006.

[48] Alejandro Satz. Then again, how often does the unruh-dewitt detector click if we switch it carefully? *Class.Quant.Grav.*, 24:1719–1732, 2007.

[49] Eduardo Martín-Martínez, David Aasen, and Achim Kempf. Processing quantum information with relativistic motion of atoms. *Phys. Rev. Lett.*, 110:160501, Apr 2013.

[50] William G. Unruh and Ralf Schützhold. On the universality of the hawking effect. *Phys.Rev. D*, 71:024028, 2005.

[51] Luís C. B. Crispino, Atsushi Higuchi, and George E. A. Matsas. The Unruh effect and its applications. *Rev. Mod. Phys.*, 80:787, 2008.

[52] R.M. Wald. *Quantum Field Theory in Curved Spacetime and Black Hole Thermodynamics*. Chicago Lectures in Physics. University of Chicago Press, 1994.

[53] William G. Unruh and Robert M. Wald. What happens when an accelerating observer detects a rindler particle. *Phys. Rev. D*, 29:1047–1056, Mar 1984.

[54] Alessandro Fabbri and Jose Navarro-Salas. *Modeling black hole evaporation*. World Scientific, London (United Kingdom), June 2005.

[55] V. Mukhanov and S. Winitzki. *Introduction to Quantum Effects in Gravity*. Cambridge University Press, 2007.

[56] J. S. F. Chan and R. B. Mann. Scalar wave falloff in asymptotically anti-de sitter backgrounds. *Phys. Rev. D*, 55:7546–7562, Jun 1997.

[57] Matt Visser. Some general bounds for one-dimensional scattering. *Phys. Rev. A*, 59:427–438, Jan 1999.

[58] Petarpa Boonserm, Tritos Ngampitipan, and Matt Visser. Regge-wheeler equation, linear stability, and greybody factors for dirty black holes. *Phys. Rev. D*, 88:041502, Aug 2013.

[59] Petarpa Boonserm and Matt Visser. Bounding the bogoliubov coefficients. *Annals of Physics*, 323(11):2779 – 2798, 2008.

[60] Petarpa Boonserm and Matt Visser. Transmission probabilities and the millergood transformation. *Journal of Physics A: Mathematical and Theoretical*, 42(4):045301, 2009.

[61] S. W. Hawking. Black hole explosions? *Nature*, 248(5443):30–31, Mar 1974.

[62] Steven B. Giddings. Black hole information, unitarity, and nonlocality. *Phys. Rev. D*, 74:106005, Nov 2006.

[63] Thomas Banks, Leonard Susskind, and Michael E. Peskin. Difficulties for the evolution of pure states into mixed states. *Nuclear Physics B*, 244(1):125 – 134, 1984.

[64] Steven B. Giddings. Modulated hawking radiation and a nonviolent channel for information release. *Physics Letters B*, 738:92 – 96, 2014.

[65] Steven B. Giddings. Nonviolent unitarization: basic postulates to soft quantum structure of black holes. *arXiv:1701.08765*, 2017.

[66] Kostas D. Kokkotas and Bernard F. Schutz. Normal modes of a model radiating system. *General Relativity and Gravitation*, 18(9):913–921, 1986.

[67] Sai Iyer and Clifford M. Will. Black-hole normal modes: A wkb approach. i. foundations and application of a higher-order wkb analysis of potential-barrier scattering. *Phys. Rev. D*, 35:3621–3631, Jun 1987.

[68] Sai Iyer. Black-hole normal modes: A wkb approach. ii. schwarzschild black holes. *Phys. Rev. D*, 35:3632–3636, Jun 1987.

[69] Antonino Flachi and José P. S. Lemos. Quasinormal modes of regular black holes. *Phys. Rev. D*, 87:024034, Jan 2013.

[70] Kostas D. Kokkotas and Bernd G. Schmidt. Quasi-normal modes of stars and black holes. *Living Reviews in Relativity*, 2(1):2, 1999.

[71] Emanuele Berti, Vitor Cardoso, and Andrei O Starinets. Quasinormal modes of black holes and black branes. *Classical and Quantum Gravity*, 26(16):163001, 2009.

[72] Steven B. Giddings and Yinbo Shi. Quantum information transfer and models for black hole mechanics. *Phys. Rev. D*, 87:064031, Mar 2013.

[73] Patrick Hayden and John Preskill. Black holes as mirrors: quantum information in random subsystems. *JHEP*, 09:120, August 2007.

[74] Donald Marolf. The black hole information problem: past, present, and future. *arXiv:1703.02143*, 2017.

[75] Gerard 't Hooft, Steven B. Giddings, Carlo Rovelli, Piero Nicolini, Jonas Mureika, Matthias Kaminski, Marcus Bleicher. The good, the bad, and the ugly of gravity and information. *arXiv:1609.01725*, 2016.

[76] N. Obadia and M. Milgrom. Unruh effect for general trajectories. *Phys. Rev. D*, 75:065006, Mar 2007.

[77] Lee Hodgkinson and Jorma Louko. Static, stationary and inertial unruh-dewitt detectors on the btz black hole. *Phys. Rev. D*, 86:064031, June 2012.

[78] Eric G. Brown, Eduardo Martín-Martínez, Nicolas C. Menicucci, and Robert B. Mann. Detectors for probing relativistic quantum physics beyond perturbation theory. *Phys. Rev. D*, 87:084062, December 2013.

[79] David Edward Bruschi, Antony R. Lee, and Ivette Fuentes. Time evolution techniques for detectors in relativistic quantum information. *J. Phys. A: Math. Theor.*, 46:165303, 2013.

[80] Wilson G. Brenna, Eric G. Brown, Robert B. Mann, and Eduardo Martín-Martínez. Universality and thermalization in the unruh effect. *Phys. Rev. D*, 88:064031, 2013.

[81] S. Chandrasekhar. *The Mathematical Theory of Black Holes*. Oxford University Press, 1994.

[82] T.S. Bunch and L. Parker. Feynman Propagator in Curved Space-Time: A Momentum Space Representation. *Phys.Rev.*, D20:2499–2510, 1979.

[83] Robert H. Jonsson, Eduardo Martín-Martínez, and Achim Kempf. Quantum signaling in cavity QED. *Phys. Rev. A*, 89:022330, Feb 2014.

[84] L Sriramkumar and T Padmanabhan. Finite-time response of inertial and uniformly accelerated unruh - dewitt detectors. *Classical and Quantum Gravity*, 13(8):2061, 1996.

[85] Luis J. Garay, Mercedes Martín-Benito, and Eduardo Martín-Martínez. Echo of the quantum bounce. *Phys. Rev. D*, 89:043510, Feb 2014.

[86] Andrzej Dragan, Ivette Fuentes, and Jorma Louko. Quantum accelerometer: Distinguishing inertial bob from his accelerated twin rob by a local measurement. *Phys.Rev.D.*, 83:085020, 2011.

[87] Vittorio Giovannetti, Seth Lloyd, and Lorenzo Maccone. Quantum-enhanced positioning and clock synchronization. *Nature*, 412:417–419, 2001.

[88] Vittorio Giovannetti, Seth Lloyd, and Lorenzo Maccone. Quantum metrology. *Phys. Rev. Lett.*, 96:010401, 2006.

[89] Vittorio Giovannetti, Seth Lloyd, and Lorenzo Maccone. Advances in quantum metrology. *Nature Photonics*, 5:222, 2011.

[90] Neil Ashby. Relativity in the global positioning system. *Living Rev. Relativity*, 6, 2003.

[91] Mehdi Ahmadi, David Edward Bruschi, Nicolai Friis, Carlos Sabin, Gerardo Adesso, and Ivette Fuentes. Relativistic quantum metrology: Exploiting relativity to improve quantum measurement technologies. *Sci. Rep.*, 4:4996, 2014.

[92] Marlan O. Scully, Vitaly V. Kocharovsky, Alexey Belyanin, Edward Fry, and Federico Capasso. Enhancing acceleration radiation from ground-state atoms via cavity quantum electrodynamics. *Phys. Rev. Lett.*, 91:243004, 2003.

[93] B. L. Hu and Albert Roura. Comment on "enhancing acceleration radiation from ground-state atoms via cavity quantum electrodynamics". *Phys. Rev. Lett.*, 93:129301, 2004.

[94] Marlan O. Scully, Vitaly V. Kocharovsky, Alexey Belyanin, Edward Fry, and Federico Capasso. Scully et al. reply:. *Phys. Rev. Lett.*, 93:129302, Sep 2004.

[95] Alvaro M. Alhambra, Achim Kempf, and Eduardo Martin-Martinez. Casimir forces on atoms in optical cavities. *Phys. Rev. A*, 89:033835, 2014.

[96] Dawood Kothawala and T. Padmanabhan. Response of unruh-dewitt detector with time-dependent acceleration. *Phys. Lett. B*, 690:201–206, 2010.

[97] Luis C. Barbado and Matt Visser. Unruh-dewitt detector event rate for trajectories with time-dependent acceleration. *Phys. Rev. D*, 86:084011, Oct 2012.

[98] C. Moller. *The Theory Of Relativity*. At The Clarendon Press, 1952.

[99] Marvellous Onuma-Kalu, Robert B. Mann, and Eduardo Martín-Martínez. Mode invisibility as a quantum nondemolition measurement of coherent light. *Phys. Rev. A*, 90:033847, Sep 2014.

[100] Luís C. B. Crispino, Atsushi Higuchi, and George E. A. Matsas. Comment on "hawking radiation, unruh radiation, and the equivalence principle". *Phys. Rev. Lett.*, 108:049001, Jan 2012.

[101] Douglas Singleton and Steve Wilburn. Singleton and wilburn reply:. *Phys. Rev. Lett.*, 108:049002, Jan 2012.

[102] L. Susskind and J. Lindesay. *An Introduction to Black Holes, Information and the String Theory Revolution: The Holographic Universe*. World Scientific, 2005.

[103] D. Harlow. Jerusalem lectures on black holes and quantum information. *Rev. Mod. Phys.*, 88:015002, Feb 2016.

[104] Christoph Adami and Greg L. Ver Steeg. Classical information transmission capacity of quantum black holes. *Class. Quant. Grav.*, 31:075015, 2014.

[105] Philip R. Johnson and B. L. Hu. Stochastic theory of relativistic particles moving in a quantum field: Scalar abraham-lorentz-dirac-langevin equation, radiation reaction, and vacuum fluctuations. *Phys. Rev. D*, 65:065015, Feb 2002.

[106] John Archibald Wheeler and Richard Phillips Feynman. Interaction with the absorber as the mechanism of radiation. *Rev. Mod. Phys.*, 17:157–181, Apr 1945.

[107] Morgan H. Lynch. Accelerated Quantum Dynamics. *Phys. Rev.*, D92(2):024019, 2015.

[108] Jason Doukas, Shih-Yuin Lin, B. L. Hu, and Robert B. Mann. Unruh effect under non-equilibrium conditions: oscillatory motion of an unruh-dewitt detector. *Journal of High Energy Physics*, 2013(11):119, 2013.

[109] Paulina Corona-Ugalde, Eduardo Martín-Martínez, C. M. Wilson, and Robert B. Mann. Dynamical casimir effect in circuit qed for nonuniform trajectories. *Phys. Rev. A*, 93:012519, Jan 2016.

[110] Shih-Yuin Lin. Radiation by an unruh-dewitt detector in oscillatory motion. *arXiv:1709.08506*, 2017.

[111] David C.M. Ostapchuk, Shih-Yuin Lin, Robert B. Mann, and B.L. Hu. Entanglement Dynamics between Inertial and Non-uniformly Accelerated Detectors. *JHEP*, 1207:072, 2012.

[112] M.M.O. Scully and M.S. Zubairy. *Quantum Optics*. Cambridge University Press, 1997.

[113] P. C. W. Davies and Adrian C. Ottewill. Detection of negative energy: 4-dimensional examples. *Phys. Rev. D*, 65:104014, May 2002.

[114] Samuel L. Braunstein and Peter van Loock. Quantum information with continuous variables. *Rev. Mod. Phys.*, 77:513–577, Jun 2005.

[115] Christian Weedbrook, Stefano Pirandola, Raúl Garcí a Patrón, Nicolas J. Cerf, Timothy C. Ralph, Jeffrey H. Shapiro, and Seth Lloyd. Gaussian quantum information. *Rev. Mod. Phys.*, 84:621–669, May 2012.

[116] A. Peres. *Quantum Theory: Concepts and Methods*. Kluwer, Dordrecht, 1995.

[117] Wojciech Hubert Zurek. Decoherence, einselection, and the quantum origins of the classical. *Rev. Mod. Phys.*, 75:715–775, May 2003.

[118] Luca Lusanna and Massimo Pauri. On the transition from the quantum to the classical regime for massive scalar particles: A spatiotemporal approach. *The European Physical Journal Plus*, 129(8):178, 2014.

[119] Claus Kiefer. *Quantum gravity*. Oxford University Press, Oxford New York, 2007.

[120] Wayne Boucher and Jennie Traschen. Semiclassical physics and quantum fluctuations. *Phys. Rev. D*, 37:3522–3532, Jun 1988.

[121] Arlen Anderson. Quantum backreaction on "classical" variables. *Phys. Rev. Lett.*, 74:621–625, Jan 1995.

[122] T. N. Sherry and E. C. G. Sudarshan. Interaction between classical and quantum systems: A new approach to quantum measurement. ii. theoretical considerations. *Phys. Rev. D*, 20:857–868, Aug 1979.

[123] Hans Thomas Elze. Linear dynamics of quantum-classical hybrids. *Phys. Rev. A*, 85:052109, May 2012.

[124] Alvin J. K. Chua, Michael J. W. Hall, and C. M. Savage. Interacting classical and quantum particles. *Phys. Rev. A*, 85:022110, Feb 2012.

[125] Daniel Terno Asher Peres. Hybrid classical-quantum dynamics. *Phys. Rev. A*, 63:022101, 2001.

[126] Daniel R. Terno. Inconsistency of quantumclassical dynamics, and what it implies. *Foundations of Physics*, 36(1):102–111, 2006.

[127] Carlos Barceló, Raúl Carballo-Rubio, Luis J. Garay, and Ricardo Gómez-Escalante. Hybrid classical-quantum formulations ask for hybrid notions. *Phys. Rev. A*, 86:042120, Oct 2012.

[128] Stephen D. Bartlett, Terry Rudolph, and Robert W. Spekkens. Reconstruction of gaussian quantum mechanics from liouville mechanics with an epistemic restriction. *Phys. Rev. A*, 86:012103, Jul 2012.

[129] David Jennings and Matthew Leifer. No return to classical reality. *Contemporary Physics*, 56, 2015.

[130] S. Olivares. Quantum optics in the phase space. *The European Physical Journal Special Topics*, 203(1):3–24, 2012.

[131] M. Hillery, R.F. O'Connell, M.O. Scully, and E.P. Wigner. Distribution functions in physics: Fundamentals. *Physics Reports*, 106(3):121 – 167, 1984.

[132] M. Reed and B. Simon. *Methods of Modern Mathematical Physics: Functional analysis*, volume 1. Academic Press, 1980.

[133] M. Reed and B. Simon. *Methods of Modern Mathematical Physics: Fourier analysis, self-adjointness*, volume 2. Academic Press, 1975.

[134] J. E. Moyal. Quantum mechanics as a statistical theory. *Mathematical Proceedings of the Cambridge Philosophical Society*, 45:99–124, 1 1949.

[135] Thomas L. Curtright Cosmas K. Zachos, David B. Fairlie, editor. *Quantum Mechanics in Phase Space: An Overview with Selected Papers*, volume 34. World Scientific, 2005.

[136] P. Ahrendt. The multivariate gaussian probability distribution. Technical report, jan 2005.

[137] L. E. Ballentine and S. M. McRae. Moment equations for probability distributions in classical and quantum mechanics. *Phys. Rev. A*, 58:1799–1809, Sep 1998.

[138] David Brizuela. Classical and quantum behavior of the harmonic and the quartic oscillators. *Phys. Rev. D*, 90:125018, Dec 2014.

[139] N. Hugget and C. Callender. *Phil. Sci.*, 68(S382), 2001.

[140] W. G. Unruh. *Steps towards a Quantum Theory of Gravity*, page 234. Adam Hilger Ltd, 1984.

[141] Kenneth Eppley and Eric Hannah. The necessity of quantizing the gravitational field. *Foundations of Physics*, 7(1):51–68, 1977.

[142] Don N. Page and C. D. Geilker. Indirect evidence for quantum gravity. *Phys. Rev. Lett.*, 47:979–982, Oct 1981.

[143] J. Rogers. Detector for the Temperaturelike Effect of Acceleration. *Phys. Rev. Lett.*, 61:2113–2116, 1988.

[144] Ralf Schützhold, Gernot Schaller, and Dietrich Habs. Signatures of the unruh effect from electrons accelerated by ultrastrong laser fields. *Phys. Rev. Lett.*, 97:121302, Sep 2006.

[145] Pisin Chen and Toshi Tajima. Testing unruh radiation with ultraintense lasers. *Phys. Rev. Lett.*, 83:256–259, Jul 1999.

[146] Eduardo Martín-Martínez, Ivette Fuentes, and Robert B. Mann. Using berry's phase to detect the unruh effect at lower accelerations. *Phys. Rev. Lett.*, 107:131301, Sep 2011.

[147] B. F. Svaiter and N. F. Svaiter. Inertial and noninertial particle detectors and vacuum fluctuations. *Phys. Rev. D*, 46:5267–5277, Dec 1992.

[148] Sebastian Schlicht. Considerations on the unruh effect: Causality and regularization. *Class.Quant.Grav.*, 21:4647–4660, 2004.

[149] Esteban A. Calzetta and Bei-Lok B. Hu. *Nonequilibrium Quantum Field Theory.* Cambridge Monographs on Mathematical Physics. Cambridge University Press, 2008.

[150] Michael R. R. Good, Paul R. Anderson, and Charles R. Evans. Mirror reflections of a black hole. *Phys. Rev. D*, 94:065010, Sep 2016.

[151] S. A. Fulling and P. C. W. Davies. Radiation from a moving mirror in two dimensional space-time: Conformal anomaly. *Proceedings of the Royal Society of London A: Mathematical, Physical and Engineering Sciences*, 348(1654):393–414, 1976.

[152] P. C. W. Davies and S. A. Fulling. Radiation from moving mirrors and from black holes. *Proceedings of the Royal Society of London A: Mathematical, Physical and Engineering Sciences*, 356(1685):237–257, 1977.

APPENDICES

Appendix A

A.1 Details of the Koopmanian calculation

Pursuing the classical-quantum analogy, similar to the quantum-mechanical creation and annihilation operators which are

$$a = \tfrac{1}{\sqrt{2}}\left(\bar{q} + \mathrm{i}\bar{p}\right), \qquad a^\dagger = \frac{1}{\sqrt{2}}\left(\bar{q} - \mathrm{i}\bar{p}\right), \tag{A.1}$$

we also introduce classical creation and annihilation operators:

$$b_x = \tfrac{1}{\sqrt{2}}\left(\bar{x} + \mathrm{i}\bar{p}_x\right), \qquad b_x^\dagger = \frac{1}{\sqrt{2}}\left(\bar{x} - \mathrm{i}\bar{p}_x\right), \tag{A.2}$$

$$b_k = \tfrac{1}{\sqrt{2}}\left(\bar{k} + \mathrm{i}\bar{p}_k\right), \qquad b_k^\dagger = \frac{1}{\sqrt{2}}\left(\bar{k} - \mathrm{i}\bar{p}_k\right) \tag{A.3}$$

where $p_x = -\mathrm{i}\partial/\partial x$ ($\bar{p}_x = \lambda p_x$) and $p_k = -\mathrm{i}\partial/\partial k$ ($\bar{p}_k = \lambda_k p_k$). Similarly to their quantum analog,

$$[b_x, b_x^\dagger] = 1, \qquad [b_k, b_k^\dagger] = 1. \tag{A.4}$$

Since $[x, k] = 0$, their respective creation/annihilation operators commute. The Liouvillian (the time-translation generator) is given by

$$L = \kappa\omega_c\left(\bar{k}\bar{p}_x - \bar{x}\bar{p}_k\right) = \mathrm{i}\kappa\omega_c\left(b_x^\dagger b_k - b_k^\dagger b_x\right), \tag{A.5}$$

while the Hamiltonian (the energy operator) is

$$H_c = \frac{\kappa\omega_c}{4}\left(b_x^2 + b_x^{\dagger 2} + b_k^2 + b_k^{\dagger 2} + 2b_x b_x^\dagger + 2b_k^\dagger b_k\right). \tag{A.6}$$

The rescaled equations of motion have now an identical appearance

$$\mathrm{i}\frac{d\bar{O}_c}{dt} = [\bar{O}_c, L/\kappa], \qquad \mathrm{i}\frac{d\bar{A}_q}{dt} = [\bar{A}_q, H_q/\hbar] \tag{A.7}$$

in both the classical and quantum sectors.

The most general bilinear Hermitian term coupling the quantum and classical systems is

$$K_i = \mathrm{i}\left(\beta^*_{0x} a b_x - \beta_{0x} b^\dagger_x a^\dagger + \beta^*_{0k} a b_k - \beta_{0k} b^\dagger_k a^\dagger\right) + \alpha_{0x} a^\dagger b_x + \alpha^*_{0x} b^\dagger_x a + \alpha_{0k} a^\dagger b_k + \alpha^*_{0k} b^\dagger_k a, \tag{A.8}$$

and so we obtain

$$\begin{aligned}
\dot{a} &= -\mathrm{i}\omega_q a - \beta_{0x} b^\dagger_x - \beta_{0k} b^\dagger_k - \mathrm{i}\alpha_{0x} b_x - \mathrm{i}\alpha_{0k} b_k, \\
\dot{a}^\dagger &= \mathrm{i}\omega_q a^\dagger - \beta^*_{0x} b_x - \beta^*_{0k} b_k + \mathrm{i}\alpha^*_{0x} b^\dagger_x + \mathrm{i}\alpha^*_{0k} b^\dagger_k, \\
\dot{b}_x &= \omega_c b_k - \beta_{0x} a^\dagger - \mathrm{i}\alpha^*_{0x} a, \\
\dot{b}^\dagger_x &= \omega_c b^\dagger_k - \beta^*_{0x} a + \mathrm{i}\alpha_{0x} a^\dagger, \\
\dot{b}_k &= -\omega_c b_x - \beta_{0k} a^\dagger - \mathrm{i}\alpha^*_{0k} a, \\
\dot{b}^\dagger_k &= -\omega_c b^\dagger_x - \beta^*_{0k} a + \mathrm{i}\alpha_{0k} a^\dagger.
\end{aligned} \tag{A.9}$$

for the coupled equations of motion.

We can write the general form of the equations of motion in terms of both quantum and classical position, momentum and shift operators. Using the relations $\alpha_{0x} = \alpha^{(1)}_{0x} + \mathrm{i}\alpha^{(2)}_{0x}$ and $\beta_{0x} = \beta^{(1)}_{0x} + \mathrm{i}\beta^{(2)}_{0x}$, and similar ones for α_{0k} and β_{0k}, the equations of motion take the following form

$$\begin{aligned}
\dot{\bar{q}} &= \omega_q \bar{p} + (\alpha^{(2)}_{0x} - \beta^{(1)}_{0x})\bar{x} + (\alpha^{(2)}_{0k} - \beta^{(1)}_{0k})\bar{k} + (\alpha^{(1)}_{0x} - \beta^{(2)}_{0x})\bar{p}_x + (\alpha^{(1)}_{0k} - \beta^{(2)}_{0k})\bar{p}_k, \\
\dot{\bar{p}} &= -\omega_q \bar{q} - (\beta^{(2)}_{0x} + \alpha^{(1)}_{0x})\bar{x} - (\beta^{(2)}_{0k} + \alpha^{(1)}_{0k})\bar{k} + (\beta^{(1)}_{0x} + \alpha^{(2)}_{0x})\bar{p}_x + (\beta^{(1)}_{0k} + \alpha^{(2)}_{0k})\bar{p}_k, \\
\dot{\bar{x}} &= \omega_c \bar{k} - (\beta^{(1)}_{0x} + \alpha^{(2)}_{0x})\bar{q} + (\alpha^{(1)}_{0x} - \beta^{(2)}_{0x})\bar{p}, \\
\dot{\bar{k}} &= -\omega_c \bar{x} - (\beta^{(1)}_{0k} + \alpha^{(2)}_{0k})\bar{q} + (\alpha^{(1)}_{0k} - \beta^{(2)}_{0k})\bar{p}, \\
\dot{\bar{p}}_x &= \omega_c \bar{p}_k + (\beta^{(1)}_{0x} - \alpha^{(2)}_{0x})\bar{p} - (\beta^{(2)}_{0x} + \alpha^{(1)}_{0x})\bar{q}, \\
\dot{\bar{p}}_k &= -\omega_c \bar{p}_x + (\beta^{(1)}_{0k} - \alpha^{(2)}_{0k})\bar{p} - (\beta^{(2)}_{0k} + \alpha^{(1)}_{0k})\bar{q}.
\end{aligned} \tag{A.10}$$

The presence of the unobservable classical operators p_x and p_k in the equations of motion for quantum position and momentum act as driving forces. This leads to a violation of the correspondence principle, in the sense that the new equations for p and q are different

from both purely classical and quantum equations of motion. Those terms generally result in non-conservation of energy in the quantum system [125, 126]. If we demand that no unobservable operators couple to the quantum sector, we obtain

$$\begin{aligned} \alpha_{0x}^{(1)} &= \beta_{0x}^{(2)} \qquad \alpha_{0k}^{(1)} = \beta_{0k}^{(2)} \\ \alpha_{0x}^{(2)} &= -\beta_{0x}^{(1)} \qquad \alpha_{0k}^{(2)} = -\beta_{0k}^{(1)}. \end{aligned} \tag{A.11}$$

Therefore, equations of motion will take the form (7.24).

A.2 Details of the phase space calculation

Here we derive the moment equations for $\langle \delta p^2 \rangle$, $\langle \delta q^2 \rangle$, and $\langle \delta p \delta q \rangle$. If we consider the most general form of a classical moment for a system of two oscillators in one dimension to be [137]

$$\left\langle (\delta p)^{k_1} (\delta k)^{k_2} (\delta q)^{n_1} (\delta x)^{n_2} \right\rangle \equiv S[k_1, k_2, n_1, n_2], \tag{A.12}$$

therefore we have its time derivative to be

$$\begin{aligned} \frac{d}{dt} S[k_1, k_2, n_1, n_2] &= n_1 S[k_1 + 1, k_2, n_1 - 1, n_2] + n_2 S[k_1, k_2 + 1, n_1, n_2 - 1] \\ &- k_1 \frac{dP}{dt} S[k_1 - 1, k_2, n_1, n_2] - k_2 \frac{dK}{dt} S[k_1, k_2 - 1, n_1, n_2] \\ &- k_1 \sum_{l=0}^{n_{max}} \sum_{j=0}^{l} \frac{S[k_1 - 1, k_2, n_1 + l - j, n_2 + j]}{(l-j)!j!} \frac{\partial^{l+1} V(Q, X)}{\partial Q^{l-j+1} \partial X^j} \\ &- k_2 \sum_{l=0}^{n_{max}} \sum_{j=0}^{l} \frac{S[k_1, k_2 - 1, n_1 + l - j, n_2 + j]}{(l-j)!j!} \frac{\partial^{l+1} V(Q, X)}{\partial Q^{l-j} \partial X^{j+1}} \end{aligned} \tag{A.13}$$

where we restrict the series by $n_{max} = 6$ and $V(Q, X)$ is a general potential. Also we have $Q \equiv \langle q \rangle$, $X \equiv \langle x \rangle$, $P \equiv \langle p \rangle$, $K \equiv \langle k \rangle$, which their time derivatives are given by

$$\begin{aligned} \frac{dQ}{dt} &= P, \qquad \frac{dX}{dt} = K, \\ \frac{dP}{dt} &= -\sum_{l=0}^{n_{max}} \sum_{j=0}^{l} \frac{S[0, 0, l - j, j]}{(l-j)!j!} \frac{\partial^{l+1} V(Q, X)}{\partial Q^{l-j+1} \partial X^j}, \\ \frac{dK}{dt} &= -\sum_{l=0}^{n_{max}} \sum_{j=0}^{l} \frac{S[0, 0, l - j, j]}{(l-j)!j!} \frac{\partial^{l+1} V(Q, X)}{\partial Q^{l-j} \partial X^{j+1}}. \end{aligned} \tag{A.14}$$

Now as a simple example we can derive a moment equation for $\langle \delta q^2 \rangle$ as follows

$$\frac{d}{dt} S[0,0,2,0] = 2S[1,0,1,0], \tag{A.15}$$

which is equivalent to

$$\frac{d}{dt} \left\langle \delta q^2 \right\rangle = 2 \left\langle \delta p \delta q \right\rangle . \tag{A.16}$$

Equations for $\langle \delta p^2 \rangle$ and $\langle \delta p \delta q \rangle$ can be derived similarly.